AN INVESTIGATION INTO POLYMERIC MATERIALS FOR THE DESIGN OF HIGH PERFORMANCE SHOCK TUBES

by

CHRISTIAN YAKAN - A - NWAJI

Thesis submitted in fulfilment of the requirements for the degree

MASTER OF TECHNOLOGY
Chemical Engineering

in the Faculty of Engineering

Cape Peninsula University of Technology

Cape Peninsula
University of Technology

AN INVESTIGATION INTO POLYMERIC MATERIALS FOR THE DESIGN OF HIGH PERFORMANCE SHOCK TUBES

by

CHRISTIAN YAKAN-A-NWAI

Thesis submitted in fulfilment of the requirements for the degree

Master of Technology: Chemical Engineering

in the Faculty of Engineering

at the Cape Peninsula University of Technology

Supervisor: Professor Samir Mukhopadhyay

Cape Town
October 2011

DECLARATION

I, Christian Yakan-A-Nwai, declare that the contents of this thesis represent my own unaided work, and that the thesis has not previously been submitted for academic examination towards any qualification. Furthermore, it represents my own opinions and not necessarily those of the Cape Peninsula University of Technology.

Signed **Date**

ABSTRACT

Shock tube initiators are small-diameter hollow plastic tubing used in blasting systems to remotely convey an initiation signal in the form of shock wave to a detonating cap. Over the past years, few researchers have reported the development of various shock tube designs consisting of single, double, and triple polymeric layers. Despite the disclosure of the development of different shock tube designs, none of the researchers presented experimental data enabling one to predict how shock tubes' properties and performance could be affected by the number of polymeric layers and the nature of polymeric materials present in the shock tube. The aim of this investigation was, therefore, to experimentally determine to which extent changing the number of polymeric layers and the type of polymeric materials could vary the properties and performance of a multi-layered shock tube.

The methodology used during the investigation involved the extrusion and testing of a standard three-layered shock tube similar to the commercially available high performance shock tube and samples of different recipes of two-layered shock tubes. The three-layered shock tube was made of high density polyethylene in the outer layer, ethylene based ionomer in the inner layer and ethylene acrylic acid copolymer in the intermediate layer. Samples of two-layered shock tubes were made of ethylene based ionomer in the inner layer and various blends of polyethylene/Adhesion promoter in the outer layer. The adhesion promoters used included ethylene based ionomers, high density polyethylene grafted with maleic anhydride (HDPE-g-MAH), and ethylene methacrylic acid copolymers (EMA). Two types of polyethylene were blended to the adhesion promoter in the outer layer of two-layered shock tubes; high density polyethylene (HDPE) and linear low density polyethylene (LLDPE). The properties of both three-layered and two-layered shock tubes were then evaluated using series of tests which included: breaking strength, elongation at break, burst strength, oil ingression, linear thermal shrinkage and peel-off adhesion.

Results generated from the tests performed have demonstrated that two-layered shock tubes might exhibit a couple of properties superior, inferior, or similar to the standard three-layered shock tube depending on the nature of the polymeric materials used in the outer layer. In particular, the use of the blends of HDPE/HDPE-g-MAH in the outer layer of two-layered shock tubes was found to produce shock tubes with enhanced resistance to oil ingression. It was also found that varying the outer layer compositions of two-layered shock tubes could modify the tube's properties and performance to some extent. Based on the results obtained, a new material design for the manufacture of high performance two-layered shock tubes was proposed.

The proposed materials design involved blends of 60%HDPE/40%HDPE-g-MAH in the outer layer, and ethylene based ionomer in the inner layer. When compared to commercially available high performance shock tubes, the new material design was found to produce shock tubes with higher sleep times but poorer linear thermal shrinkage, and structural integrity.

DEDICATION

This thesis is dedicated to:

- The God of Abraham, Isaac, and Jacob for giving me strength, health, perseverance, and motivation throughout the completion of this work.
- My father, Mr. Nwai Yakan for giving me the best gift ever; education.
- My mother, Mrs. Nwai Genevieve for her unconditioned love and support.
- My family, friends, and colleagues for always cheering me up in difficult times.
- All my teachers and lecturers for contributing in shaping my life.

"Trust in the LORD with all your heart, and do not lean on your own understanding. In all your ways acknowledge him, and he will make straight your paths" **(Proverbs 3: 5-6)**

ACKNOWLEDGEMENTS

I wish to thank:

- The Cape Peninsula University of Technology for accommodating me throughout my undergraduate and postgraduate studies.

- Professor Samir Mukhopadhyay for his rich and fruitful advices, as well as his supervisory role throughout the completion of this work.

- Professor Irina Masalova for her moral support.

- Nazeem George, Victor Ncongwane, Francois De Bruyn, Noah Mhlongo, Siyakudumisa Mcimeli, and all the staff and students of the Material Science and Technology Centre for their continuous support.

- AEL mining service for the sponsorship, the experimental support and all the relevant research expenses.

TERMS AND CONCEPTS CITED

Adhesion promoter: Polymeric material capable of enhancing the adhesive properties of a polymer when blended therewith

Adhesion strength: Minimum force to be applied in order to separate the shock tube outer layer from the inner layer

Burst strength: Extent to which the shock tube can convey the shock wave without being physically damaged

Breaking strength: Minimum longitudinal force to be applied in order to tear the shock tube apart

Cold drawing: Irreversible extension of the shock tube after melt consolidation

Compatible blend: Blend that can be mechanically processed without exhibiting phase separation

Core load: Mass of explosive powders per linear meter of shock tube

Desensitizing agent: Substance capable of reducing the sensitivity of an explosive

Detonating cap: Device receiving the shock wave which is transmitted by the shock tube

Elongation at break: Maximum extension a shock tube can undergo when it is gradually stretched

Ionomer: Polymer having a hydrocarbon backbone and bearing pendant acid groups which are first ionized, then partially (or completely) neutralized by either a metal ion or a quaternary ammonium ion to form salts

Linear thermal shrinkage : Extent to which the shock tube shrinks when subjected to high temperature for a defined period of time

Miscible blend: Polymeric blend consisting of components homogeneously mixed at a molecular level in such a way that there is only one phase present

Misfire : Failure to transmit the initiating signal

Shock tube:	Hollow plastic tubing having an inner surface upon which explosive powders are dispersed as adherent particles at a core load sufficiently low to avoid rupture of the tubing in use
Shock wave:	Initiating signal in the form of high-pressure gaseous phase. It is produced by the combustion of explosive powders present in the shock tube
Sleep time:	The maximum time a shock tube can spend in fuel oil and still fire
Structural integrity:	Extent to which the components of a multi-layered shock tube are bonded
Surlyn:	Trade name of ionomers manufactured by DuPont Industrial Polymer
Velocity of detonation:	The rate at which the shock wave travels inside the shock tube
Zytel:	Trade name of polymeric material manufactured by DuPont Industrial Polymer and consisting of blend of polyethylene and polyamide

CONTENTS

LIST OF FIGURES

LIST OF TABLES

ABBREVIATIONS

Al:	Aluminium
B:	Boron
$BaSO_4$:	Barium Sulphate
$KClO_4$:	Potassium perchlorate
EAA:	Ethylene acrylic acid copolymer
EMA:	Ethylene methacrylic acid copolymer
EVA:	Ethylene vinyl acetate
HDPE:	High density polyethylene
HMX:	High melting explosive; Cyclotetramethylenetetranitramine
LDPE:	Low density polyethylene
LLDPE:	Linear low density polyethylene
Pb_3O_4:	Lead oxide
PETN:	Pentaerythritol-tetranitrate
PVC:	Polyvinyl chloride
RDX:	Cyclotrimethylenetrinitramine
Si:	Silicone
TiH_2:	Titanium hydride
TNT:	Trinitrotoluene
UHDPE:	Ultra high density polyethylene
VOD:	Velocity of detonation
W:	Tungsten
Zr:	Zirconium

Chapter 1 : Introduction

1.1 Background

One of the most significant advances in the 1960's for mining, construction, and quarrying operations was the industrial development of shock tube initiators. A shock tube initiator is a signal transmitting fuse made of a small-diameter hollow plastic tubing, which is loaded with dusts of explosive powders onto its inner surface. It is generally used as initiating device for blasting (Brent & Harding, 1993). Shock tubes operate by conveying an initiating signal in the form of shock wave (or impact wave) to a detonating cap. The shock wave is driven by the continuous combustion of explosive powders present inside the shock tube (Persson, 1968). Figure 1.1 shows a schematic illustration of shock wave displacement in an initiated shock tube.

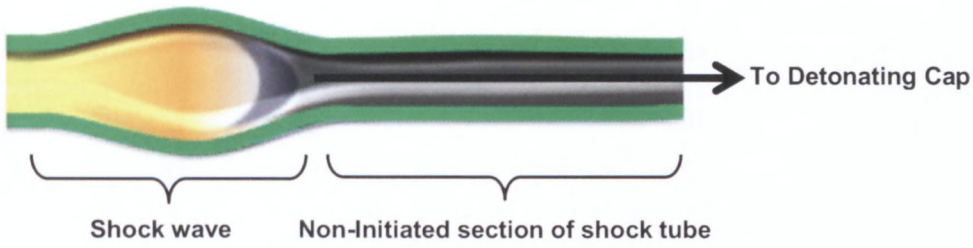

Figure 1.1: Schematic illustration of shock wave displacement in an initiated shock tube

Per-Anders Persson of Nitro Nobel AB originally invented the concept of shock tube initiators in 1968. Ever since, few researchers reported the development of different shock tube designs consisting of various polymeric layers. These included the following:

- **Single-layered shock tubes:** by Stewart (1992), Brent & Harding (1993), and Stewart et al. (2002)
- **Double-layered shock tubes:** by Kristensen et al. (1982), Simon & Welburn (1985), and Thureson & Gladden (1986)
- **Triple-layered shock tube:** by Gladden et al. (1997)

Despite reporting the development of different shock tube designs, none of the researchers presented experimental data showing explicitly how the numbers of polymeric layers of a shock tube could impact the tubes' properties and performance. Furthermore, because the science behind shock tubes' material design is not comprehensively detailed in the published literature, it is very difficult to accurately predict the response of polymeric materials on the properties and performance of shock tubes.

Since the 1960's, shock tube initiators have been widely adopted by the blasting industry and today are considered to be crucial parts of initiating systems. High performance shock tubes currently manufactured in the industry consist generally of three polymeric layers: an inner layer made of ethylene based ionomer, an outer layer made of high density polyethylene, and a relatively thin adhesive layer made of acrylic based copolymer. Figure 1.2 highlights the configuration of polymeric layers in a commercial high performance three-layered shock tube.

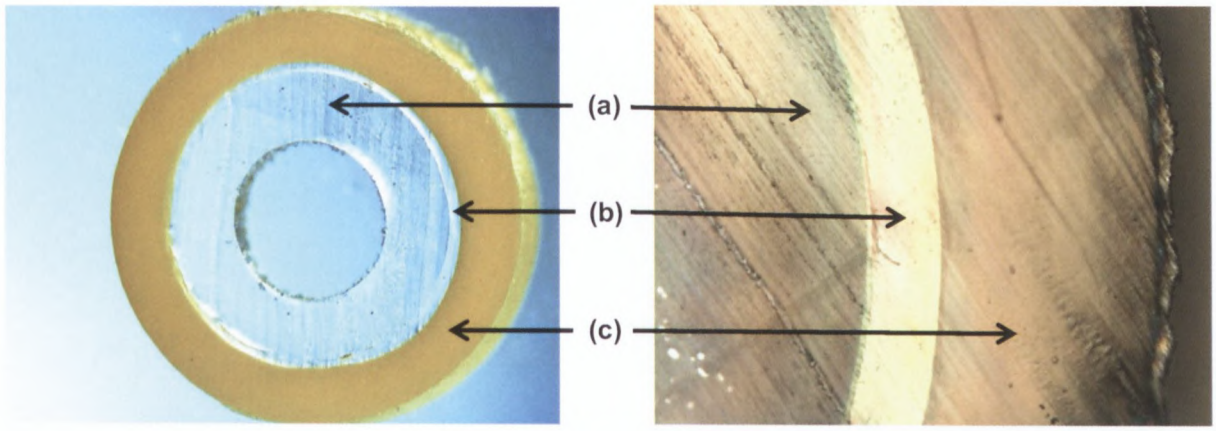

Figure 1.2: Cross sectional view of a high performance three-layered shock tube: (a) inner layer; (b) adhesive layer; (c) outer layer

Due to the presence of three layers in their structure, high performance three-layered shock tubes are often found to have a complex and costly manufacturing sequence. Hence, the elimination of a polymeric layer from the structure of these tubes is seen as a means to simultaneously reduce the shock tube manufacturing cost and simplify the manufacturing sequence. Unfortunately, early research work conducted on shock tube design does not provide experimental data enabling the prediction of how

eliminating a polymeric layer from the structure of a multi-layered shock tube could impact the properties and performance of the tube.

The aim of this study was, therefore, to investigate the influence of the numbers of polymeric layers on shock tubes' properties and performance. The study was conducted by eliminating the adhesive layer from the structure of a standard three-layered shock tube and adding adhesion promoters to the polyethylene of the outer layer.

1.2 Problem statement

The removal of a polymeric layer from the structure of a high performance three-layered shock tube could simplify its manufacturing sequence and reduce the manufacturing cost. However, the literature lacks experimental data enabling one to predict how structure adjustment and material modification could affect the properties and performance of a multi-layered shock tube.

1.3 Objectives

The objectives of this work were set out as follows:

- Compare the properties of various recipes of two-layered shock tubes against a standard three-layered shock tube, then deduce the influence of the numbers of polymeric layers on the properties and performance of multi-layered shock tubes.

- Determine the effects of varying the outer layer composition of two-layered shock tubes on the tubes' properties and performance.

- Review the properties of the experimental two-layered shock tubes, and then recommend a new material design for the manufacture of high performance two-layered shock tubes.

1.4 Research design and methodology

In order to meet the objectives, the following methodology was used:

- A three-layered shock tube made of high density polyethylene in the outer layer, acrylic based copolymer in the adhesive layer, and ethylene based ionomer in the

inner layer was extruded. The extrusion conditions were similar to the standard commercial three-layered shock tubes.

- A process of making two-layered shock tubes with no adhesive layer, involving blends of polyethylene with an adhesion promoter in the outer layer, was developed using a commercial extrusion line. The inner layer material was identical to the one used in the inner layer of the three-layered shock tube. The process conditions were modified to meet the extrusion needs of the blends used to construct the two-layered shock tubes, but they were not too dissimilar to the process of commercial three-layered shock tubes.

- The properties of the experimental shock tubes were determined using a series of tests which included: breaking strength, elongation at break, oil ingression, linear thermal shrinkage, velocity of detonation, and burst strength. A peel-off test especially designed and developed for the purpose of this work was used to measure the adhesion strength between the inner and outer layers of these experimental shock tubes.

- The properties of two-layered shock tubes were compared against the standard three-layered shock tube extruded and the influence of the number of polymeric layers on shock tubes' properties and performance was deduced.

- The properties of experimental two-layered shock tubes were analysed, and the effect of varying the outer layer compositions of two-layered shock tubes on the tubes' properties and performance was determined.

- Based on the results obtained, a new material design for the manufacture of high performance two-layered shock tubes was proposed.

1.5 Scope

This work involved an investigation into polymeric materials for the design of multi-layered shock tubes. The inner layer material (ethylene based ionomer) was not modified. The materials investigated in the outer layer were restricted to polyethylene blends. The process conditions were only changed as required, but no attempt was made towards optimization.

1.6 Importance and benefits

This experimental investigation was expected to enrich the literature with data that could be used as reference point for future research work on shock tube design. The work was also expected to be value-adding to the explosive and polymer industries, with regards to the optimum design of high performance two-layered shock tubes for commercial implementation.

Chapter 2 : Review of Literature

2.1 Introduction

The scientific understanding of materials design for shock tubes is still at an early stage. Very few published articles on the subject are available. This chapter presents a summary of previous research works conducted on shock tubes' design. A review on shock tubes' operation mechanisms and materials is also presented. The average properties of current commercial high performance shock tubes are provided as well. Furthermore, since this investigation involves materials design, a theoretical review on polymer blends, adhesion promoters, and polymer adhesion is presented.

2.2 Definition

A shock tube initiator can be defined as a hollow plastic tubing having an inner surface upon which explosive powders are dispersed as adherent particles at a core load sufficiently low to avoid rupture of the tubing in use (Brent & Harding, 1993). Shock tubes were used extensively for many years as a means for studying the combustion of gases and gas/solid dispersions in both deflagrations and detonation mode before being adopted as initiating device for blasting systems (Gaydon & Hurle, 1963). The adoption of the shock tube as an initiating device for blasting systems has demonstrated that the gas/solid combustion could be contained and propagated in a small tube of plastic construction (Gaydon & Hurle, 1963).

2.3 Operating mechanism of shock tubes

Shock tubes operate by transmitting a pressurised shock wave (or impact wave) along with hot particles and gases to a detonating cap (Persson, 1968). The shock wave is generated by the ignition of explosive powders present onto the inner wall of the tubing. The purpose of explosive powders dispersed inside the tubing is to sustain the shock wave while adding enough energy, as to compensate for the losses caused by the deformation of the tube wall and friction of the gas along the wall (Persson, 1968). The shock wave propagates in the longitudinal direction of the tube at a very high temperature (≈ 2000 K). In order to ensure a steady dissemination of the shock wave, the distribution of explosive powders inside the shock tube must not be discontinued (Persson, 1968).

2.4 Research trend in shock tubes

Before the invention of shock tubes, three methods were largely used in blasting systems to ignite the detonating cap: electric ignition, powder fuse ignition, and detonating fuse ignition (Persson, 1968).

- **Electric ignition**

  Electric ignition was carried out by means of electric current. This method involved the risk of being disturbed by electromagnetic fields and other factors such as lightning, earth currents, electrical high voltage conductors, or broadcasting stations. Electric ignition was therefore unreliable (Persson, 1968).

- **Powder fuse ignition**

  This method involved the ignition of the detonating cap via combustion of black powder located in a plastic fuse. The combustion reaction was propagated along the fuse at an unsteady velocity varying between 0.01 and 200 m/s. The unavoidable variation in the velocity of detonation made this method difficult for applications with very short intervals (Persson, 1968).

- **Detonating fuse ignition**

  This method was performed using a small-diameter tubing containing about 10 grams of explosive powders per linear meter of tubing. The tube was initiated at one end, and the reaction could propagate with a velocity of about 6000 m/s. The high level of explosive powders in these tubes was found to produce a strong shock wave which caused damages to objects positioned nearby during the initiation process. This ignition method was very hazardous and couldn't be used in applications were time delay was required (Persson, 1968).

2.4.1 Original shock tube design

In order to solve the problems encountered with the methods of electric ignition, powder fuse ignition, and detonating fuse ignition, Persson (1968) invented the shock tube. Persson's (1968) shock tube consisted of a single polymeric layer internally coated with light deposits of explosive powders. The explosive powders used were chosen from the following substances: pentaerythritol-tetranitrate (PETN), cyclotrimethylenetrinitramine (RDX), cyclotetramethylenetetranitramine (HMX), trinitrotoluene (TNT), tetryl, dinitroethylurea, or a mixture of two or more of the aforementioned substances (Persson, 1968). Because these substances were very

sensitive and were able to release large amount of energy when initiated, Persson (1968) recommended a desensitizing agent, such as paraffin or wax, be added to the explosive powders. Persson (1968) established that the primary condition for shock tube operation was the initiation of a chemical reaction in the explosive powders dispersed along the interior wall of the tube.

One of the most attractive aspects of Persson's (1968) shock tube was the small quantity of explosive powders used per linear meter of shock tube, also known as the core load. In fact, the core load was so small that the shock wave was able to propagate along the tube without producing any damages in the vicinity of the tube. The lower limit of the core load was determined by the losses encountered within the tube during the propagation of the shock wave. The upper limit of the core load was defined by the radial strength of the material present in the tubing. Persson (1968) recommended the core load to be lower than 0.1 grams per linear meter of tubing for a tube with a corresponding inside diameter varying between 1 and 4 mm. Persson (1968) also reported that the polymeric material to be used in the tubing should have fair mechanical properties and should allow the shock wave to only propagate in the longitudinal direction of the tube at a velocity of about 1500 m/s. In order to illustrate his invention in a more practical way, Persson (1968) presented a few material designs for his shock tube. These included the following:

- **Material design 1**

  A polymeric tube made of soft polyvinyl chloride, and having a length of 3 m, an outer diameter of 5 mm, and an inner diameter of 3 mm was coated with a thin layer of petroleum jelly. PETN powders were then dispersed onto the inner wall of the tube in such a way that, the layer of powders adhered to the layer of petroleum jelly. The layer of powder corresponded to a quantity of 0.3 grams per linear meter of tubing. After ignition, the shock tube was successfully detonated but was partially ruptured along its length.

- **Material design 2**

  Three polymeric hoses made of soft polyvinyl chloride, measuring 0.8, 3, and 10m long respectively, with outer diameters of 5 mm, and inner diameters of 3 mm which were loaded with PETN powders at a core load of 0.05 grams per linear meter of tubing. Unlike the previous material design, no petroleum jelly was used. After ignition, the shock tubes were successfully detonated and no physical damages were

observed in the tube. The velocities of detonations for each tube were measured by means of an electronic counter and were found to be about 2100 m/s.

- **Material design 3**

  A tube made of paper reinforced Bakeline having a length of 1 m, an outer diameter of 4 mm, and an inner diameter of 3 mm was constructed. Explosive powders were dispersed onto the inner wall of the tube at a core load of 0.3 grams per linear meter of tubing. After ignition, the shock tube was successfully detonated.

- **Material design 4**

  An elastic hose made of soft polyvinyl chloride, and having a length of 10 m with an outer diameter of 5 mm, and an inner diameter of 3 mm was loaded with PETN powder at a core load of 0.05 grams per linear meter of tubing. The tube was equipped with a delay action element having a pyrotechnic burning for a delay of 200 milliseconds. After ignition, the tube was successfully detonated and the actual delay time in the delay action element was calculated and found to be 268 milliseconds.

2.4.2 Two-layered shock tubes

2.4.2.1 Kristensen et al. (1982) shock tube design

Almost one decade after Person (1968)'s invention, Kristensen et al. (1982) reported the development of a sandwich type of double-layered shock tube, comprising two adjacent polymeric layers. The explosive powders dispersed along the tube's inner wall consisted of a mixture of cyclotetramethylene tetranitramine and aluminium. The mixture's ratio was about 91% cyclotetramethylene tetranitramine and 9% aluminium. The Kristensen et al. (1982) shock tube had an outer diameter of 3 mm and an inner diameter of 1.3 mm. The powder density on the inner wall was in the order of 2.7 grams per square meter of inner surface. The powder density used was reported to ensure a steady propagation of the shock wave. The inner layer material of Kristensen et al. (1982) shock tube was selected from polymer suitable for adhesive film. The polymer used in the inner layer was expected to provide the inner wall with good adhesive ability with respect to the explosive powders. Kristensen et al. (1982) expressly recommended the inner layer's polymer to have an attractive force around 5.5 g/m^2 (with respect to explosive powders). The outer layer material was chosen amongst polyamide, polyethylene, and polymers with similar mechanical properties. The role of the outer layer was to enhance the tube's resistance to external damages.

Figure 2.1 highlights the configuration of polymeric layers in Kristensen et al. (1982) shock tube design.

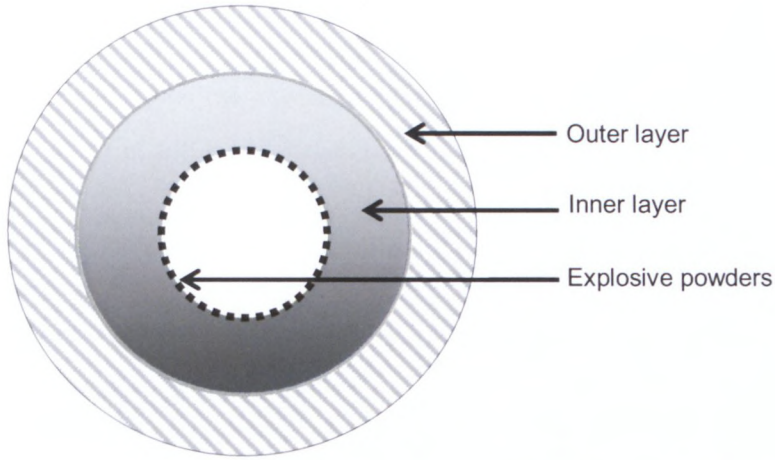

Figure 2.1: Schematic representation of the layers' configuration in Kristensen et al. (1982) shock tube design

Experiments conducted by Kristensen et al. (1982) with various types of ionomers as inner layer materials (Surlyn 1554, Surlyn 1706, Surlyn 1707, and Surlyn 1855) have shown that, Surlyn 1855 is the material providing the most effective adhesion strength.

2.4.2.2 Simon & Welburn (1985) shock tube design

Because shock tubes were made of polymeric materials, they were often found to be susceptible to elongation and possible breakage when handled in warm environments (Simon & Welburn, 1985). Elongation was found to have the particularly negative effect of thinning out the shock tube and dislodging the explosive powders present on the inner wall, which in turn caused the shock tube to malfunction during the initiation. In order to solve the problems of elongation and breakage in warm environments, Simon & Welburn (1985) proposed a two-layered shock tube design with improved resistance to stretching and breaking especially in hot mediums. Simon & Welburn's (1985) shock tube consisted of two polymeric layers similar the shock tube proposed earlier by Kristensen & Gladden (1982). Textile filaments were, however, intercalated at the layers' interface. Figure 2.3 shows a structural representation of Simon & Welburn (1985) shock tube design (Simon & Welburn, 1985).

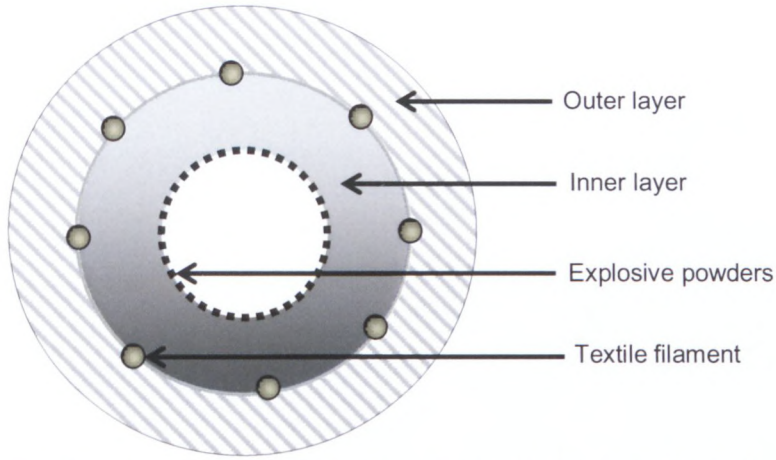

Figure 2.2: Schematics representation of the layers' configuration in Simon & Welburn's (1985) shock tube design

The inner layer material of Simon & Welburn's (1985) shock tube was chosen from polymers with good adhesion properties with regards to the explosive powders. Ethylene based ionomers known as Surlyn were found to be exceptionally suitable materials for the inner layer. The outer layer was chosen amongst polyethylene resins with a density of about 0.93 g/cm^3. Polypropylene, polyvinyl chloride, polyamide, and polyurethane were also reported to be suitable polymers for the outer layer. The textile filaments were selected from cords showing no elongation under longitudinal stress (even at temperature of the order 65°C). Low elongation filaments made from viscose rayon, polyesters, polypropylene, and polytetrafluororthylene were also reported to be very useful. The number of textile filaments was a function of the filaments fineness and was typically varying from 5 to 10 (Simon & Welburn, 1985).

Simon & Welburn's (1985) shock tube was manufactured by first extruding the inner tube, then applying the filaments linearly along the tube. The inner tube with the filaments was then passed through a second extruder where it was coated over with the outer layer material. Tensile tests performed by Simon & Welburn (1985) revealed that, the presence of the textile filament could increase the breaking strength by 68 %.

2.4.2.3 Thureson & Gladden (1986) shock tube design

Only one year after the publication of Simon & Welburn's (1985) shock tube design, Thureson & Gladden (1986) reported the invention of a two-layered shock tube similar to that disclosed by Kristensen et al. (1982), but with enhanced mechanical

properties. The inner layer of Thureson & Gladden's (1986) shock tube was made of an ethylene based ionomer known as Surlyn 8940 and was manufactured by DuPont Industrial Polymers. Ethylene/acrylic acid copolymer (EAA), Ethylene vinyl acetate (EVA), and polymers having comparable adhesive properties were also reported to be useful as inner layer materials. The outer layer consisted of polyolefin such as linear low density polyethylene (LLDPE), low density polyethylene (LDPE), blends of LLDPE with ionomer, polypropylene, polyamide, and blends of polyamide with co-extrudible adhesives. The explosive powders used included mixtures of materials such as PETN, RDX, HMX, and 2, 6-bis (picrylamino)-3, 5- dinitropyridine.

Thureson & Gladden's (1986) shock tube design was manufactured using a dual operation process, wherein the inner tube was initially extruded, then stretched considerably before being sent to a secondary extruder where it was coated with the outer layer material. Thureson & Gladden (1986) reported that, the stretching step could be made more beneficial by heating the inner tube above its softening point. However, the tube temperature should be maintained below the flush point of the explosive powders. Figure 2.3 shows a schematic illustration of the manufacturing process used by Thureson & Gladden (1986).

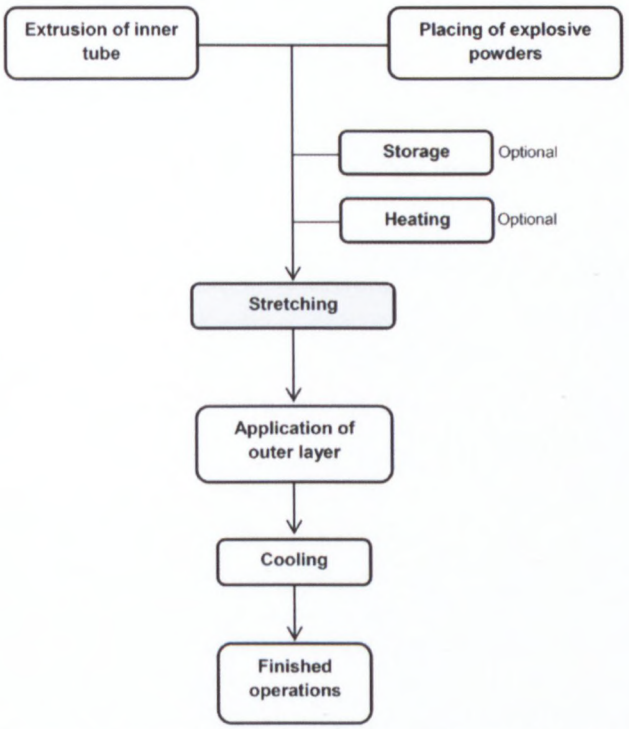

Figure 2.3: Schematics illustration of Thureson & Gladden (1986) shock tube manufacturing sequence, (Thureson & Gladden, 1986)

Thureson & Gladden (1986) reported that, such a shock tube would offer various advantages such as low manufacturing cost, improved handling characteristics, and improved quality control during manufacturing while retaining the essential characteristics of a shock tube.

2.4.2.4 Gladden et al. (1989) shock tube design

Then, Gladden et al. (1989) disclosed the development of a two-layered shock tube comprising the ethylene based ionomer Surlyn 8940 in the inner layer, and polyethylene in the outer layer. The tube had an outer diameter of 3 mm, and an inner diameter of 1.27 mm. The explosive powders present on the inner wall were made of mixture of substances such as silicon (Si) / red lead (Pb_3O_4), molybdenum (MO) / Potassium perchlorate ($TiH_2/KClO_4$), Boron (B) / red lead (Pb_3O_4), Zirconium (Zr) / Barium sulphate ($BaSO_4$) and Tungsten (W) / Potassium perchlorate ($KClO_4$).

In order to control the velocity of signal transmission, also known as the velocity of detonation (VOD), discrete restrictions, which reduced the inner tube interior axial cross sectional area, were formed along the tube. The presence of discrete restrictions in the tube provided means to mechanically attenuate the propagation of chemical reactions inside the shock tube. Experiments performed by Gladden et al. (1989) demonstrated that, the restrictions could effectively reduce the VOD.

2.4.3 Three-layered shock tubes

2.4.3.1 Gladden et. al (1997) shock tube design

Several years later, Gladden et al. (1997) also reported the invention of polymeric shock tubes consisting of three layers; an outer layer, an inner layer, and an intermediate layer. The Gladden et al. (1997) shock tube had an outer diameter varying from 0.397 to 2.380 mm, hence was much smaller than all the previous shock tube designs. The tube's inner diameter varied from 0.198 to 1.321 mm. The explosive powders used in the tube consisted of mixture of aluminium and one of the following substances: HMX, PETN, RDX, 2,6-bis (picrylamino)-3,5-dinitropyridine and ammonium perchlorate. The powder surface density was comprised between 0.45 and 7 grams of explosive powder per square meter of inner surface. The inner layer material was chosen from polymers with good adhesion characteristics with respect to the explosive powders. Ethylene based ionomers known as Surlyn were once again found to be suitable materials for the inner layer. The outer layer material was

chosen amongst polyamides such as nylon 6 and polyethylene resins, both low and medium density. The intermediate layer's material was selected from polymers capable of adhering to both the outer and inner layer material. The intermediate layer was much thinner than both the inner and outer layer.

2.4.4 Single-layered shock tubes

2.4.4.1 Stewart (1992) shock tube design

In the early 90's, Stewart (1992) reported the invention of a single-layered shock tube. The tube consisted of a main polymeric layer, coated with an outer skin. The explosive powders consisted of blends of HMX/Aluminum. The main polymeric layer was made from polymer with fair adhesive properties and acceptable process-ability. The outer skin consisted of polymers such as polyvinyl alcohol and polyvinyl acetate. Stewart (1992) reported that, shock tubes having such skins would last 2.5 times longer in fuel oil than shock tubes without the skin. Figure 2.4 shows a schematic illustration of Stewart (1992) shock tube design.

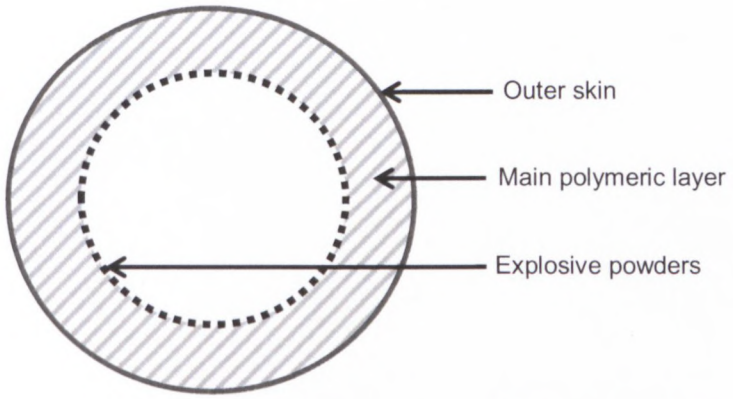

Figure 2.4: Schematic representation of the layer's configuration in Stewart's (1992) shock tube design

2.4.4.2 Stewart (2002) shock tube design

A decade later, Stewart (2002) disclosed the invention of another single layered shock tube made of one polymeric layer. The polymeric material that was used, consisted of a blend of draw orientable polymer resins and a minor amount of a surface modifier capable of enhancing the adhesive properties of the polymeric blend. Suitable materials for Stewart's (2002) tube was comprised of blends varying from 60 to 97% (by weight) of a polyolefin resin such as linear low density polyethylene,

optionally 5 to 45% of a second polymer, which is polyolefin miscible and can improve the melt strength of the blend, and 2 to 25% of a third polyolefin miscible or compatible polymer which is a surface modifying agent such as an ethylene/acrylic or methylacrylic acid copolymer that may be wholly or partially neutralised (e.g. The ethylene based ionomer Surlyn 1855) (Stewart 2002).

Stewart (2002) also reported that, when dealing with orientable polymers, most favourable results are achieved by orientating the polymer linearly. Linear orientation can be carried out by cold drawing the shock tube after consolidation of the melt. The term "cold drawing" refers to the irreversible extension of the tube after the polymer has cooled sufficiently to take a permanent structure (Stewart, 2002). Cold drawing can be carried out at any stage of the extrusion process. It is achieved by applying stress to orientate the crystallite in the direction of the tube length. The cold drawing temperature should not be higher than the glass transition temperature of the polymeric tube. Additionally, an intermediate or final relaxation stage may also be performed to "stress relieve" the cold drawn tube, therefore improving the dimensional stability of the tube (Stewart, 2002). In order to illustrate his invention, Stewart (2002) developed and tested different single-layered shock tubes made from blends of various polymeric materials. Table 2.A summarises the composition of some of the shock tubes tested by Stewart (2002).

Table 2.A: Composition of single-layered shock tubes tested by Stewart (2002)

Components	Tube 1	Tube 2	Tube 3
LLDPE	80 %	80 %	80 %
EVA	10 %	10 %	10 %
Ethylene based ionomer	10 %	-	-
EAA	-	10 %	10 %

The role of LLDPE was to provide the tube with the necessary mechanical strength, while the presence of EVA was intended to strengthen the melt and allow for a more uniform product. The addition of ethylene based ionomer or ethylene acrylic acid copolymer (EAA) was used to provide the tube with excellent powder adhesion. The characteristics and properties of the single-layered shock tubes tested by Stewart (2002) are summarised in Table 2B.

Table 2.B: Characteristics and properties of single-layered shock tubes tested by Stewart (2002)

Characteristics and Properties	Tube 1	Tube 2	Tube 3
Outer diameter (mm)	3.1	3	3.1
Inner diameter (mm)	1.4	1.3	1.4
Core load (mg/m)	18.9	17.9	18.6
Shrinkage (after 1 hr @ 80 °C)	2.2	2.6	2.3
Tensile strength (N/mm^2)	43	48	48
Elongation (%)	690	520	520

2.5 Commercial shock tubes

***N.B:** Information provided in this section were obtained from private communications and the trade literature.

Since the 1960's, shock tubes have been produced and commercialized by several chemical and explosive manufacturers. Commercial shock tubes are available in single-layered, double-layered and triple-layered tubing. These shock tubes have versatile sets of characteristics that can include the following:

- Good resistance to bursting
- Low resistance to shock propagation
- Good resistance to abrasion
- Good handling and flexibility characteristics (memory)
- Good tensile properties for durability and handling performance
- Good radial strength to contain the shock reaction
- Good resistance to oil and fuel diffusion
- High structural integrity and function (Good bonding strength between layers)
- Ability to withstand and function between -50°C and 80°C
- Impermeable to water
- Moderate but uniform thermal shrinkage

Shock tubes capable of meeting all of the above characteristics are often referred to as "high performance shock tubes".

2.5.1 Structure of commercial high performance shock tubes

Commercial high performance shock tubes currently manufactured in the industry are generally made of three adjacent polymeric layers. Their inner surface is coated with explosive powders, which consists of blends of HMX and Aluminium. These shock tubes are sold worldwide under various trade names. Their outer diameter lies generally between 2.85 and 3.15 mm, while their inner diameter can vary from 1.10 to 1.30 mm. The thicknesses of their inner and outer layers are between 0.3 and 0.5 mm, while the thickness of their adhesive layer often ranges between 0.2 and 0.08 mm. The core load of these shock tubes is typically between 11 and 17 mg of explosive powders per linear meter of tubing.

2.5.2 Industrial methods of testing shock tubes

Tests used in the industry to evaluate the properties and performance of shock tubes vary from one manufacturer to another and generally include the following trials: breaking strength and elongation at break, linear thermal shrinkage, oil ingression, burst strength, and velocity of detonation.

2.5.2.1 Breaking strength and elongation at break

When used in the mines, shock tubes are often subjected to pulling and stretching phenomena. The breaking strength and elongation at break tests are therefore performed to estimate the extent to which the shock tube could be stretched without being torn apart. These tests are carried out in the industry on a tensiometer. The testing procedure is similar to that used for the tensile strength of common polymers, and it involves the longitudinal stretching of a shock tube specimen until it ruptures. The breaking strength and elongation at break tests are carried out to evaluate the extent to which the shock tube could be longitudinally stretched without being torn apart. The breaking strength is expressed in Newton (N), while the elongation at break is expressed in percentage (%).

2.5.2.2 Linear thermal shrinkage

During the extrusion process, stresses are imposed on the polymeric materials at a high temperature, and some residual stresses remains when the polymer is cooled to room temperature (Buchanan, 1992). Subsequently, if the polymer is heated, individual molecules, or group of molecules, tend to retract from an ordered conformation to a more disordered and entangled one. Depending on the molecular

interactions, chain entanglements and other steric hindrances, the molecular chain segments would contract and shrinkage can be observed (Buchanan, 1992). Because shock tubes are made of polymeric materials, they are susceptible to thermal shrinkage. The linear thermal shrinkage test is therefore performed to estimate the extent to which the shock tube would shrink when exposed to high temperatures. The testing method involves the heating of a given shock tube specimen for a defined period of time. The heating temperature depends on the nature of polymers used in the shock tube and is generally around 80°C. The percentage by which the tube shrinks after being heated is called linear thermal shrinkage.

2.5.2.3 Oil ingression

Shock tubes are often operated in combination with explosive emulsions. The hydrocarbon fuel phase of such emulsions is generally a petroleum fraction such as diesel or paraffin (Stewart, 1992). The petroleum fraction, also known as fuel oil, is known to diffuse through the shock tube at a slow rate when in prolonged contact therewith (Stewart, 1992). The ingression rate depends on the nature of the fuel oil, the chemical and physical structure of the polymer present in the shock tube, the contact time, and the temperature of the fuel oil (Stewart, 1992). The diffusion of fuel oil through shock tubes has the negative effect of reducing the lifespan of shock tubes. The maximum time a shock tube can remain in contact with fuel oil and still detonates is referred to as "sleep time" (Stewart, 1992). An oil ingression test is therefore performed in the industry to estimate the sleep time of a shock tube in the fuel oil. It is carried out by submerging specimens of shock tubes into a warm bath of fuel oil. The samples are taken out of the oil at given periods of time, and then initiated recurrently until at least one misfire is obtained. The maximum time after which all the specimens are initiated without exhibiting a single misfire is recorded as the sleep time.

2.5.2.4 Bursts strength

Once a shock tube has been initiated, the shock wave produced causes a sudden expansion of the polymeric tubing in use (refer to Figure 1.1). The expansion often results in physical damages of tubing, also known as tube bursts. During the formation of a burst, the gases forming the shock wave are partially released into the atmosphere resulting in reduction of signal strength. The bursts strength test is

therefore carried out to evaluate the extent to which the shock wave can be contained within the polymeric tubing without producing any bursts. The test is carried out by heating a specimen of shock tube for a given period of time. The specimen is then initiated and observed. The number of bursts per linear meter of shock tube is recorded and used to estimate the tube's radial strength. Shock tubes with poor radial strength would exhibit more bursts than shock tubes with good radial strength.

2.5.2.5 Velocity of detonation

The velocity at which the shock wave travels inside a shock tube is referred to as velocity of detonation. It is measured in the industry with a special apparatus capable of monitoring the initiating signal (the shock wave) and computing the speed at which it is travelling. The velocity of detonation (VOD) is expressed in meter per second, and can have a critical importance when the blasting requires time delay.

2.5.3 Average properties of commercial high performance shock tubes

Commercial high performance shock tubes are made of three adjacent polymeric layers and can exhibit versatile sets of properties that might vary from one manufacturer to another. The average properties of commercial high performance shock tubes currently manufactured the industry are summarised in the table 2.C. These properties were obtained from different manufacturers.

Table 2.C: Summary of average properties of commercial high performance three-layered shock tubes

Properties	Approximate range
Breaking strength (rate of extension: 70 mm/min)	160 N – 200 N
Elongation at break (rate of extension: 70 mm/min)	200 – 300 %
Linear thermal shrinkage (After 1hr in an oven @ 80°C)	6 – 10 %
Oil penetration (50°C in Paraffin)	45 – 50 hrs
Burst strength (After 20min in an oven @ 80°C)	Normally 2 to 5 bursts per 5 meters of tubing
Velocity of detonation (over a length of 60 cm)	1800 - 2200 m/s

***Source:** Commercial literature and private communications

2.5.4 Materials used in commercial high performance shock tubes

2.5.4.1 Outer layer of high performance shock tubes

The deployment of shock tubes in mines is generally accompanied by pulling, twisting, bending and rubbing phenomena. Therefore, the polymeric materials used in the outer layer should give the overall structure good handling characteristics. Polyethylene in low, medium, and high densities are the materials generally used in the outer layer of commercial high performance shock tubes. The structure and properties of polyethylene are reviewed in the next section.

2.5.4.2 Structure and properties of polyethylene

a) Structure

The morphology of polyethylene depends on the molecular characteristics and preparation conditions. HDPE, for instance, is synthesized at a low temperature and low pressure, thus yielding molecules bearing few branches (see figure 2.5(a)). The small quantity of branches allows the molecules of HDPE to easily pack close together. The molecular packing is achieved in an orderly but incomplete manner, giving the polymer a semi-crystalline structure with a relatively high density and high molecular weight (Peacock, 2000). The high molecular weight of HDPE combined with its low coefficient of friction gives the polymer good resistance to abrasion (Vasile & Pascu, 2005). HDPE is stiffer than lower density polyethylene (Peacock, 2000). Figure 2.5 shows schematic representations of the molecular structure of different types of polyethylene (high density, low density, linear low density, and very low density).

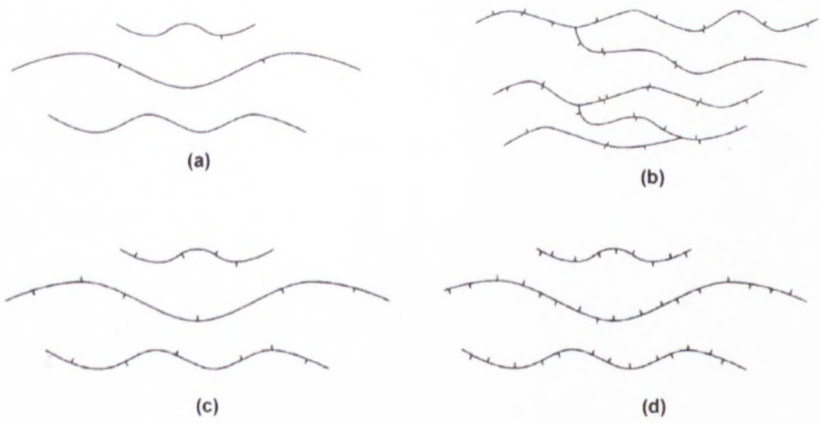

Figure 2.5: Schematic representation of molecular structures of different types of polyethylene: (a) high density; (b) low density; (c) linear low density; (d) very low density, (Peacock, 2000)

b) Properties of polyethylene

The properties of polyethylene in general are flexible and depend on its molecular structure. Polyethylene with fewer numbers of branches, such as HDPE, tend to propagate cracks readily, and would be less tough than the polyethylene with considerable numbers of branches (Peacock, 2000). Linear low density polyethylene would require more energy input for rupture than HDPE (Peacock, 2000).

The wear resistance of polyethylene increases with an increasing molecular weight, and a decreasing level of branching. Thus, polyethylene with a higher density would exhibit higher resistance to abrasion (Peacock, 2000). Polyethylene in its natural state is highly resistant to wear. In fact, no other unmodified polymer exhibits such a high wear resistance (Peacock, 2000). Abrasive wear in polyethylene only occurs when its surface is rubbed by a rougher counter surface. The wear resistance of polyethylene is particularly high for HDPE and ultra-high molecular weight polyethylene (Peacock, 2000).

Polyethylene is also susceptible to thermal expansion. Thermal expansion can be defined as the length increase that some polymers undergo when exposed to high temperatures (Peacock, 2000). Thermal expansion in polyethylene in general is a function of the amount of crystals present in the polymer's structure and their orientation axes with respect to the direction in which the expansion is being measured. Due to a greater degree of freedom of movement, amorphous regions would expand greater than in crystalline regions (Peacock, 2000).

Polyethylene resins are permeable, to some extent, to liquids, gases and vapours. However, these polymers are hardly permeable to solvents whose solubility is similar to theirs (Peacock, 2000). The permeability of polyethylene to polar and organic molecules decreases with an increasing degree of crystallinity (Peacock, 2000); hence polyethylene resins with higher density are less permeable to polar and organic molecules. The degree of permeability of polyethylene by polar and organic molecules in increasing order is as follows: Alcohols, acids, nitro derivatives, aldehydes and ketones, esters, ethers, hydrocarbons and, halogenated hydrocarbons (Peacock, 2000).

2.5.5 Inner layer of high performance shock tubes

The inner layer of commercial high performance shock tubes has two primary functions. First, to hold the explosive powders onto the inner surface, and secondly, to reinforce the shock tube resistance to oil and fuel ingression. Ethylene based ionomers are currently used in the inner layer of commercial high performance shock tubes. The structure and properties of these ionomers are presented in the next section.

2.5.5.1 Structure and properties of ionomers

An ionomer is a polymer having a hydrocarbon backbone and bearing pendant acid groups which are first ionized, then partially (or completely) neutralized by either a metal ion or a quaternary ammonium ion to form salts (Halliday, 1975). Ionomers were developed in 1964 by Du Pont Industrial Polymers and are currently known under the trade name of Surlyn® (Longworth, 1975). Although the percentage of metal ions in ionomers is very small, it is enough to give the ionomer a cross-link structure in the glassy state (Longworth, 1975). The cross-link structure of ionomers can be broken when the polymer is molten, allowing polymer chains to freely slide one on top of the other. Ionomers can, therefore, exhibit both characteristics of thermoplastics and thermosetting polymers (Longworth, 1975). Despite their cross-link structure in the glassy state, ionomers are generally considered to be thermoplastic and have a melting range between 150°C and 250°C (Chanda & Roy, 2006). The presence of ionic aggregates in the structure of ionomers gives them a special set of properties which cannot be obtained with non-ionic polymers (Vanhoorne and Nicolai, 1995). Figure 2.6 shows two representations of ionic aggregates in ionomers.

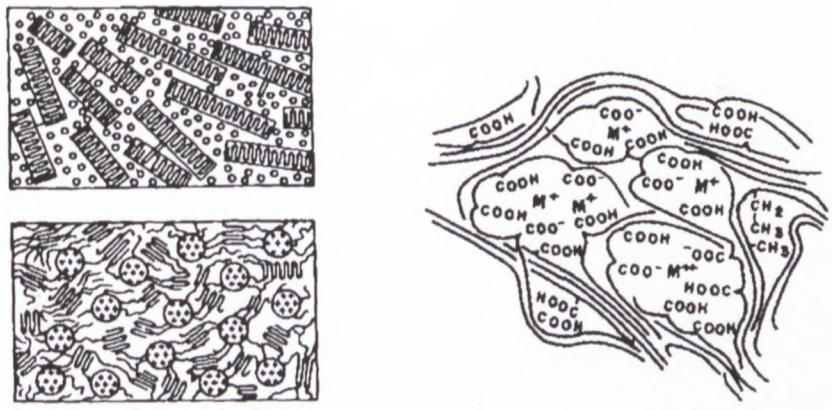

Figure 2.6: Schematic representation of ionic aggregates: (a) Longworth-Vaughan model for acid copolymer and dry ionomer; (b) Bonnotto model, (Longworth, 1975)

Ethylene based ionomers, are generally tougher than their parent hydrocarbon polymer (polyethylene), and have relatively high melt strength (Longworth, 1975). Their high melt strength allows them to be considerably drawn during processing without tearing. Ethylene based ionomers would therefore exhibit good resistance to puncture (Longworth, 1975). Because of their unconventional structure, ethylene based ionomers also have better resistance to solvent ingression than their parent hydrocarbon. In fact, these ionomers are often too ionic to dissolve in non-polar solvents and too organic to dissolve in polar solvents (Nicholson, 2006).

2.5.6 Adhesive layer of high performance shock tubes

The adhesive layer is the component that binds the inner and outer layers together. The presence of the adhesive layer enhances the tube's structural integrity. The adhesive layer of commercial three-layered shock tubes is generally made from an ethylene acrylic copolymer.

2.6 The theory of adhesion

Multi-component shock tubes consist of adjacent polymeric layers adhering one to the other. The extent to which adhesion occurs is a function of the materials present in each layer. This next section reviews the mechanisms of adhesion, methods for evaluating adhesion strength, and factors promoting interfacial adhesion.

2.6.1 Adhesion mechanisms

Adhesion is the result of interatomic and intermolecular interaction at the interface of the two surfaces (Awaja et al., 2009). It is a subject that involves various disciplines such as physics, surface chemistry, rheology, polymer chemistry, and stress analysis (Awaja et al., 2009). Adhesion can be theoretically explained by three main mechanisms: mechanical coupling, molecular bonding and thermodynamic adhesion.

2.6.1.1 Mechanical coupling

Mechanical coupling is also known as interlocking adhesion mechanism. According to this theory, adhesion is the result of surface locking at the interface. Adhesion here is favoured by presence of void and micro-voids at the surface of substrates. (Awaja et al., 2009).

Mechanical coupling has been the subject of much controversy as some researchers believe that the presence of voids on the surface simply increases the surface area of substrates and allows more molecular bonding. Mechanical coupling generally occurs when an adhesive fluid is poured onto a solid substrate (Awaja et al., 2009). Figure 2.4 shows an illustration of mechanical coupling between substrates.

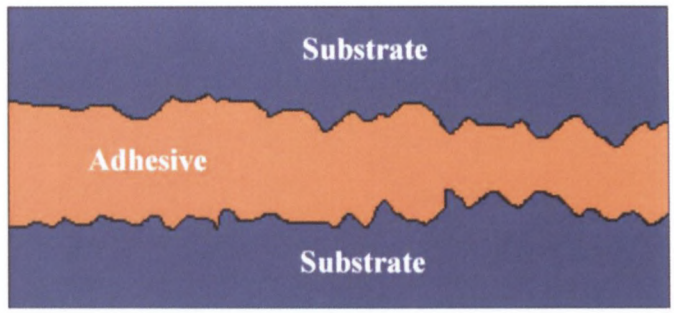

Figure 2.7: Illustration of mechanical coupling between substrates (Awaja et al., 2009)

2.6.1.2 Molecular bonding

Molecular bonding is the more popular of the three adhesion mechanisms. It comprises dipole-dipole interactions, van der Waal forces and chemical interactions (Awaja et al., 2009). According to the molecular bonding theory, adhesion results from interfacial interactions caused by the presence of high energy functional groups located at the surface of two components in intimate contact (Awaja et al., 2009). Figure 2.5 shows a schematic illustration of molecular bonding taking place at the interface of two surfaces in intimate contact.

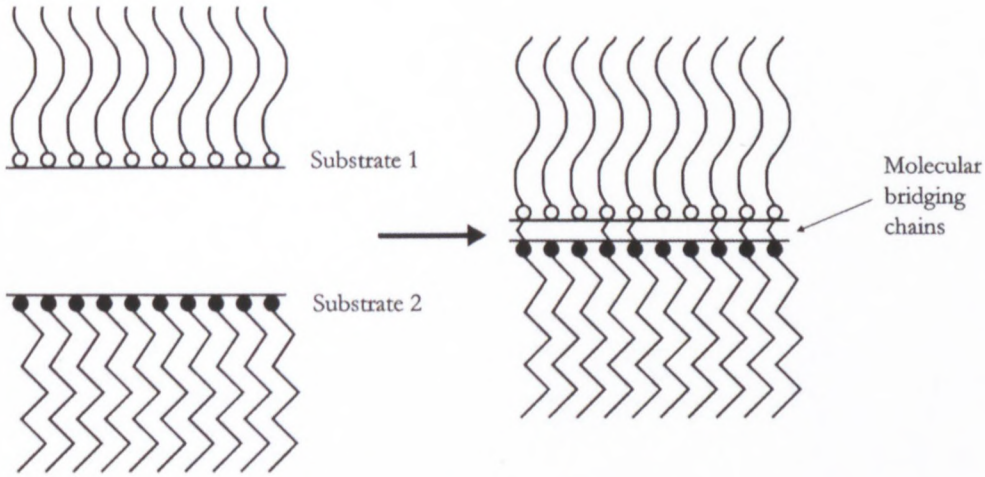

Figure 2.8: Illustration of molecular bonding between substrates (Awaja et al., 2009)

Research conducted by Basin (1984) has shown that, as the numbers of chemical bonds at the interface increases, it passes through a maximum value. Once the maximum value is passed, the concentration of mechanical stresses at the interface cause the adhesion strength to be weakened. Therefore, having excessive chemical bonding at the interface might compromise the adhesion strength.

Voyutskii (1963) reported that for composite interfaces with an adhesive layer, the adhesion strength is a function of the thickness of the adhesive layer and the interfacial adhesion strength increases with a decreasing thickness of adhesive layer as stress dissipates easily through the interface.

Studies performed by Lauren et al. (2004) have shown that, for copolymer systems, adhesion is partially controlled by the architecture of the copolymer and the stress at the interface. Lauren et al. (2004) added that, adhesion can also be controlled by the crystalline structure at the interface, the molecular weight, the molecular architecture, and the annealing condition. The findings from Lauren et al. (2004) were supported by Toro et al. (2005) and Zhang et al. (2006).

2.6.1.3 Thermodynamic mechanism

Adhesion can also be explained by the phenomenon of thermodynamic adsorption. Unlike molecular bonding, the thermodynamic mechanism does not require intermolecular interaction for strong adhesion. Instead, the equilibrium process at the interface promotes adhesion (Awaja et al., 2009). Good adhesion would only occur if the interfacial tension is kept to a minimum (Qin et al., 1999).

2.6.2 Evaluation of adhesion strength

The extent to which adhesion occurs at the interface of two polymer surfaces in contact can be assessed using a peel-off test (Bateup, 1981). The test involves the gradual separation of two surfaces in contact. The peel-off test can be performed on polymers as well as other materials. When dealing with polymeric materials, the test should be performed at a reasonable speed because for all polymers, the adhesion force increases with an increasing speed of separation. The rate of increase is generally a function of the polymeric composition (Bateup, 1978). The increase in adhesion force with increasing rate of separation is due to the augmentation of energy dissipation within the polymer during the peeling process. Stiff and inflexible

polymers generally have lower peel strength than soft and flexible polymers (Bateup, 1978).

2.6.3 Factors Promoting Interfacial Adhesion

The forces involved in the adhesion of substrates are similar to those involved in holding the molecules of a material together (Petrie, 2007). These forces are either chemical or physical in nature. In general, interfacial adhesion can be promoted by many factors which include the following (Petrie, 2007):

2.6.3.1 Good wetting of the substrate

In order for adhesion to occur, the adhesive fluid must be evenly spread over the surface of the solid substrate in a process nown as wetting (Petrie, 2007). Wetting allows molecules of the fluid and substrate to come in contact, hence promoting strong forces of attraction (Petrie, 2007).

The wetting process occurs in two steps; the spreading of adhesive fluid over the solid substrate and the penetration of adhesive fluid into the substrate's micro-pores or micro-voids. The first step is a function of the relative surface energy of the fluid and substrate while the second step depends upon the roughness of the substrate and the viscosity of the fluid. In order for good wetting to occur, the free energy of the solid substrate should be less than that of the fluid (Petrie, 2007). Although proper wetting of substrate is necessary for good adhesion, it is not a significant condition (Rostami & Miles, 1992).

2.6.3.2 Presence of high energy functional groups at the interface

The extent to which two surfaces adhere one to the other could be influenced by the nature of molecules and functional groups present at the interface (Koberstein et al., 2003). The surface properties of components in contact would define the adhesion strength. Achieving the desired surface properties depends on the ability to locate specific functional groups at the surface (Koberstein and O'rourke-muinsener, 2003). The presence of high energy functional groups at the surface would particularly enhance the adhesion strength of polymers (Koberstein and O'rourke-muinsener, 2003).

Studies performed by Elman et al., (1994) on the distribution of polymer terminal groups at the surface and interface have shown that, functional groups having a surface energy higher than that of the polymer backbone tend to remain in the polymer bulk layers instead of being concentrated at the interface where they are most needed for adhesion.

2.7 Modification of adhesive properties of polymers

Polymers such as polyolefin have a generally low surface energy because of their organic nature (Wolfensberger et al., 1995). Hence they are expected to have poor adhesive abilities. The surface properties of these polymers can be modified considerably by incorporating functional groups at the surface. This is achieved via surface treatments such as fluorination (Hennemann et al., 1994) or corona treatment (Wolfensberger et al., 1995). The surface properties of polymers can also be modified by adding polymers with high energy functional groups to the polymeric matrix (Tanabe et al., 1996); this can be achieved via blending. In this case, the functional polymer migrates to the surface of the resulting blend and adjusts the surface energy of the overall system (Tanabe et al., 1996). Falsafi et al. (2000) have demonstrated that the delocalization of high energy functional groups from the bulk to the interface promotes strong adhesion.

2.8 Polymer blends

A polymer blends have previously been reported by Thureson and Gladden (1986) and Stewart et al. (2002) to be useful materials for shock tubes. This section reviews some relevant aspects on the theory behind polymer blend.

Polymer blend can be defined as the physical mixture of different polymers. It is generally carried out in an extruder (Kumar and Gupta, 1998). Polymers are usually blended for various reasons. One reason is to fill the deficiency in performance and price of some existing homopolymers (Rostami & Miles, 1992). Another reason is to obtain a material that has a combination of the properties of both constituents (Bower, 2002). Polymers can also be blended to achieve specific surface properties. One of the most attractive aspects of polymer's surface modification via blending is the phenomenon of preferential segregation of constituents; the constituents of the blend are relatively free to move from the bulk to the surface, or the other way around since

they are not chemically bonded (Tsukruk, 2004). Their movement is driven by the tendency to lower the overall free energy of the system (Tsukruk, 2004).

Polymer blends have now become very common in the industry. This is because it requires a relatively shorter period of time and less effort for preparation compared to polymer synthesis. However, the science behind polymer blending is complex and includes disciplines such as interfacial science, rheology, physic, chemistry, thermodynamics, morphology and polymer processing (Rostami & Miles, 1992). The next section discusses the factors influencing the miscibility and compatibility of polymeric blends.

2.9 Miscible and compatible polymer blends

When two different polymers are blended, the properties of the resulting blend depend on the level of intimate mixing and the chemical reactions between the components of the blend (Bower, 2002). The most intimate form of mixing takes place at a molecular level. Unfortunately, only few polymers can be blended homogeneously at a molecular level in such a way that there is only one phase present (Bower, 2002). Blends capable of doing so are referred to as "miscible blends" (Rostami & Miles, 1992). An immiscible blend can be called compatible if it is mechanically processable, and can overcome phase separation while exhibiting the desired properties (Rostami & Miles, 1992). Blends that are miscible in certain ranges of composition and temperature, but immiscible in others, are also sometimes called compatible blends (Bower, 2002).

Since the entropy of mixing of macromolecules is generally low, polymer blends will hardly be homogeneous (Rostami & Miles, 1992). The necessary condition for two different polymers to be miscible is that the Gibbs free energy of the mixture must be less than the sum of the Gibbs free energy of the separate constituents (Bower, 2002). Currently, there is no general theory that can accurately predict the homogeneity of two different polymers. However, favourable interactions such as hydrogen-bonding and electron donor-electron acceptor molecular formation can promote good compatibility and miscibility (Kumar and Gupta, 2003).

2.10 Polymer processing

Polymer processing can be defined as "the engineering activity concerned with operations carried out on polymeric materials or systems to increase their utility"

(Tadmor and Gogos 2006). Polymer processing involves the conversion of raw polymeric materials into finished products, and might include, not only shaping, but also compounding and chemical reactions, leading to a polymer having a modified structure and morphology (Tadmor and Gogos 2006).

One of the most important steps of polymer processing is the shaping operation. The shaping operation can be seen as the essence of polymer processing, its objective is to give the final polymer a clearly defined form. The shaping operation is preceded by a melting phase, where by the polymer is molten in an extruder (Tadmor and Gogos 2006). Polymers can only be processed between the glass transition and the degradation temperature (Kumar and Gupta, 2003).

Understanding polymer processing requires a good knowledge of the machinery used as well as the polymer being extruded. The behaviours of the extrusion process are generally governed by the physical and thermal properties of the polymer extruded (Kumar et al., 2003).

2.11 Conclusion

This chapter presented a summary of previous research works conducted on shock tube designs. The operating mechanism of shock tubes was described. In addition, the structure of commercial high performance shock tubes was presented. Methods used in the industry to evaluate the properties of shock tubes were also discussed. The average properties of current commercial high performance shock tubes were provided. Since this investigation involved polymeric materials, the chapter also presented a theoretical review on polymer blends and polymer adhesion. The next section will highlight the main research topics that were identified from the literature review.

2.12 Research topics identified

It is apparent from the literature review, that many aspects of shock tube materials design are still unclear and need further investigation; these include the following:

- The influence of the numbers of polymeric layers on shock tubes' properties and performance is not clearly established.

- The properties and performance of the different shock tubes disclosed are not comprehensively compared.
- Polymeric blends have been mentioned as potential materials for shock tubes. However, the influence of compatibility and miscibility of polymeric components on shock tubes properties and performance is non-existent.

In this study, the response of the number of polymeric layers on shock tubes' properties and performance is investigated. The study is carried out by eliminating the intermediate layer from the structure of a standard three-layered shock tube then adding different adhesion promoters to polyethylene of the outer layer. The next chapter will discuss the methodology used for this study in detail.

Chapter 3 : Experimental

3.1 Introduction

The experimental procedure was conducted at the manufacturing plant of AEL Mining Services at Modderfontein. It involved the extrusion and testing of a standard three-layered shock tube similar to the commercially available high performance shock tubes and samples of two-layered shock tubes containing different recipes of polymer blends in the outer layer. This chapter discusses the selection of raw materials, the experimental process of manufacturing shock tubes, and tests used to measure the properties and performance of the shock tubes produced during the experimental work.

3.2 Selection of raw materials for experimental shock tubes

3.2.1 Outer layer of experimental two-layered shock tubes

The materials used in the outer layer of the experimental two-layered shock tubes consisted of blends of a polyethylene resin and an adhesion promoter. Polyethylene represented the major component of the blend and was chosen to provide the outer layer with mechanical strength. The role of the adhesion promoter was to improve the adhesive capability of polyethylene, in order to allow the outer layer to firmly adhere to the inner layer. The next section describes the different types of polyethylene resins and adhesion promoters used.

3.2.1.1 Polyethylene resins

Two types of polyethylene resins were used in the outer layer of the experimental two-layered shock tubes; high density polyethylene (HDPE) and linear low density polyethylene (LLDPE). HDPE was selected for its fair mechanical properties, good resistance to abrasion, and low permeability to polar solvents. LLDPE was chosen for its relatively high tensile strength and low melt viscosity, which improves the processability. HDPE and LLDPE were respectively blended with the adhesion promoters in various ratios.

The HDPE used in this study was supplied by Bamberger Polymer and is known under the trade name of Fortiflex, while the LLDPE used was provided by Sabic

Innovative Plastic and is known as Ladene. Some characteristics of HDPE and LLDPE resins used are displayed in Table 3.A.

Table 3.A: Characteristics of polyethylene resin used in the study

Polymer	Density (g/cm^3)	Melting point (°C)	Melt flow index (g/10min) ASTM D1238
HDPE	0.948	145	0.3
LLDPE	0.935	115	5

3.2.1.2 Adhesion promoters

Three different adhesion promoters were used in the outer layer of two-layered shock tubes. These included; ethylene-methacrylic acid copolymers (EMA), ethylene based ionomers, and maleic anhydride modified high density polyethylene (HDPE-g-MAH) also known as HDPE grafted with maleic anhydride.

a) Ethylene methacrylic acid copolymers (EMA)

These copolymers were mainly chosen for their excellent adhesion capability in the melt stage. Two grades of ethylene methacrylic acid copolymers were used in this study. Both grades had identical percentages of methacrylic acid (9% wt), but with different densities and melt flow indexes. These copolymers were provided by DuPont Industrial Polymer and are currently commercialised under the trade name of Nucrel. Table 3.B shows some characteristics of the two EMA used as adhesion promoters in the study. These copolymers are labelled in Table 3.B as EMA (a) and EMA (b).

Table 3.B: Characteristics of EMA used as adhesion promoters in the study

Polymer	Density (g/cm^3)	Melting point (°C)	Melt flow index (g/10min) ASTM D1238
EMA (a)	0.93	101	2.5
EMA (b)	0.93	100	10

b) Anhydride modified high density polyethylene (HDPE-g-MAH)

The choice of anhydride modified high density polyethylene as adhesion promoter was motivated by its ability to firmly adhere to polar substrates such as ionomers, and the presence of HDPE backbone in its structure. The presence of HDPE backbone in the structure of HDPE-g-MAH was expected to promote compatibility with HDPE resins when blended therewith. Two grades of HDPE-g-MAH were used during the experimental work. One of the grades was provided by DuPont Industrial Polymer and was labelled HDPE-g-MAH (a), while the other grade was provided by Dow Chemical Company and was labelled HDPE-g-MAH (b). Some characteristics of HDPE-g-MAH (a) and HDPE-g-MAH (b) are listed in Table 3.C.

Table 3.C: Characteristics of HDPE-g-MAH used as adhesion promoters in the study

Polymer	Density (g/cm^3)	Melting point (°C)	Melt flow index (g/10min) ASTM D1238
HDPE-g-MAH (a)	0.960	135	2
HDPE-g-MAH (b)	0.954	134	2

c) Ethylene based ionomers

These materials were chosen for their excellent tackiness in the melt stage, low permeability to organic and polar solvents, and the presence of ethylene monomer in their structure, which might promote compatibility with polyethylene resins. The choice of ethylene based ionomers as adhesion promoters was also motivated by the presence of a similar material in the inner layer, in other words, similarities between the adhesion promoter and the inner layer material were expected to enhance adhesion strength between the shock tube layers.

Four different grades of Ethylene based ionomers, having various metal ions and acid contents were used in the study. These ionomers were all provided by DuPont Industrial Polymers and are known under the trade name of Surlyn. Some characteristics of ethylene based ionomers used are shown in Table 3.D. The ionomers were labelled ionomer (a), ionomer (b) ionomer (c) and ionomer (d).

Table 3.D: Characteristics of ionomers used as adhesion promoters in the study

Ionomer	Metal ions	Acid contents (%)	Melting points (°C)	Melt flow index (g/10min) ASTM D1238
Ionomer (a)	Na+	≈ 15	94	2.4
Ionomer (b)	Zn2+	≈ 10	96	2.4
Ionomer (c)	Zn2+	≈ 10	95	1
Ionomer (d)	Zn2+	≈ 10	87	5

3.2.2 Inner layer material

The polymeric material used in the inner layer of both two-layered and three-layered shock tubes produced was an ethylene based ionomer similar to that used in the inner layer of commercially available high performance three-layered shock tubes. This material was chosen for its good resistance to oil and fuel diffusion, combined with its excellent adhesive properties in the melt stage, which allows for good adhesion of explosive powders onto the inner surface. The ionomer used in the inner layer is listed in Table 3.D under the label "ionomer (a)".

3.2.3 Materials for three-layered shock tube

A three-layered shock tube similar to commercially available high performance shock tube was extruded during the experimental work. The outer layer consisted of high density polyethylene (HDPE) marketed under the trade name of Fortiflex (refer to Table 3.A for the characteristics) and the inner layer was made of an ethylene based ionomer. The ionomer used in the inner layer is listed in Table 3.D under the name "ionomer (a)". The material present in the adhesive layer was an ethylene acrylic copolymer (EAA) marketed by Dow Chemical Company under the trade name of Primacor (Refer to Table 3.E for the characteristics).

The explosive powders present in all of the shock tubes produced, both three-layered and two-layered shock tubes, consisted of a blend of 92% HMX and 8% Aluminium. HMX was the main energetic material while aluminium acted as a sensitizer. The moisture content of explosive powders was kept below 0.08% before processing in order to avoid agglomerations.

Figure 3.1 Illustrates the configuration of polymeric layers in both three-layered and two-layered shock tubes extruded, while Table 3.E shows the characteristics of the EAA used in the adhesive layer.

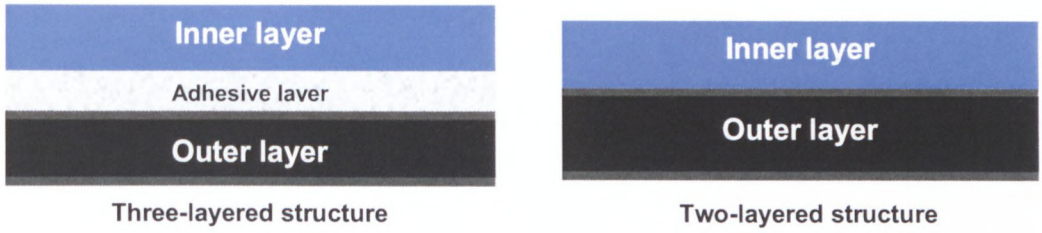

Figure 3.1: Configuration of polymeric layers in two-layered and three-layered shock tubes

Table 3.E: Characteristics of the ethylene acrylic acid copolymer used in the adhesive layer of the three-layered shock tube

Polymer	Density (g/cm^3)	Melting point (°C)	Melt flow index (g/10min) ASTM D1238
EAA	0.935	103	2.6

3.3 Nomenclature of experimental two-layered shock tubes

During the experimental work, the blending compositions of two-layered shock tubes were adjusted until processable blends were obtained. Initial evaluations involved various blending compositions but the focus of the work was ultimately narrowed down to the following four combinations:

1. HDPE + HDPE-g-MAH
2. HDPE + EMA
3. HDPE + Ionomer
4. LLDPE + Ionomer

HDPE was therefore respectively blended with HDPE-g-MAH, EMA, and ionomers while LLDPE was only blended with the ionomers. The label used to identify experimental two-layered samples consisted of an alphabetical letter preceded by a

number (e.g. A1). Each alphabetical letter represented a blend with defined components as shown below:

"A" → HDPE + HDPE-g-MAH
"B" → HDPE + EMA
"C" → HDPE + Ionomer
"D" → LLDPE + Ionomer

The ratios of polyethylene and the adhesion promoter were altered. The blending combinations and their respective labels are presented in Table 3.F. The nomenclature shown in Table 3.F was used to identify experimental two-layered shock tubes throughout the entire work. No nomenclature was used for experimental three-layered shock tubes.

Table 3.F: Nomenclature of experimental two-layered samples

Sample's label	Outer layer material	Inner layer material
A1	90% HDPE + 10% HDPE-g-MAH (a)	Ionomer (a)
A2	70% HDPE + 30% HDPE-g-MAH (a)	Ionomer (a)
A3	80% HDPE + 20% HDPE-g-MAH (b)	Ionomer (a)
A4	60% HDPE + 40% HDPE-g-MAH (b)	Ionomer (a)
B1	60% HDPE + 40% EMA (b)	Ionomer (a)
B2	70% HDPE + 30% EMA (b)	Ionomer (a)
B3	60% HDPE + 40% EMA (a)	Ionomer (a)
B4	50% HDPE + 50% EMA (a)	Ionomer (a)
C1	70% HDPE + 30% Ionomer (d)	Ionomer (a)
C2	70% HDPE + 30% Ionomer (b)	Ionomer (a)
C3	70% HDPE + 30% Ionomer (a)	Ionomer (a)
C4	70% HDPE + 30% Ionomer (c)	Ionomer (a)
D1	70% LLDPE + 30% Ionomer (d)	Ionomer (a)
D2	70% LLDPE + 30% Ionomer (a)	Ionomer (a)
D3	70% LLDPE + 30% Ionomer (b)	Ionomer (a)

3.4 Manufacturing sequence of experimental shock tubes

The manufacturing sequence of experimental shock tubes was similar to the sequence used for commercial shock tubes. The extrusion equipment included three twin screw extruders mounted in a series, a silo (used as dryer), chillers (used as water cooling units), outer and inner diameters monitors, and capstans (used as pullers). Figure 3.2 shows a schematic representation of the complete extrusion process.

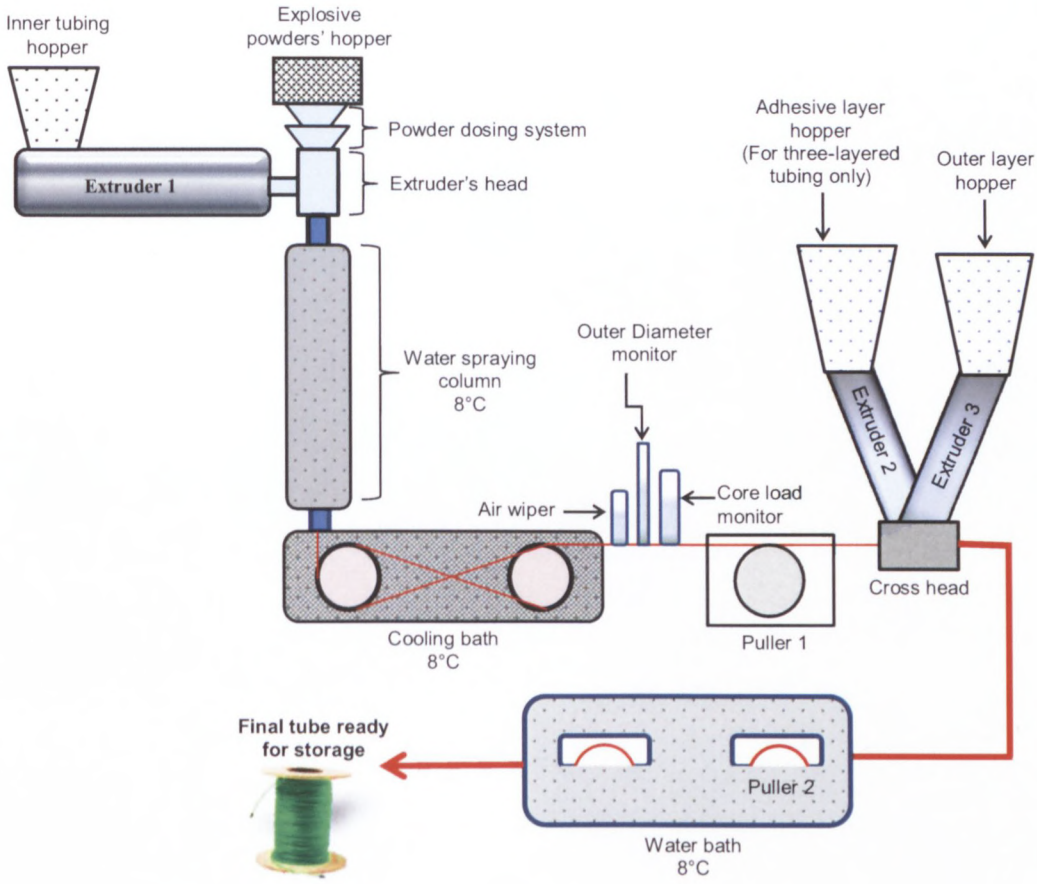

Figure 3.2: Schematic representation of the complete extrusion process

The following sequence was followed during the manufacturing process:

1. The extruders were switched on and the temperatures were set accordingly. ***NB:** Extruder 2 was disconnected during the extrusion of two-layered shock tubes.

2. The inner layer material (Ionomer (a)) was fed to the silo where it was dried using dry air at a temperature of 40°C for an hour. The purpose of drying was to reduce the moisture content and avoid possible melt breakage during melt draw down.

3. The dried inner layer material was fed to the first extruder were it was extruded as a small-diameter tubing (outer diameter ≈ 2.5 mm).

4. The explosive powders which consisted of blends of HMX and aluminium were fed to the powder's hopper, and then were spread onto the tube's inner wall at a constant rate. The inner tube containing explosive powders was then sent to the water spraying column where it was quenched. Figure 3.3 shows a schematic representation of the inner tube extrusion.

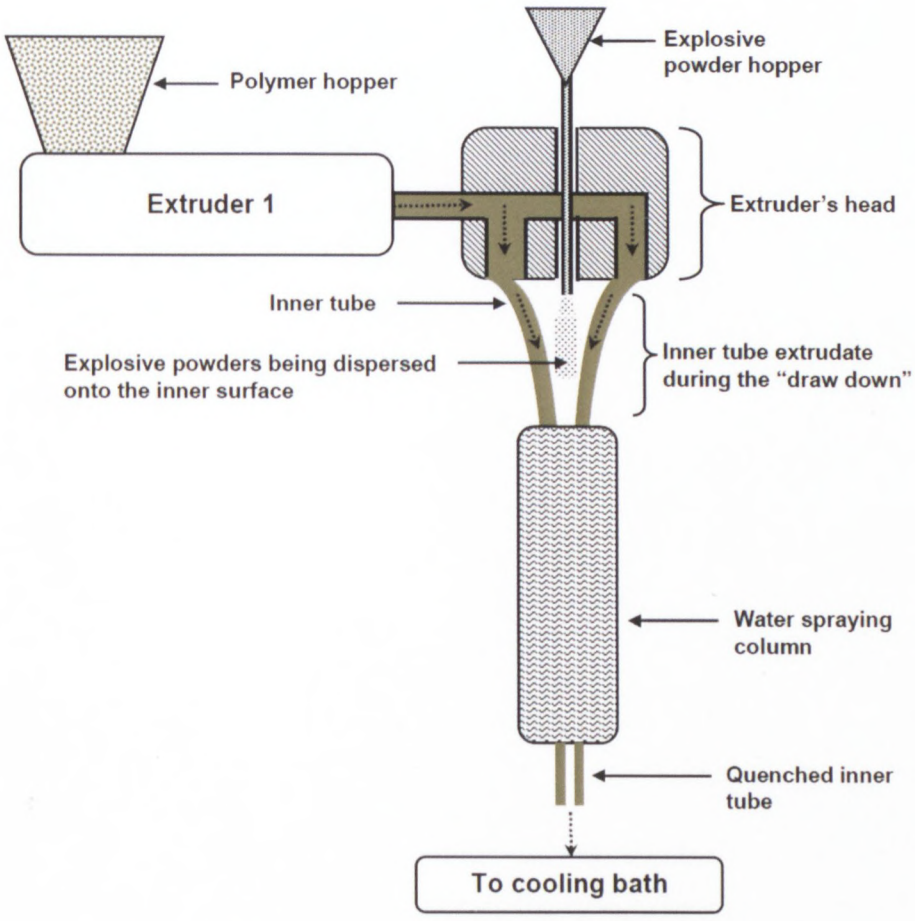

Figure 3.3: Schematic representation of the inner tube extrusion

5. The dosing rate of explosive powders was adjusted until the core load monitor was indicating values varying between 11 and 16 mg/m.

6. Polyethylene and the adhesion promoter were mixed using a concrete mixer. The blending ratios were as described in Table 3.F. The mixing was carried out for 10 minutes at a speed of about 20 rpm.

7. Extruder 2 was disconnected and the blend prepared in step No. 6 was fed to extruder 3. The inner tube extruded in steps No. 3 & 4 was pulled by puller 1 which was running at the speed of 140 m/min. The tube was then sent through the cross head of extruder 2 & 3 where it was coated with the molten polymeric blend.

   ***N.B:** Steps No. 6 & 7 were followed for two-layered shock tubes only

8. HDPE was fed to the third extruder, while EAA was fed to the second extruder. The inner layer extruded in steps 3 & 4 was pulled by puller 1, which was running at the speed of 140 m/min. The tube was then sent through the cross head of extruder 2 & 3 where it was coated with EAA and HDPE respectively.

   ***N.B:** This step was followed for the extrusion of the three-layered shock tube only

9. The tube coming from extruder 3 was pulled by puller 2, which was running at the speed of 300 m/min then cooled down using cool water.

10. The tubing obtained was then collected and stored for 48 hours at a temperature of about 25°C before being tested.

3.5 Operating conditions

3.5.1 Temperature profiles of extruders

The inner layer material (ionomer (a)) had a melting point of 94°C. In order to allow a homogeneous flow of the molten material, the extrusion temperature of extruder 1 was varied from 100°C at the first zone to 210°C at the nozzle. The exact temperature for each extruder zone can be found in Table A1 of the appendix section. The

temperature profile of the first extruder was kept unchanged for all the samples produced.

The outer layer of all the shock tubes produced was extruded using extruder 3. The temperature profile of this extruder was not identical for all the two-layered shock tubes; this is because two-layered shock tubes were made of various polymeric blends in the outer layer. The components of each blend had a different melting point and melt flow index. In order to ensure a steady and homogenous flow of these blends, the temperature profile was adjusted to the need of every blend. The temperature profile of extruder 3 for each two-layered shock tube can be found in the appendix A Table A2.

The outer layer of three-layered shock tube was made of high density polyethylene with a melting point of 145°C. The extrusion temperature, therefore, varied from 140°C at the first zone to 220°C at the nozzle. The exact temperature for each extruder zone can be found in the appendix A.

The adhesive layer material was an ethylene acrylic acid copolymer with a melting point of 103°C. This material was only used for the three-layered shock tube. The temperature profile of the second extruder ranged from 120°C at the first zone to 205°C at the nozzle.

3.5.2 Cooling water, stretching ratios, and extruder speeds

The temperature of the cooling water used in the chillers, cooling bath, and water spraying unit was maintained at 8°C. The shock tube samples were stretched once during the manufacturing process. The stretching took place between the first and second pullers. The stretching ratio was 7/15. The extruders' speeds were slightly adjusted in order to obtain consistent shock tubes' dimensions.

3.6 Testing of experimental shock tubes

After being extruded and conditioned for 48 hours at 25°C, the shock tube samples produced were tested in order to determine their properties and performance indicators. The tests performed included: dimensions measurements, core load measurements, breaking strength, elongation at break, burst strength, oil ingression, velocity of detonation, and peel-off test.

3.6.1 Dimensional measurements

3.6.1.1 Apparatus used for dimensional measurements

The apparatus used to measure the dimension of experimental shock tubes consisted of a Stanley knife and an electron microscope known as Axio imager. Figure 3.4 shows a picture of the type of microscope used.

Figure 3.4: Picture of the type of electron microscope used in measuring the dimensions of shock tubes (http:// zeiss.de/micro)

3.6.1.2 Procedure followed during dimensional measurements

The procedure followed to measure the dimensions of shock tube samples is outlined below:

1. A tiny circular specimen of a given shock tube sample having a thickness of about 1 mm was cut using the Stanley knife.

2. The specimen was placed under the microscope and was observed. The inner diameter, outer diameter, inner tube thickness, outer tube thinness, and adhesive layer thickness (for three-layered shock tubes only) were measured.

3. Each dimension was measured from three different angles and the average of the three values was calculated and recorded. Figure 3.5 shows a schematic representation of the dimensions of a two-layered shock tube as observed and measured under the microscope.

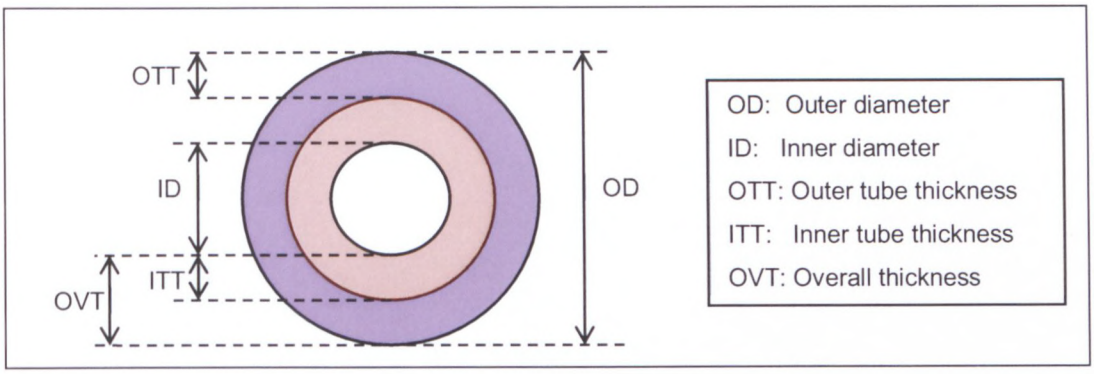

Figure 3.5: Schematic representation of the cross sectional view of a two-layered specimen observed under the microscope

4. Steps No.1, 2 and 3 were performed with a total of 10 specimens per sample. The mean of the measured dimension for a given sample was calculated as follows (see Equation 3.1 below):

$$\text{Mean OD/ID/ITT/OTT/OVT} = \frac{\text{Average dimension of (specimen 1+ } \cdots \text{+ specimen 10)}}{10} \qquad \textbf{Equation 3.1}$$

3.6.2 Core load measurements

3.6.2.1 Apparatus used for core load measurements

The apparatus used to measure the core load consisted of Stanley knife, a weight scale, meter scale, and a blow gun equipped with an air compressor.

3.6.2.2 Procedure followed for core load measurements

The test procedure was as follows:

1. 10 specimens of a shock tube sample were cut using the Stanley knife. Each of the specimens measured exactly 1 meter. The specimens were cut in such a way that, the distance between two specimens was 20 cm (See Figure 3.6).

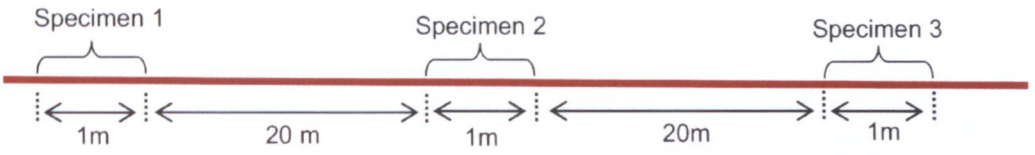

Figure 3.6: Illustration of the distance between specimens used for core load measurements

2. Each of the specimens was weighed and their weight was recorded.

3. Pressurised air was blown inside the shock tube specimens using the blow gun, and the explosive powders were completely removed from the tubes.

4. The ten shock tube specimens without explosive powders were weighed once more and the new weight was recorded.

5. The core load for each specimen was then calculated using the following equation (see Equation 3.2 below):

$$\text{Core load of a single specimen} = \text{Mass of specimen with powders} - \text{Mass of specimen without powders} \qquad \text{Equation 3.2}$$

6. Knowing the core load of each of the 10 specimens, the mean core load of the sample from which the specimens were cut was calculated as follows:

$$\text{Mean core load} = \frac{\text{core load of (specimen 1} + \cdots + \text{specimen 10)}}{10} \qquad \text{Equation 3.3}$$

3.6.3 Breaking strength and elongation at break

3.6.3.1 Apparatus used for breaking strength and elongation at break tests

The apparatus used for the breaking strength test and elongation at break tests was as follows: a LLOYD tensiometer connected to a computer which was equipped with software enabling one to monitor and record the pulling strength and elongation of specimens tested.

3.6.3.2 Procedure followed to measure the breaking strength and elongation at break

Breaking strength and elongation tests were both carried out simultaneously. The testing procedure was as follows:

1. A shock tube specimen having a length of about 10 cm was cut from a given sample. Both ends of the specimen were hooked onto the upper and lower creeps of the tensiometer as illustrated in Figure 3.7.

2. The shock tube specimen was then stretched longitudinally at the constant extension rate of 70 mm/min. The pulling strength as well as the sample's elongation were respectively monitored by the computer until rupture occurred. Figure 3.7 shows an illustration of the experimental set up used.

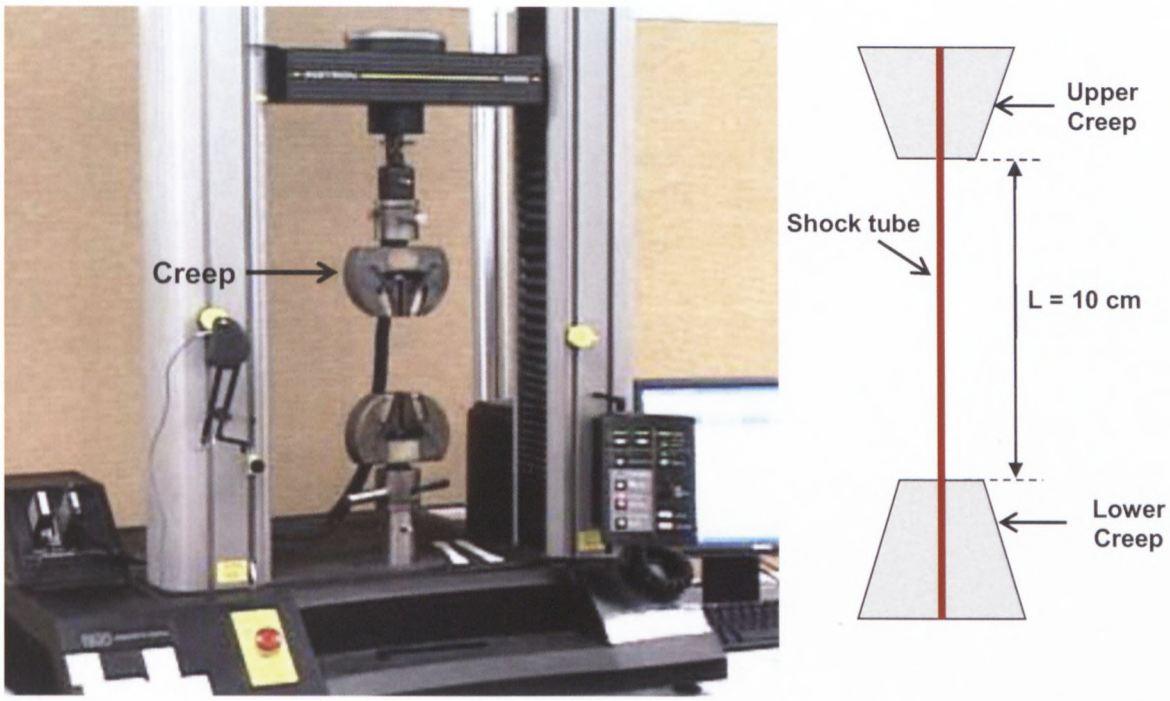

Figure 3.7: Experimental set up used for breaking strength and elongation at break tests

3. After rupture of the tube, the maximum load applied before rupture (also known as breaking strength), and the maximum elongation before rupture

(also known as elongation at break) were both displayed by the computer's software.

4. The entire procedure was performed with a total of 20 specimens for each sample.

5. The mean elongation at break and breaking strength for a given sample were calculated as follows using the equation in Equation 3.4 below:

$$\text{Mean elongation at break} = \frac{\text{Elongation at breakbreaking of (specimen 1}+\cdots+\text{specimen 20)}}{20} \qquad \textbf{Equation 3.4}$$

6. Equation 3.4 was also used to calculate the mean breaking strength. The entire testing procedure was repeated with each and every sample produced.

3.6.4 Oil ingression

3.6.4.1 Apparatus used for oil ingression test

The apparatus used for the test consisted of masking tape, a thermal bath, 10 litres of paraffin known as Fluidox 400, and an electric firing device.

3.6.4.2 Procedure followed during oil ingression test

The steps taken to perform the oil ingression test were as follows:

1. A minimum of 100 specimens of a sample were cut randomly. Each specimen had a length of about 3 meters.

2. The thermal bath was filled with 10 litres of paraffin, and the thermostat was set to 50°C.

3. Once the paraffin temperature had reached 50°C and was steady, the specimens were introduced into the thermal bath in such a way that, about 1.5 meters of the tube was totally submerged in the oil with both ends hanging outside of the bath. The thermal bath was then hermetically sealed. Figure 3.8

shows a schematic illustration of a shock tube specimen submerged into the thermal bath.

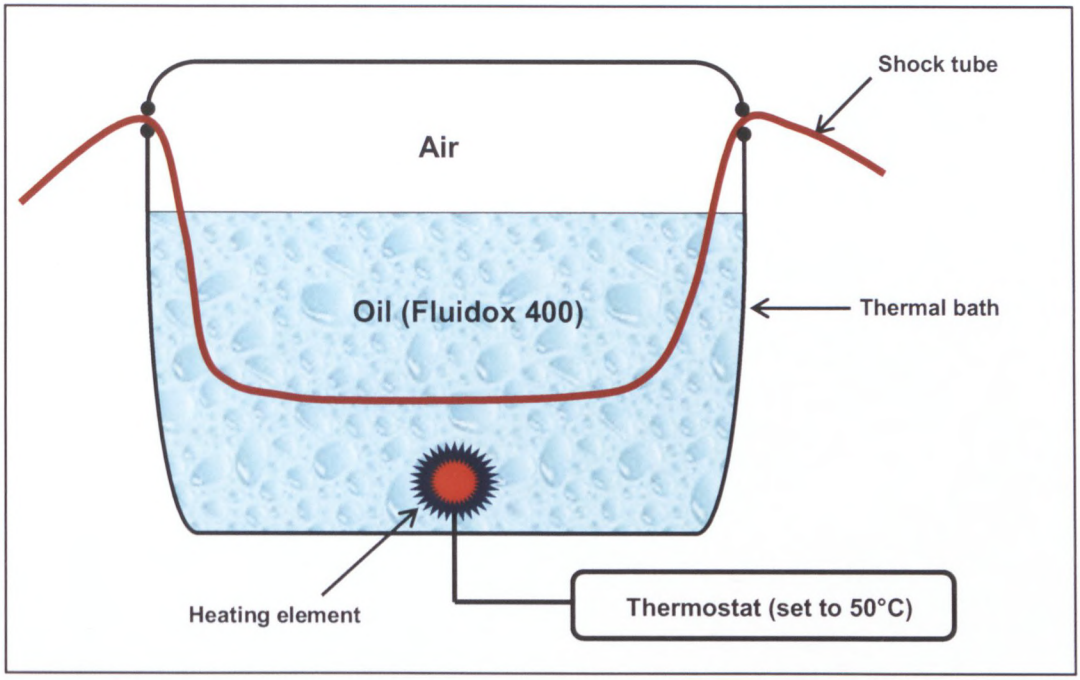

Figure 3.8: Schematic illustration of experimental set up for oil ingression test

4. After spending 24 hours inside the hot paraffin, five specimens were taken out of the thermal bath, and one end of the tube was closed with the masking tape. The specimens were initiated from the end without masking tape using the electric firing device. Figure 3.9 shows a picture of the electric firing device used.

5. After initiation of the tube, the end that was closed with the masking tape was observed: In the event that the masking tape was perforated, the specimen was said to be "passing". And in the event that the masking tape was not perforated, the specimen was said to be "failing".

   ***NB:** the term "Passing" here means that, the shock wave has successfully travelled along the shock tube. Meanwhile, the term "failing" means that the shock wave has been interrupted while travelling along the shock tube.

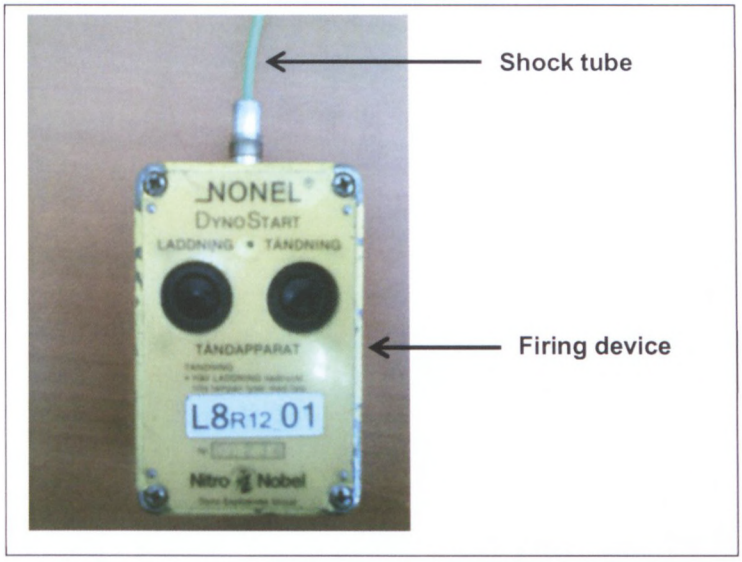

Figure 3.9: Electric firing device used

6. Steps 4 and 5 were repeated after every 2 hours until all the specimens of each samples were failing. The maximum time after which all the five specimens of a sample were passing was recorded as sleep time.

7. Steps 1 through 7 were repeated with a total of 5 sets of specimens and the sleep times obtained were recorded.

3.6.5 Linear thermal shrinkage

3.6.5.1 Apparatus used for linear thermal shrinkage test

The apparatus used for this test consisted of an oven, Stanley knife and a meter scale.

3.6.5.2 Procedure followed during linear thermal shrinkage test

The following procedure was used:

1. The oven was preheated to 80°C. A specimen measuring exactly 1 m was cut from a shock tube sample and introduced inside the preheated oven for an hour.

2. After the hour, the specimen was taken out of the oven and kept for 10 minutes in a room at temperature of about 25°C. The specimen was then measured using the meter scale and its new length was recorded. Figure 3.10 shows a schematic illustration of the tube length before and after heating.

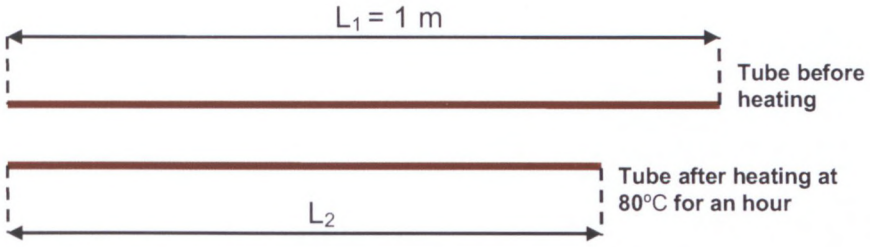

Figure 3.10: Schematic representation of shock tube sample before and after being introduced into the oven during linear shrinkage test

3. The percentage shrinkage for the specimen was calculated as follows(see Equation 3.5 below)

$$\text{Shrinkage} = \frac{L_1 - L_2}{L_1} \times 100 \qquad \text{Equation 3.5}$$

***N.B:** L_1 is the specimen length before heating and L_2 is the specimen length after being heated at 80°C for an hour.

4. Steps 1 through 5 were repeated with 9 more specimens and the mean linear shrinkage was calculated using the equation below (Equation 3.6):

$$\text{Mean linear shrinkage} = \frac{\text{Shrinkage of (specimen 1} + \cdots + \text{specimen 10)}}{10} \qquad \text{Equation 3.6}$$

5. This procedure was carried out on every shock tube produced.

3.6.6 Velocity of detonation test

3.6.6.1 Apparatus used for velocity of detonation test

The apparatus used for velocity of detonation (VOD) test consisted of a firing device and a VOD indicator. The VOD indicator is a device that measures, records and

displays the velocity at which the initiation signal (or shock wave) travels inside a shock tube.

3.6.6.2 Procedure followed during VOD test

The procedure used to measure the VOD was as follows:

1. A specimen measuring about 3 meters was cut from a shock tube sample. The specimen was then hooked onto the creeps of the VOD indicator. Figure 3.11 shows a schematic illustration of the experimental set up for the VOD test.

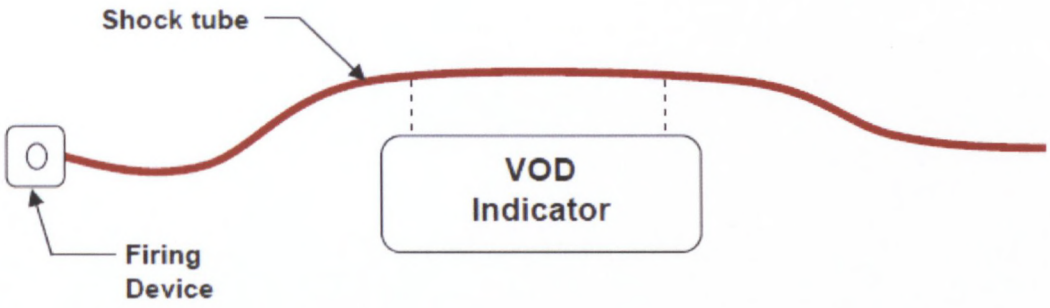

Figure 3.11: Illustration of apparatus set up for VOD test

2. The specimen was initiated from one end using the firing device.

3. The velocity of detonation was displayed on the screen of the VOD indicator and its value was recorded.

4. The entire procedure was repeated with a total of 10 specimens for each shock tube sample and the mean VOD was calculated using the following equation (Equation 3.7):

$$\text{Mean VOD} = \frac{\text{VOD of (specimen 1} + \cdots + \text{specimen 10}}{10} \qquad \textbf{Equation 3.7}$$

3.6.7 Burst strength test

3.6.7.1 Apparatus used for burst strength test

The apparatus used for this test comprised an oven, a cylindrical cardboard of 20 cm diameter and 30 cm long, an electric firing device, and a permanent marker.

3.6.7.2 Procedure followed during burst strength test

The test procedure is detailed below:

1. Five specimens of a given sample were cut randomly. Each of the specimens had a length of 7 m. A mark was put 1 m away from the tube end (see Figure 3.12).

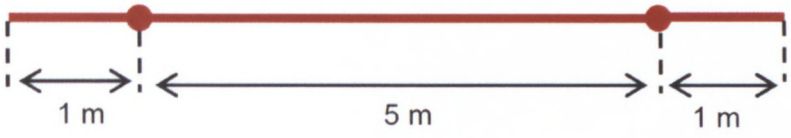

Figure 3.12: Schematic representation of specimen used for burst strength test

2. The oven was preheated to 80°C. The specimens were rolled around the cylindrical card board, then introduced inside the preheated oven in such a way that, one end of the each specimen was still hanging out of the oven.

3. The oven was hermetically closed and the specimens were left inside for 20 minutes.

4. After the 20 minutes, the shock tube specimens were initiated from the end that was left hanging out of the oven.

5. The initiated specimens were taken out of the oven, and examined with the naked eye.

6. The numbers of bursts observed along the 5 m length marked in step 1 were recorded. Figure 3.13 shows some pictures of bursts observed

Figure 3.13: Pictures of typical bursts observed during burst strength test

7. The average number of bursts per linear meter of shock tube for a single test was computed as follows:

$$\text{Average numbers of bursts for a single test} = \frac{\text{Total number of bursts within the 5m length observed}}{5} \qquad \text{Equation 3.8}$$

8. The entire procedure was repeated 10 times with each sample and the mean of numbers of bursts for a given sample was calculated as follows:

$$\text{Mean numbers of bursts} = \frac{\text{Average numbers of bursts of (test 1+ } \cdots \text{+ test 10)}}{10} \qquad \text{Equation 3.9}$$

3.6.8 Peel-off test

3.6.8.1 Apparatus used for peel-off test

Unlike the previous tests, which are currently used in the industry, the peel-off test was especially designed and developed for this work. The test was performed to determine the amount of force that has to be applied in order to separate the inner layer from the outer layer. The apparatus used consisted of a tensiometer linked to a computer, a vernier caliper, tweezers and a Stanley knife.

3.6.8.2 Procedure followed during peel-off test

The test procedure was as follows:

1. A specimen of shock tube was longitudinally cut in two equal parts using the Stanley knife. Figure 3.14 shows a schematic representation of a two-layered shock tube before and after being longitudinally cut.

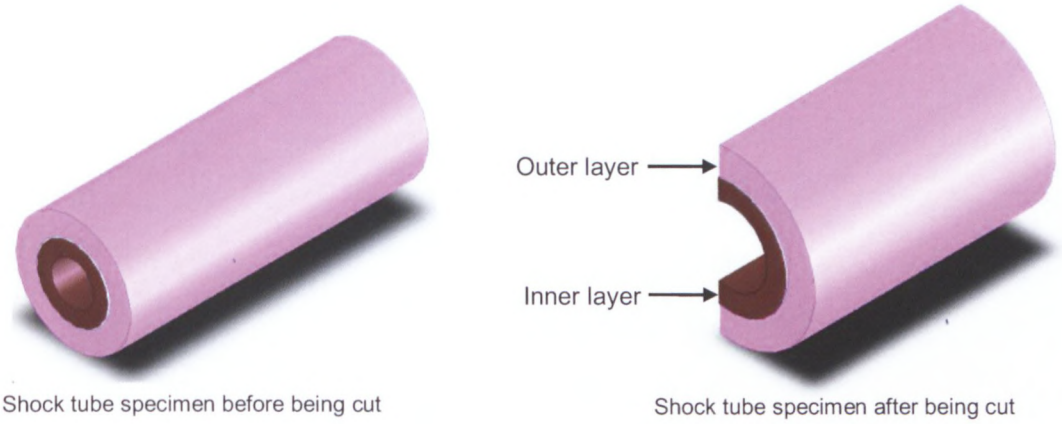

Figure 3.14: Schematic representation of the two-layered shock tube before and after being longitudinally cut

2. The inner layer was then separated from the outer layer using tweezers. The layers separation was carried out along a length of 20 cm, and 10 cm was left unseparated. Figure 3.15 shows a schematic representation of a shock tube specimen after the layers' separation.

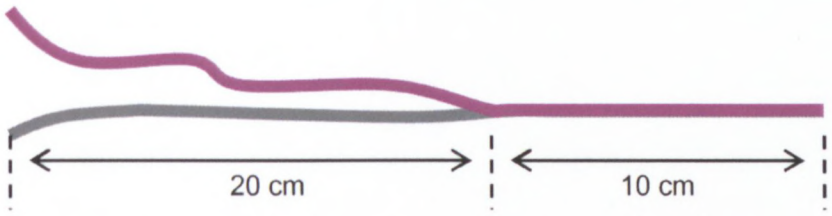

Figure 3.15: Schematic representation of shock tube specimen after the layers' separation

3. The outer layer of the specimen was hooked onto the lower creep of the tensiometer while the inner layer was hooked onto the upper creep in such a way that, both layers formed an angle of 180°. A schematic representation of the apparatus and experimental set up can be found in Figure 2.16.

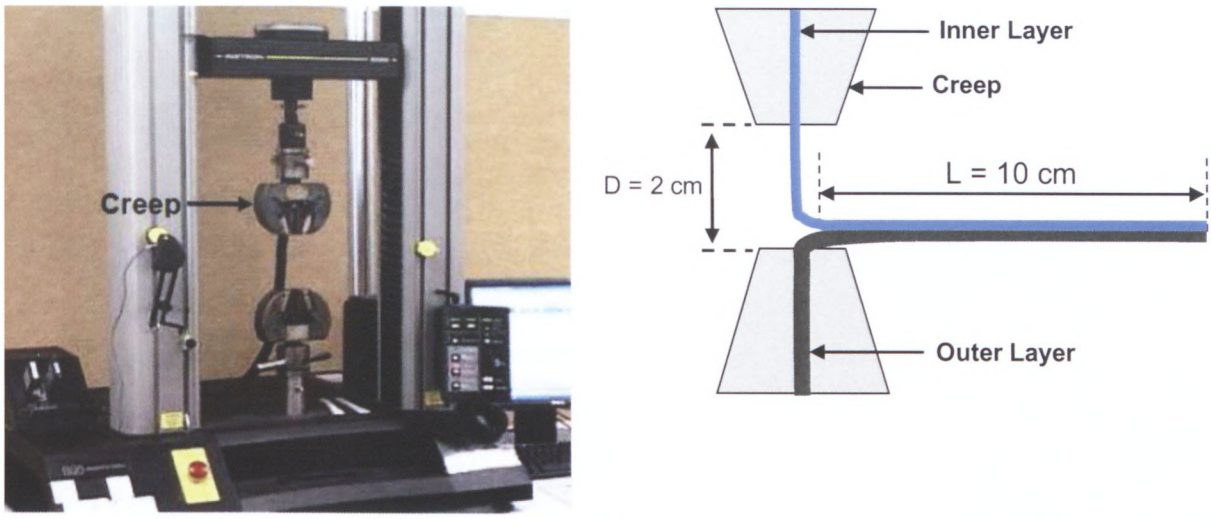

Figure 3.16: Schematic representation of apparatus set up used for peel off test

4. The upper creep was gradually moved upward at a speed of 75 mm/min, and the inner layer was separated from the outer layer. The upward force (or peel-off force) which was the force applied to carry out the layers' separation, was monitored by the computer. Readings were recorded between intervals of two seconds. The average peel-off force applied between the 20th and 120th second was calculated. Figure 3.17 shows the graphical representation of the variation of force applied as a function of time.

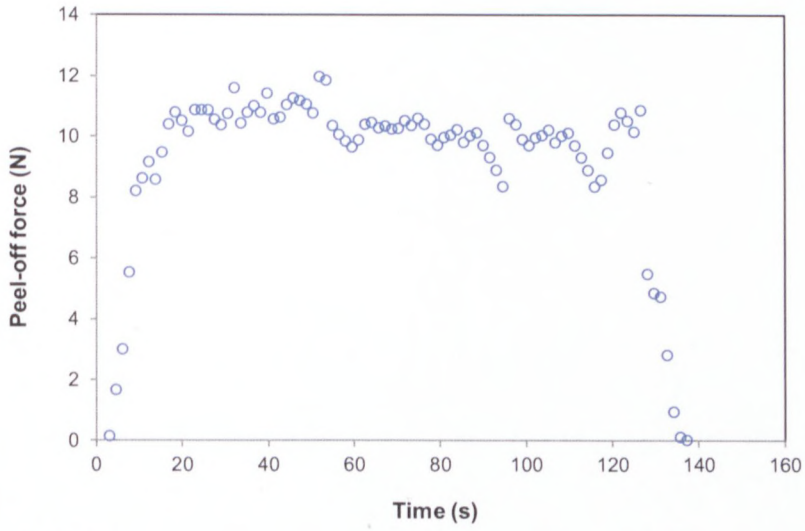

Figure 3.17: Graphical representation of the peel-off force applied as a function of time

5. Steps 1 through 5 were repeated with a total of 10 specimens per sample and the mean adhesion strength was computed as follows:

$$\text{Mean adhesion strength} = \frac{\text{Average peel-off force of (specimen 1+}\cdots\text{+specimen 10)}}{10} \qquad \textbf{Equation 3.10}$$

3.7 Experimental errors

Physical measurements cannot be completely free of uncertainties, no matter how careful the measurements are made (Taylor, 1997). Because the applications of science greatly depend on physical measurements, it is crucial to know the extent to which uncertainties occur and keep them to a minimum (Taylor, 1997).

The word "error" in science and engineering generally refers to the inevitable uncertainty that occurs in all measurements. Hence, errors do not necessarily imply mistakes and cannot be eliminated by being careful (Taylor, 1997). There are three main types of errors: gross errors, random errors, and systematic errors.

- Gross errors are generally caused by equipment failures (e.g. mechanical failure or power failure) and always result in an automatic rejection of the measured values (Taylor, 1997).

- Random errors are due to the imperfection of the measuring device which affects the precision. Precision here is defined as the repeatability or reproducibility of values obtained during measurements. Random errors are generally revealed by repeating the measurements several times and can be assessed by statistical analysis. Precision can be improved by increasing the number of specimens being tested (Taylor, 1997).

- Systematic errors always tend to push the measured values to the same direction and are often attributed to improper calibration of measuring devices or malfunctioning instruments. Unlike random errors, systematic errors are not revealed by repeating the measurements several times. Hence, systematic errors cannot be assessed by statistical analysis based on repeated measurements (Taylor, 1997). A typical example of systematic error would be a stop watch that runs slow and always leads to the overestimation of the

measured time. In this case, the measured values might have a good precision but a poor accuracy.

During the experimental work, all data generated after encountering gross errors were automatically rejected. The potential sources of systematic errors were minimized checking the calibrations. Random errors were assessed using statistical equations. These equations included calculations of the standard error also known as standard deviation of the mean. The standard deviation of the mean (SDOM) is an evaluation of the margin of error incorporated in the mean (Taylor, 1997). Equations 3.11, 3.12 and 3.13 respectively show the formulae used in calculating the mean, standard deviation, and standard deviation of the mean.

$$\bar{x} = \frac{\sum_{i=1}^{i=N} x_i}{N} \qquad \textbf{Equation 3.11}$$

$$\sigma_x = \sqrt{\frac{1}{N-1}\sum_{i=1}^{i=N}(x_i - \bar{x})^2} \qquad \textbf{Equation 3.12}$$

$$SDOM = \frac{\sigma_x}{\sqrt{N}} \qquad \textbf{Equation 3.13}$$

Where N is the total number of specimens tested per sample,

x_i is the measurement obtained for a single specimen i

$\bar{x}$ is the mean of all recorded measurements for a given sample x

σ_x is the standard deviation of measurements obtained for a given sample x

Equation 3.13 was used to evaluate the random errors that occurred during dimensional measurements, core load measurement, breaking strength and elongation at break tests, bursts strength test, linear thermal shrinkage test, and peel off test. Results were expressed as follows (see equation 3.14):

$$Results = \bar{x} \pm SDOM \qquad \textbf{Equation 3.14}$$

Figure shows a graphical representation of the error bar used for the estimation of results.

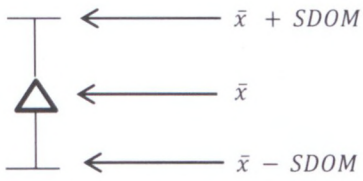

Figure 3.18: Representation of the error bar for estimation of results

Equations 3.11, 3.12 and 3.13 were not used for the evaluation of errors for the oil ingression test. Rather, the upper and lower bones of the error bar were respectively represented by the highest and lowest sleep time obtained.

3.6 Conclusion

This chapter has reviewed the sequence that was followed in selecting the raw materials for experimental samples. A description of the samples' compositions and extrusion process was also given. In addition, the tests used to evaluate the properties of shock tube samples were described. The chapter also presented the method used to estimate errors encountered during the experimental tests. The next chapter will present and discuss the results obtained.

Chapter 4 : Results and Discussion

4.1 Introduction

Results outlining the properties and performance of experimental shock tubes are presented and discussed in this chapter. The nomenclature used for two-layered shock tubes is the same as described in section 3.3 of chapter three. The properties of two-layered shock tubes are compared to the standard three-layered shock tube extruded, and the influence of the numbers of polymeric layers on the properties and performance of a multi-layered shock tube is deduced. The effect of varying the outer layer compositions of two-layered shock tubes on the tubes' properties and performance is also discussed. Based on the results obtained, a material design for the manufacture of high performance two-layered shock tubes is proposed. The properties of the shock tube obtained with the proposed material design are compared to the properties of Stewart's (2002) single-layered shock tubes and commercially available high performance three-layered shock tubes. The advantages and limitations of the shock tube obtained with the proposed material design are also presented.

4.2 Tubes' dimensions

The dimensions measured for two-layered shock tubes included the outer diameter, inner diameter, outer tube thickness, and inner tube thickness. Then, the dimensions measured for the three-layered shock tube included the outer diameter, inner diameter, outer tube thickness, inner tube thickness, and adhesive layer thickness. Table 4.A displays the dimensions obtained for the three-layered shock tube.

Table 4.A: Dimensions of experimental three-layered shock tube

	Outer diameter	Inner diameter	Outer tube thickness	Inner tube thickness	Adhesive layer thickness
Mean (mm)	2.98	1.11	0.42	0.45	0.10
Standard error (mm)	± 0.05	± 0.03	±0.02	±0.04	±0.01

Figures 4.1(a), (b), (c) and (d) show graphical representations of dimensions of two-layered shock tubes. The dimensions are plotted on a single axis (Y-axis). Due to the difference in structure, the dimensions of two-layered shock tubes were not compared to the three-layered shock tube.

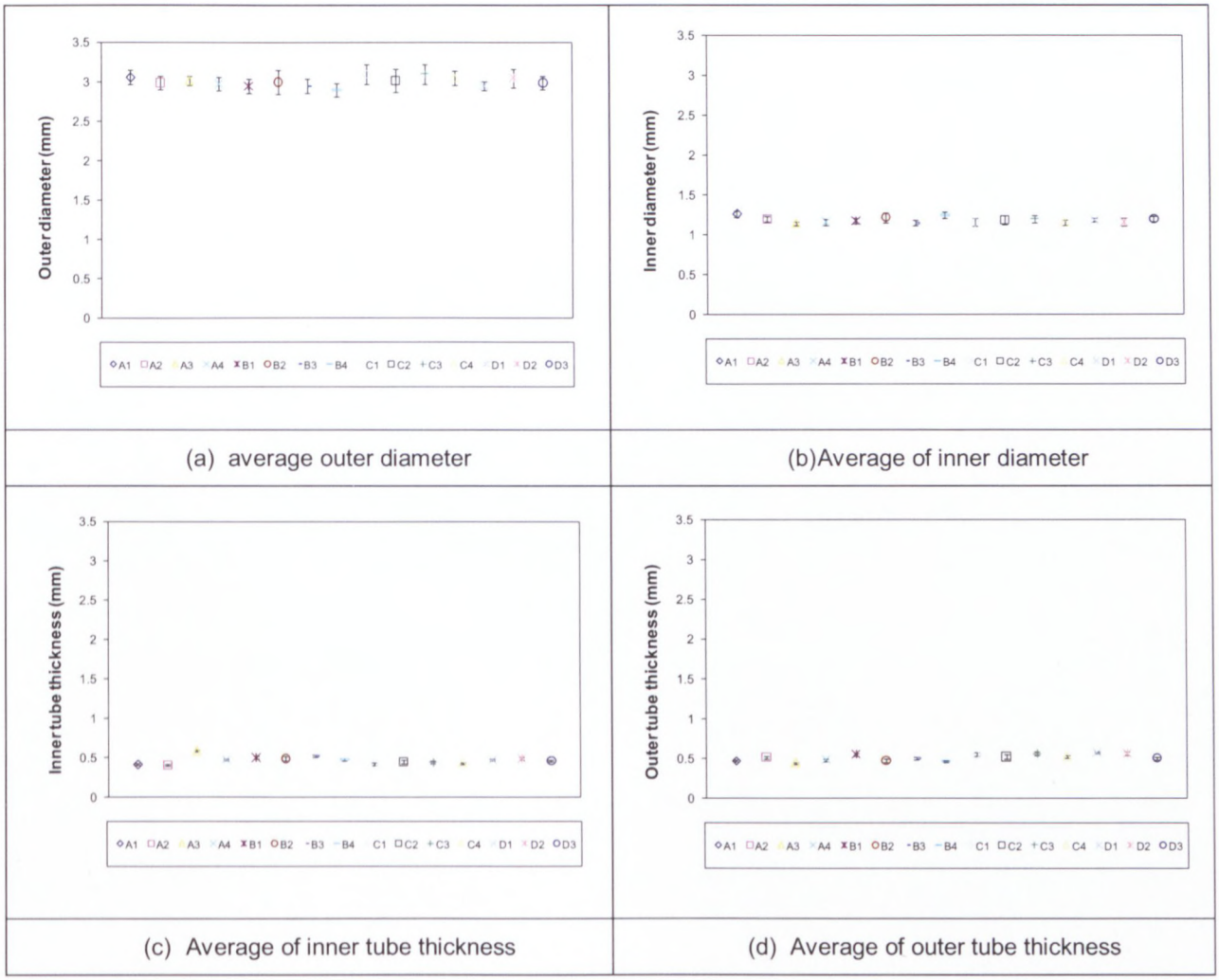

(a) average outer diameter

(b)Average of inner diameter

(c) Average of inner tube thickness

(d) Average of outer tube thickness

Figure 4.1: Dimensions of experimental shock tubes

It can be seen from Figures 4.1(a), (b), (c) and (d) that, all the experimental two-layered shock tubes have comparable dimensions; hence, should any difference be observed between the properties of experimental two-layered shock tubes, discrepancy in dimensions would unlikely be the cause.

4.3 Core loading

Figure 4.2 shows a graphical representation of core load ranges obtained with the experimental shock tubes. The ranges are plotted on a single axis (Y-axis). The grey area on the graph represents the core load range for the three-layered shock tube which spans from 12 to 16 mg / m. The points plotted on the graph represent the core load ranges of experimental two-layered shock tubes.

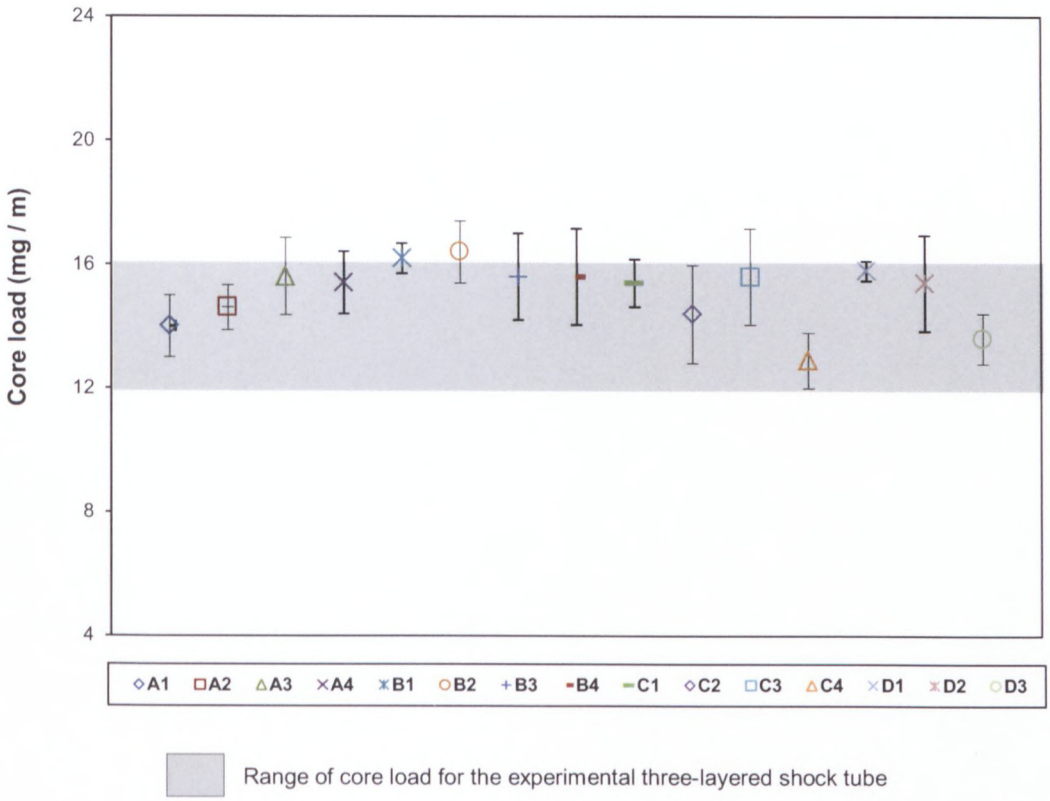

Figure 4.2: Graphical representation of core load range of experimental two-layered shock tubes

It can be observed from Figure 4.2 that, all the points plotted on the graph are within the same core load range as the three-layered shock tube. Hence, two-layered shock tubes and the three-layered shock tube are loaded with a comparable quantity of explosive powders per linear meter of tubing. The similarity observed in the core load implies that the properties and performance of the experimental shock tubes would only be a function of the compositions of polymeric layers, rather than the core loading responses.

4.4 Burst strength

The burst strength test was performed to evaluate the radial strength of various shock tube samples. The test was carried out at a temperature of 50°C. This section compares the burst strength of the two-layered shock tubes to the three-layered shock tube. The influence of the outer layer compositions of two-layered shock tubes on the burst strength is also discussed.

4.4.1 Bursts strength comparison between two-layered shock tubes and the three-layered shock tube

Figure 4.3 shows a graphical representation of the ranges of numbers of bursts obtained per linear meter of shock tubes. The ranges are plotted on a single axis (Y-axis). The grey area on the graph represents the range obtained with the experimental three-layered shock tube, while the points plotted represent the ranges obtained with experimental two-layered shock tubes.

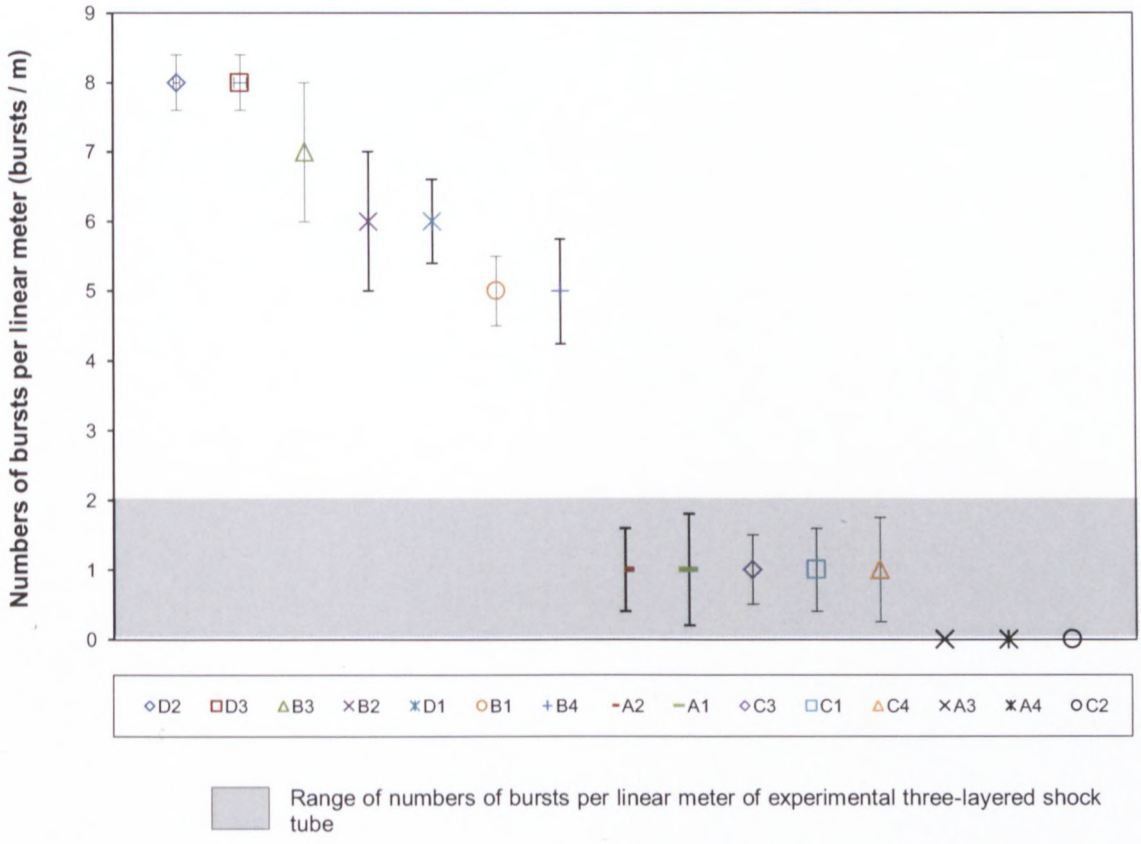

Figure 4.3: Graphical representation of the numbers of bursts per linear meter of shock tubes (at 50°C)

It can be seen from Figure 4.3 that some points representing two-layered shock tubes are within the grey area, while other points also representing two-layered shock tubes are above it. The points within the grey area represent two-layered shock tubes with bursting characteristics similar to those of the three-layered shock tube, and the points above the grey area, represent two-layered shock tubes with bursting characteristics poorer than the three-layered shock tube.

The coexistence of both two-layered shock tubes with bursting characteristics poorer than the three-layered shock tube and two-layered shock tubes with bursting characteristics similar to the three-layered shock tube suggests that the burst strength of a multi-layered shock tube is more dependent on the type of polymeric materials present in the shock tube rather than the numbers of polymeric layers.

4.4.2 Influence of outer layer compositions of two-layered shock tubes on the burst strength

Table 4.B shows the outer layer compositions of two-layered shock tubes having bursting characteristics similar to the three-layered shock tube, while Table 4.C shows the outer layer compositions of two-layered shock tubes having bursting characteristics poorer than the three-layered shock tube.

Table 4.B: Outer layer compositions of two-layered shock tubes exhibiting bursting characteristics similar to the three-layered shock tube

Sample label	Outer layer composition
A1	90% HDPE + 10% HDPE-g-MAH (a)
A2	70% HDPE + 30% HDPE-g-MAH (a)
A3	80% HDPE + 20% HDPE-g-MAH (b)
A4	60% HDPE + 40% HDPE-g-MAH (b)
C1	70% HDPE + 30% ionomer (d)
C2	70% HDPE + 30% ionomer (b)
C3	70% HDPE + 30% ionomer (a)
C4	70% HDPE + 30% ionomer (c)

Table 4.C: Outer layer compositions of two-layered shock tubes exhibiting bursting characteristics poorer than the three-layered shock tube

Sample label	Outer layer composition
B1	60% HDPE + 40% EMA (b)
B2	70% HDPE + 30% EMA (b)
B3	60% HDPE + 40% EMA (a)
B4	50% HDPE + 40% EMA (a)
D1	70% LLDPE + 30% Ionomer (d)
D2	70% LLDPE + 30% Ionomer (a)
D3	70% LLDPE + 30% Ionomer (b)

By looking at Tables 4.B and 4.C, it becomes evident that, the burst strength of a two-layered shock tube can be affected by variations in outer layers' compositions. Moreover, two-layered shock tubes with outer layers made of blends of HDPE/HDPE-g-MAH and HDPE/ionomer would have a better resistance to bursting than two-layered shock tubes with blends of HDPE/EMA and LLDPE/Ionomer.

4.4.2.1 Blends of HDPE/HDPE-g-MAH and HDPE/Ionomer

Two-layered shock tubes were found to be significantly affected by the composition of the outer layer. In particular, the presence of blends of HDPE/HDPE-g-MAH and HDPE/Ionomer in the outer layer was found to generate shock tubes with very few bursts (less than 2 per linear meter of tubing). The relatively good burst strength obtained with these outer layer compositions could be attributed to the presence of HDPE. In fact, HDPE is a polymer consisting of molecules bearing few branches. It is expected that the low level of branches would allow the molecules of HDPE to pack close together, hence strengthening the intermolecular forces. The strong intermolecular forces would enable the outer layer to overcome the sudden stress applied by the shock wave. The shock wave would, therefore, be constrained to propagate in the longitudinal direction of the tube without causing physical damages to the tubing.

Furthermore, the presence of adhesion promoters such as HDPE-g-MAH and ionomers might have added some value to the strength of the outer layer. HDPE-g-

MAH for instance, possesses a HDPE backbone, which can promote compatibility with HDPE of the main polymeric matrix. It could therefore allow the resulting blend to retain the mechanical strength of HDPE. While the ionomer has a molecular structure comprising ionic crosslinks; the presence of ionic crosslink provides the polymer with exceptional intermolecular forces. The exceptional intermolecular forces would enable the shock tube to contain the shock wave without being ruptured.

4.4.2.2 Blends of HDPE/EMA and LLDPE/Ionomer

The presence of LLDPE/Ionomer and HDPE/EMA blends in the outer layer of two-layered shock tubes was found to generate shock tubes with relatively poor burst strengths (between 4 to 8 bursts per linear meters of tubing).

The poor burst strength obtained with blends of HDPE/EMA could be a result of the poor interfacial adhesion between HDPE and EMA which results in high entropy of mixing, and segregation of microphases. The segregation of microphases combined with the poor interfacial adhesion would weaken the radial strength of the shock tube, leading to diminished burst strength.

On the other hand, the poor burst strength observed with blends of LLDPE/Ionomer could result from the presence of LLDPE as main component of the blend. In fact, as opposed to HDPE, LLDPE is polymer consisting of molecules bearing considerable amounts of short branches. The presence of these branches would prevent the molecules from packing close together, hence weakening the intermolecular forces. The weak intermolecular forces of LLDPE would cause the outer layer of the shock tube to have a relatively poor burst strength, despite the presence of ethylene based ionomers as adhesion promoters.

4.5 Breaking strength

The breaking strength test was performed to determine the maximum amount of longitudinal force shock tubes can handle without being torn apart. The test was performed at ambient temperature (about 25 °C). In this section, the breaking strengths of two-layered shock tubes are compared to the three-layered shock tube. The influence of the outer layer compositions of two-layered shock tubes on the breaking strength is also discussed.

4.5.1 Breaking strength comparison between two-layered shock tubes and the three-layered shock tube

Figure 4.4 shows a graphical representation of the breaking strengths of experimental shock tubes. The breaking strengths are plotted here on a single axis (Y-axis). The grey area on the graph represents the range obtained with the three-layered shock tube which varies from 160 to 220 N, while the points plotted represent the ranges obtained with two-layered shock tubes.

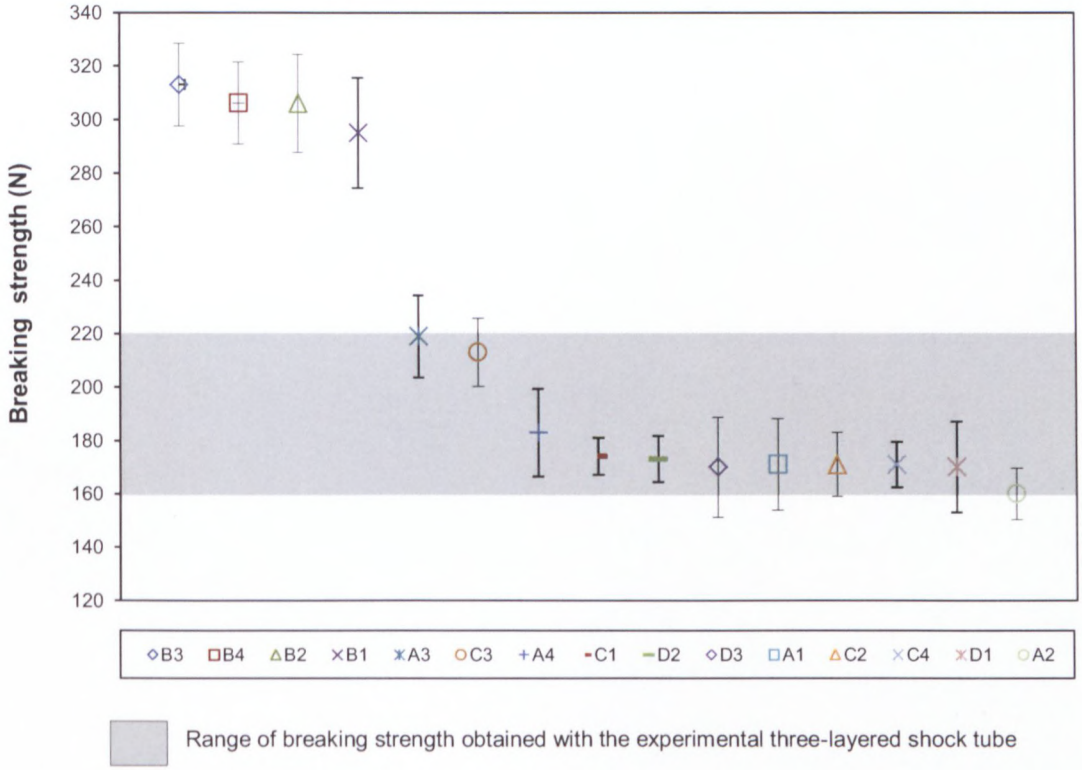

Figure 4.4: Breaking strengths range of experimental shock tubes

It can be observed from Figure 4.4 that, none of the points representing two-layered shock tubes are below the grey area; the points are either within the grey area or above it. This means that all of the experimental two-layered shock tubes possess breaking strengths either superior or similar to the three-layered shock tube. The results obtained here suggest that the removal of the adhesive layer from the structure of a three-layered shock tube combined with the addition of adhesion promoters to polyethylene of the outer layer might not compromise the shock tube breaking strength. However, the discrepancies observed between the points plotted

on the graph indicate that the breaking strength of two-layered shock tubes might be significantly influenced by variations in outer layer compositions.

4.5.2 Influence of outer layer compositions on the breaking strength of two-layered shock tubes

By taking a closer look at Figure 4.4, it can be observe that, samples B3, B4, B2, and B1 are far above the grey area and exhibit the highest breaking strengths. The outer layer compositions of these samples are shown in Table 4.D.

Table 4.D: Outer layer compositions of shock tube samples having the highest breaking strengths

Sample label	Outer layer composition
B1	60% HDPE + 40% EMA (b)
B2	70% HDPE + 30% EMA (b)
B3	60% HDPE + 40% EMA (a)
B4	50% HDPE + 40% EMA (a)

Table 4.D reveals that, two-layered shock tubes with highest breaking strengths are all having identical outer layer components: HDPE and EMA. The use of HDPE/EMA blends in the outer layer of two-layered shock tubes therefore appears to add significant value to the tube's breaking strength. Furthermore, no major differences were observed between the breaking strength of two-layered shock tubes having HDPE as main component of the outer layer (samples C1, C2, and C3) and the corresponding two-layered shock tubes having LLDPE as main component of the outer layer (samples D1, D2, and D3). Hence the substitution of HDPE in the outer layer by LLDPE might not affect the breaking strength of two-layered shock tubes.

The similarity in the breaking strength between two-layered shock tubes having HDPE as the main component of the outer layer and the corresponding two-layered shock tubes having LLDPE as the main component of the outer layer could result from the fact that, the tensile strength of a glassy polymer is not only dependent on the intermolecular forces but also on the molecular weight distribution of the polymer.

It is expected that, polymers with wide molecular weight distribution would require more energy input for rupture.

4.6 Elongation at break

The goal of the elongation at break test was to determine the extent to which shock tubes could be stretched longitudinally without being ruptured. This section compares the elongation at break of two-layered shock tubes to the three-layered shock tube, and then discusses the influence of outer layer compositions on the elongation at break of two-layered shock tubes.

4.6.1 Comparison of elongation at break between two-layered shock tubes and the three-layered shock tube

Results obtained from elongation at break tests are presented in the form of ranges in Figure 4.5.

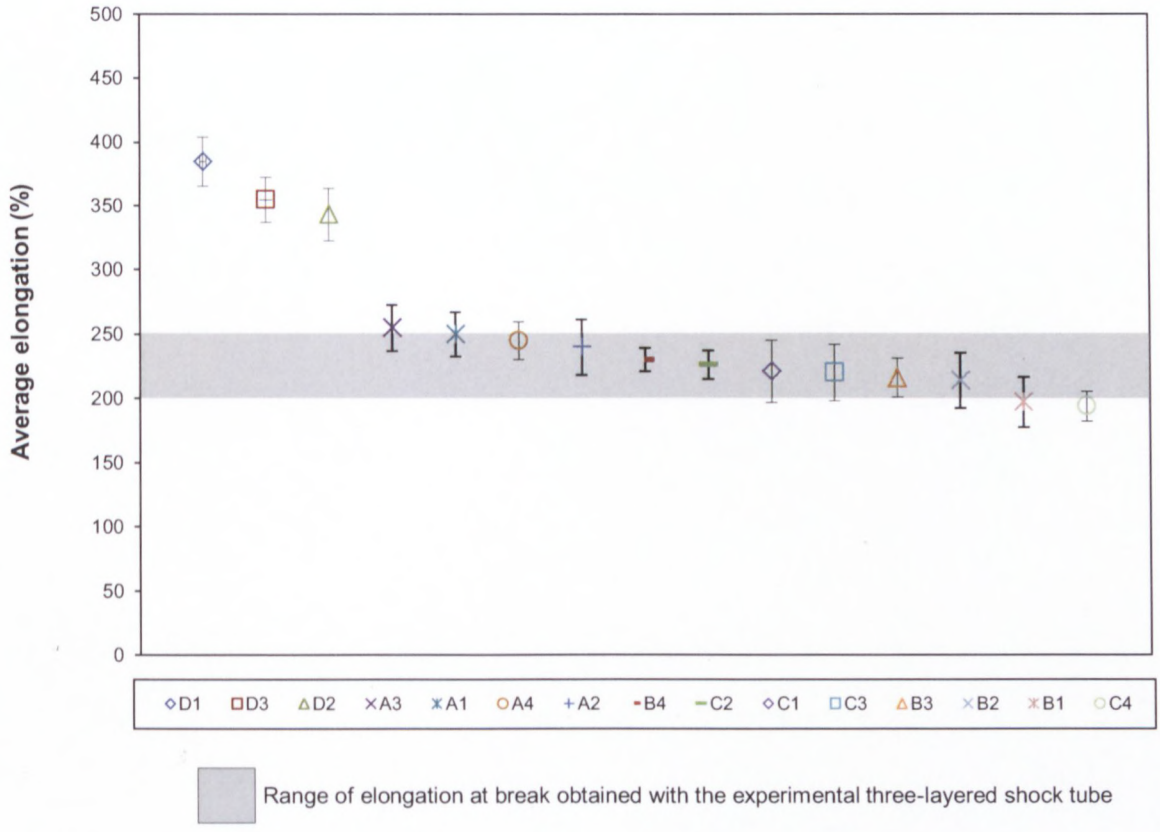

Figure 4.5: Elongation at break of experimental shock tubes

The grey area on the graph (Figure 4.5) represents the range of elongation at break obtained with the three-layered shock tube and it spans from 200 to 250%. The points plotted on the graph represent the range of elongation at break obtained with two-layered shock tubes.

Similar to the breaking strength results (refer to Figure 4.4), none of the points representing two-layered shock tubes are below the grey area; the points are either within the grey area or above it (see Figure 4.5). The results obtained here confirm that two-layered shock tubes with no adhesive layer, and that have adhesion promoters added to polyethylene of the outer layer, have the capability to exhibit mechanical properties comparable to a standard three-layered shock tube.

4.6.2 Influence of outer layer materials on the elongation at break of two-layered shock tubes

It can be observed from Figure 4.5 that samples D1, D2, and D3 have elongation at break far superior the three-layered shock tube. The outer layer compositions of these samples are given in Table 4.E.

Table 4.E: Outer layer compositions of shock tube samples having elongation at break superior to the three-layered shock tube

Sample label	Outer layer composition
D1	70% LLDPE + 30% Ionomer (d)
D2	70% LLDPE + 30% Ionomer (a)
D3	70% LLDPE + 30% Ionomer (b)

Table 4.E reveals that all the two-layered shock tubes having an elongation at break superior to the three-layered shock tube possess identical components in the outer layer, namely LLDPE and ionomer. Hence, despite generating shock tubes with relatively poor radial strength, the presence of LLDPE/ionomer blends in the outer layer of two-layered shock tubes might enhance the extent to which the shock tube is longitudinally stretched without being ruptured.

Table 4.F shows a comparison of elongation at break between two-layered shock tubes with HDPE in the outer layer and the corresponding two-layered shock tubes with LLDPE in the outer layer. It is shown in Table 4.F that, the presence of LLDPE as main component of the outer layer of two-layered shock tubes generates shock tubes with elongation at break much higher than the corresponding tubes with HDPE.

Table 4.F: Comparison between two-layered shock tubes with HDPE in the outer layer and corresponding shock tubes with LLDPE

Sample label	Outer layer composition	Mean elongation at break (%)
D1	70% LLDPE + 30% Ionomer (d)	385
C1	70% HDPE + 30% ionomer (d)	221
D2	70% LLDPE + 30% Ionomer (a)	343
C2	70% HDPE + 30% ionomer (a)	226
D3	70% LLDPE + 30% Ionomer (b)	355
C3	70% HDPE + 30% ionomer (b)	220

4.7 Oil ingression

An oil ingression test was performed to determine the sleep time of the experimental shock tubes in fuel oil. The test was carried out at a temperature of 50°C in paraffin. This section compares the sleep time of two-layered shock tubes to the three-layered shock tube. The influence of the outer layer compositions of two-layered shock tubes on the resistance to oil ingression is also discussed.

4.7.1 Sleep time comparison between two-layered shock tubes and the three-layered shock tube

The sleep time ranges obtained from experimental tests are graphically presented on a single axis (Y-axis) in Figure 4.6. The range for the three-layered shock tube is represented by the grey area and varies from 45 to 48 hours, while the points plotted on the graph represent the sleep time ranges of two-layered shock tubes.

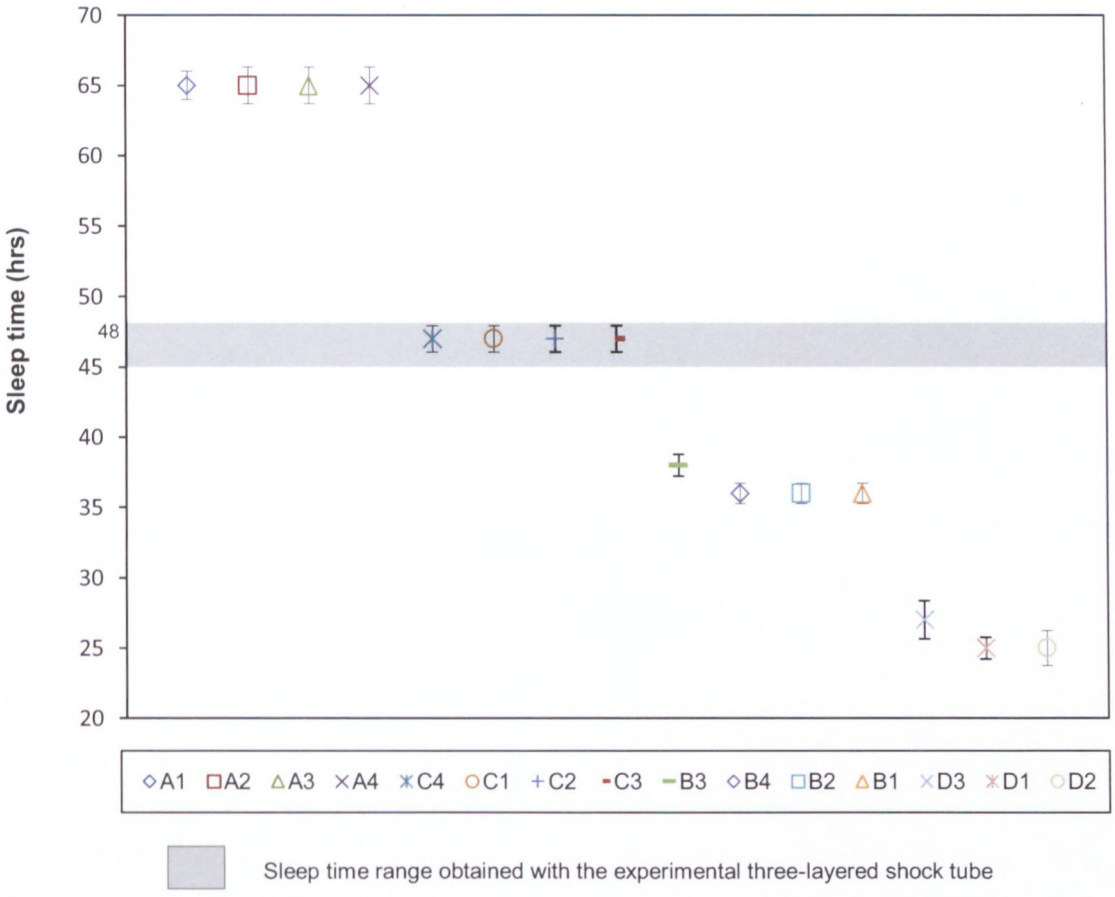

Figure 4.6: Sleep time of experimental shock tube (at 50°C)

It can be seen from Figure 4.6 that two-layered shock tubes can exhibit sleep times similar, superior, or inferior to the standard three-layered shock tube. This suggests that the sleep time of a multi-layered shock tube is dependent on the layer's compositions rather than the number of polymeric layers.

4.7.2 Influence of outer layer compositions on the sleep time of two-layered shock tubes

Tables 4.G, 4.H, and 4.I respectively show the outer layer compositions of two-layered shock tubes with sleep times superior, inferior, and similar to the three-layered shock tube.

Table 4.G: Outer layer compositions of two-layered shock tubes with sleep time superior to the three-layered shock tube

Sample label	Outer layer composition
A1	90% HDPE + 10% HDPE-g-MAH (a)
A2	70% HDPE + 30% HDPE-g-MAH (a)
A3	80% HDPE + 20% HDPE-g-MAH (b)
A4	60% HDPE + 40% HDPE-g-MAH (b)

Table 4.H: Outer layer compositions of two-layered shock tubes with sleep time inferior to the three-layered shock tube

Sample label	Outer layer composition
B1	60% HDPE + 40% EMA copolymer (b)
B2	70% HDPE + 30% EMA copolymer (b)
B3	60% HDPE + 40% EMA copolymer (a)
B4	50% HDPE + 40% EMA copolymer (a)
D1	70% LLDPE + 30% Ionomer (d)
D2	70% LLDPE + 30% Ionomer (a)
D3	70% LLDPE + 30% Ionomer (b)

Table 4.I: Outer layer compositions of two-layered shock tubes with sleep time similar to the three-layered shock tube

Sample label	Outer layer composition
C1	70% HDPE + 30% ionomer (d)
C2	70% HDPE + 30% ionomer (b)
C3	70% HDPE + 30% ionomer (a)
C4	70% HDPE + 30% ionomer (c)

4.7.2.1 Blends of HDPE/HDPE-g-MAH

Two-layered shock tubes with blends of HDPE/HDPE-g-MAH in the outer layer were found to have sleep times varying between 63 and 65 hours, which was almost 20 hours above the sleep time of the three-layered shock tube. The high sleep time obtained here suggested that, the addition of HDPE-g-MAH to HDPE of the outer layer could enhance the barrier properties of a multi-layered shock tube.

The enhancement of barrier properties by HDPE-g-MAH could be attributed to the fact that HDPE-g-MAH is an additive, which not only promotes adhesion but also, improves the thermal resistance of polymers. Its presence in the outer layer would therefore be expected to slow down the heat transfer from the hot oil to the inner tube. Because the diffusion of oil through polymers decreases with a decreasing temperature (Peacock, 2000), the hot oil would also require more time to diffuse through the outer shock tube and this would result in a shock tube with enhanced barrier properties.

4.7.2.2 Blends of HDPE/Ionomer

These blends were found to generate shock tubes with sleep times similar to the three-layered shock tube (between 46 and 47 hours). The sleep times obtained here suggest that the addition of ionomers to HDPE of the outer layer does not compromise the barrier properties of the layer. This could be attributed to the fact that ionomers have a complex molecular structure that allows them to be hardly permeable to both organic and inorganic solvents (Nicholson, 2006). The low permeability of ionomers by solvents would therefore allow the outer layer to slow down the ingression of oil and retain the barrier properties of the main polymer (HDPE).

4.7.2.3 Blends of LLDPE/Ionomer

These blends were found to generate shock tubes with very poor resistance to oil ingression (sleep time between 24 and 26 hours); the sleep time was almost 20 hours lower than both the three-layered shock tube and the corresponding two-layered shock tube with HDPE as main component of the outer layer. The very low sleep time obtained with these blends implies that, the substitution of HDPE of the outer layer by LLDPE might seriously compromise the barrier properties of the shock tube. LLDPE might therefore not be suitable for the outer layer of high performance two-layered

shock tubes. Table 4.J shows a comparison of sleep times of two-layered shock tubes with LLDPE and two-layered shock tubes with HDPE.

Table 4.J: Comparison of sleep times between shock tubes with HDPE and corresponding shock tubes with LLDPE

Sample label	Outer layer composition	Sleep time range (hrs)
D1	70% LLDPE + 30% Ionomer (d)	24 – 26
C1	70% HDPE + 30% ionomer (d)	45 – 47
D2	70% LLDPE + 30% Ionomer (a)	24 – 26
C2	70% HDPE + 30% ionomer (a)	45 – 47
D3	70% LLDPE + 30% Ionomer (b)	24 – 26
C3	70% HDPE + 30% ionomer (b)	45 – 47

The huge difference between the sleep times of two-layered shock tubes having HDPE as main component of the outer layer and the corresponding two-layered shock tubes with LLDPE could once again be due to the difference of the molecular structure of these polymers. Because LLDPE is made of molecules bearing few branches, it would be difficult for its molecules to pack close together during melt solidification. Hence, cavities and gaps would be created in the morphology, resulting in a faster diffusion of oil through the outer layer.

4.7.2.4 Blends of HDPE/EMA

The presence of HDPE/EMA blends in the outer layer of two-layered shock tubes resulted in tubes with sleep times varying between 34 and 36 hours. The sleep times of these tubes were about 10 hours lower than that obtained with the three-layered shock tube. The relatively poor barrier properties obtained here could be a result of the high entropy of mixing between HDPE and EMA. The high entropy of mixing would result in a blend with poor interfacial adhesion between dissimilar micro-phases. The poor interfacial adhesion would eventually lead to the formation of gaps within the polymeric matrix and this would speed up the diffusion of the oil through the outer layer.

4.8 Linear thermal shrinkage

A linear thermal shrinkage test was performed to determine the extent to which experimental shock tubes would shrink when subjected to a high temperature for a defined period of time. The test was carried out at a temperature of 80°C. Results obtained are graphically represented in Figure 4.7 on a single axis (Y-axis). The linear thermal shrinkage range for the three-layered shock tube is represented in Figure 4.7 by the grey area, while the points plotted on the graph represent the linear thermal shrinkage of two-layered shock tubes.

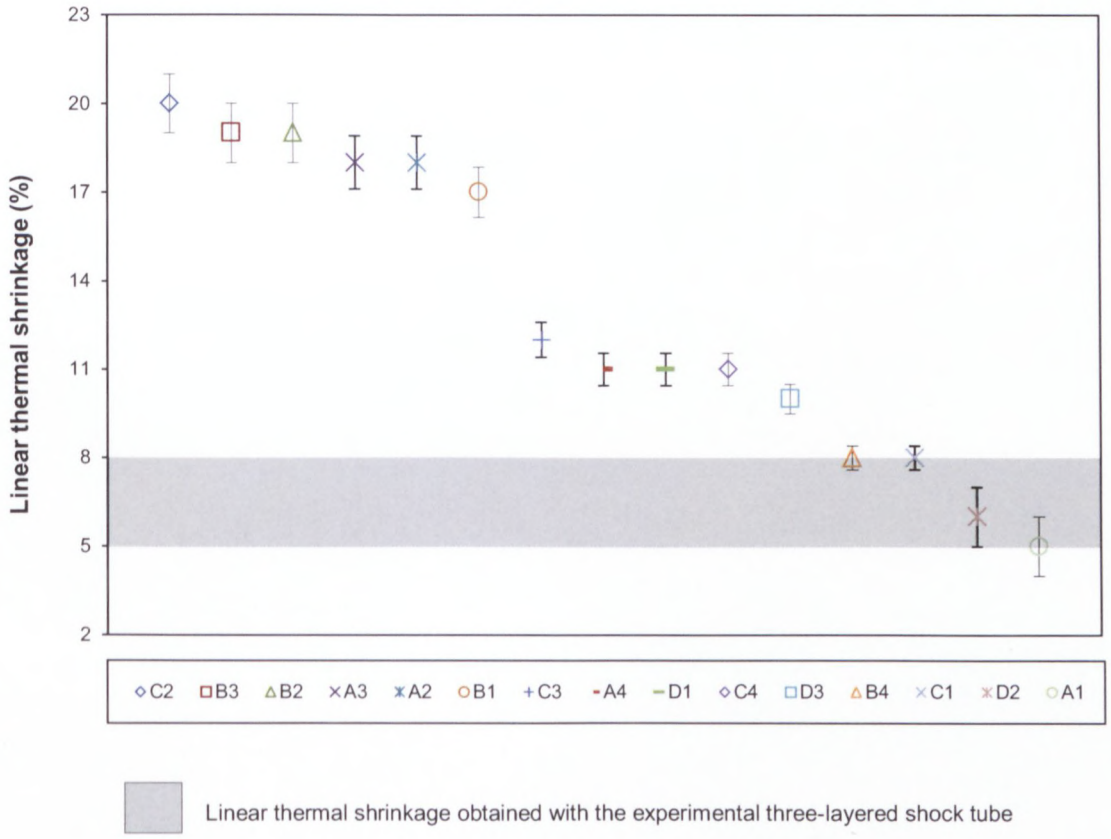

Figure 4.7: Linear thermal shrinkage of experimental shock tubes

It can be observed from Figure 4.7 that, most of experimental shock tubes have linear thermal shrinkages above that of the three-layered shock tube. Exceptions are however observed with samples A1, D2, C1, and B4. Table 4L shows the outer layer compositions of two-layered shock tubes with linear thermal shrinkage similar to the three layer shock tube.

Table 4.K: Outer layer compositions of two-layered shock tubes with linear thermal shrinkage similar to the three-layered shock tube

Sample label	Outer layer composition
A1	90% HDPE + 10% HDPE-g-MAH (a)
D2	70% LLDPE + 30% Ionomer (a)
C1	70% HDPE + 30% ionomer (d)
B4	50% HDPE + 40% EMA copolymer (a)

Table 4.K reveals that two-layered shock tubes with thermal linear shrinkage similar to the three-layered shock tube all have different polymeric compositions in the outer layer. Therefore, there is insufficient evidence to establish a relationship between the type of polymeric materials and the linear thermal shrinkage of multi-layered shock tubes.

The lack of relationship observed between the linear thermal shrinkage of two-layered shock tubes and the outer layer materials could be the result of variations in operating conditions. In fact, in order to ensure a smooth extrusion, the process conditions and particularly, the extrusion temperature was adjusted to the need. Such adjustments might have affected the thermo-mechanical properties of the shock tubes. Further investigation involving process optimization might therefore help lowering the thermal linear shrinkage.

4.9 Peel-off strength

The peel-off test was performed to evaluate the adhesion strength between the outer and inner layers of experimental shock tubes. Figure 4.8 shows a graphical representation of the adhesion strength obtained. The grey area in Figure 4.8 represents the range of adhesion strength for the three-layered shock tube, while the points plotted on the graph represent the range of adhesion strength for two-layered shock tubes.

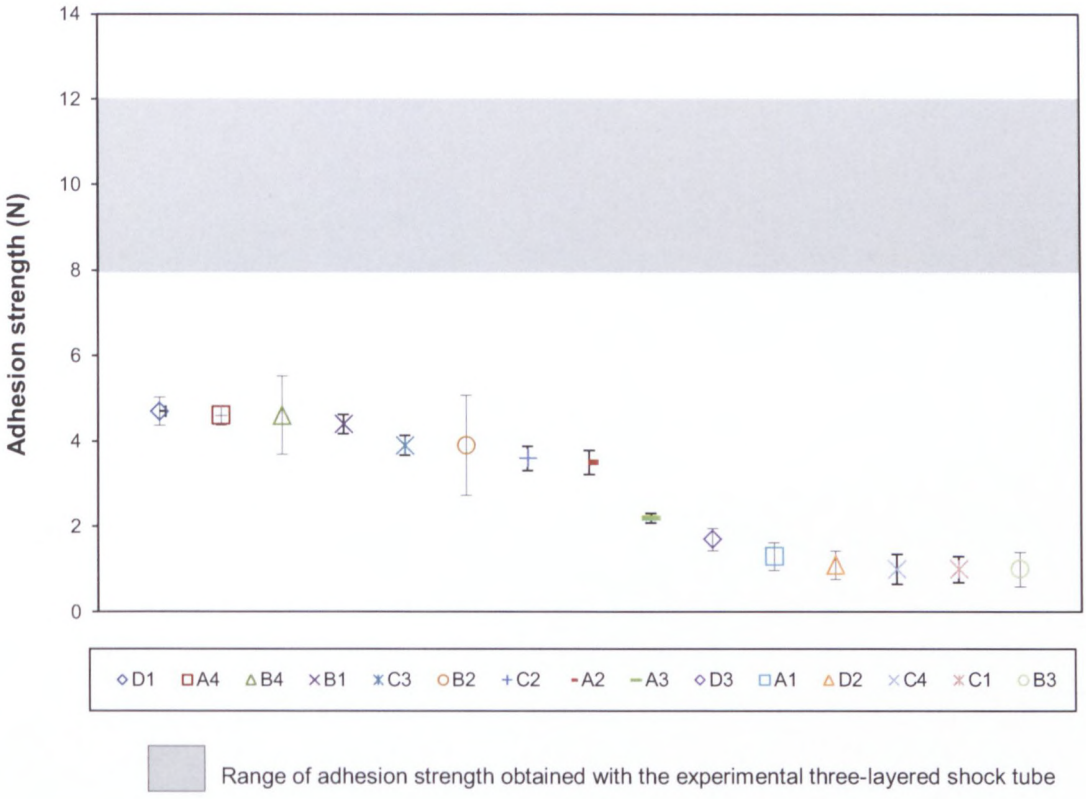

Figure 4.8: Graphical representation of peel off force obtained with experimental two-layered shock tubes

Figure 4.8 clearly indicates that, the adhesion strength between the inner and outer layers of the entire two-layered shock tubes is much poorer than the adhesion strength between the inner and outer layers of the experimental three-layered shock tube. This suggests that, the various adhesion promoters added to polyethylene of the outer layer could not provide the layer with sufficient tackiness. Hence, the removal of the adhesive layer from the structure of a three-layered shock tube combined with the addition of adhesion promoters to polyethylene of the outer layer might generate shock tubes with poor structural integrity.

The relatively poor level of adhesion obtained between the inner and outer layers of two-layered shock tubes might be a result of improper concentration of mechanical stress at the interface of the layers, which could have been caused by the non-optimized dosing of adhesion promoters. In fact, it is expected that, as the numbers of chemical bonds at the interface increases, it passes through a maximum value. Once

the maximum value is passed, the concentration of mechanical stresses at the interface causes the adhesion strength to be weakened (Basin, 1984).

Although the adhesion strength between the inner and outer layers of two-layered shock tubes was found to be lower than the adhesion strength between the inner and outer layers of the three-layered shock tube, the aging process of two-layered shock tubes might favour bonding between the layers, hence improve adhesion.

4.10 Velocity of detonation

Results obtained from velocity of detonation tests were plotted on a single axis as shown in Figure 4.9. The grey area on the graph represents the velocity of detonation (VOD) of three-layered shock tube, while the points plotted represent the VOD of two-layered shock tubes.

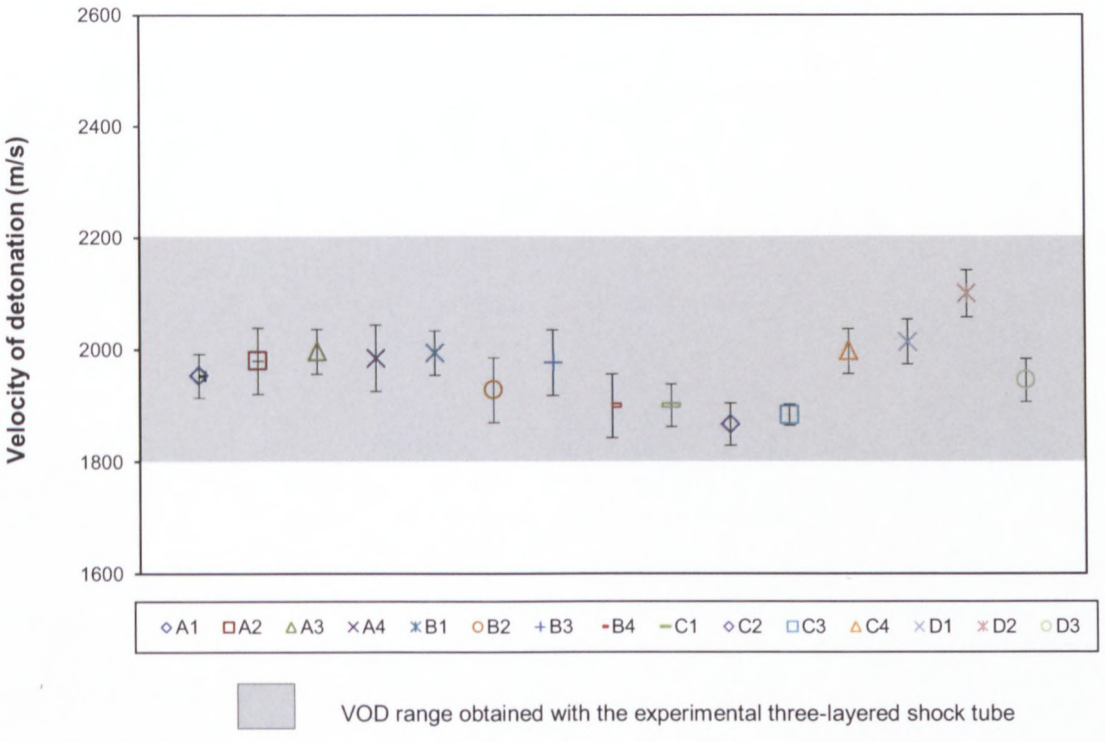

Figure 4.9: Velocity of detonation per sample

It can be seen that, all of the experimental two-layered shock tubes have velocity of detonations comparable to the three-layered shock tube. The results obtained here

suggest that, the elimination the adhesive layer from the structure of a three-layered shock tube combined with the addition of adhesion promoters to polyethylene of the outer layer does not compromise the shock tube's VOD. This was expected, since the core loading was found to be within comparable ranges and all of the experimental shock tubes had an identical inner layer material.

4.11 Summary of comparison of properties between two-layered shock tubes and the three-layered shock tube

Table 4L shows a summary of comparison of properties between the three-layered and two-layered shock tubes.

Table 4.L: Summary of properties comparison between the three-layered shock tube and two-layered shock tubes

Label	Breaking strength	Elongation at break	VOD	Burst strength	Sleep time	Linear shrinkage	Adhesion strength
A1	√	√	√	√	↑	√	×
A2	√	√	√	√	↑	×	×
A3	√	√	√	√	↑	×	×
A4	√	√	√	√	↑	×	×
B1	↑	√	√	×	×	×	×
B2	↑	√	√	×	×	×	×
B3	↑	√	√	×	×	×	×
B4	↑	√	√	×	×	√	×
C1	√	√	√	√	√	√	×
C2	√	√	√	√	√	×	×
C3	√	√	√	√	√	×	×
C4	√	√	√	√	√	×	×
D1	√	↑	√	×	×	×	×
D2	√	↑	√	×	×	√	×
D3	√	↑	√	×	×	×	×

√ Property matches the standard three-layered shock tube

× Property is poorer than the standard three-layered shock tube

↑ Property is superior to the standard three-layered shock tube

One of the goals of this investigation was to compare the properties of various recipes of two-layered shock tubes to that of the standard three-layered shock tube. It can be seen from Table 4.L that, none of the experimental two-layered shock tubes has sets of properties that entirely match the three-layered shock tube. This confirms the uniqueness of the three-layered shock tube and justifies why it is widely used in the industry.

4.12 Selection of new material design for high performance two-layered shock tube

Experimental two-layered shock tubes such as samples A1, A2, A3, A4, C1, C2, C3 and C4 were found to have sets of properties that were very close to the three-layered shock tube. The principal weaknesses of these two-layered shock tubes were their high linear thermal shrinkages and relatively poor level of adhesion strength between the inner and outer layers. Table 4.M shows the ranges of the linear thermal shrinkage, and adhesion strength of samples A1, A2, A3, A4, C1, C2, C3 and C4

Table 4.M: Ranges of linear thermal shrinkage, and peel-off force of samples A1, A2, A3, A4, C1, C2, C3 and C4

Label	Linear shrinkage (%)	Adhesion strength (N)
A1	4 – 6	1 – 2
A2	17 – 19	3 – 4
A3	17 – 19	2 – 3
A4	10 – 12	4 – 5
C1	7 – 9	1 – 2
C2	20 – 22	3 – 4
C3	11 – 13	3 – 4
C4	10 – 11	1 – 2

Property matches that of the three-layered shock tube

Property is poorer than that of the three-layered shock tube

Table 4.M clearly indicates that, sample A4 has a slightly higher level of adhesion between its inner and outer layers, with moderate linear thermal shrinkage. This

sample was also found to have excellent burst strength, moderate breaking strength, good elongation at break, and a significantly high sleep time. For these reasons, the material design used in sample A4 was proposed for manufacture of high performance two-layered shock tubes. The proposed material design consisted of ethylene based ionomer in the inner layer, and a blend of 60%HDPE/40%HDPE-g-MAH in the outer layer.

4.13 Comparison of properties between the proposed two-layered shock tube and commercial high performance three-layered shock tubes

Table 4.N shows a comparison of properties between the two-layered shock tube obtained with the proposed material design (sample A4) and commercially available high performance three-layered shock tubes.

Table 4.N: Comparison of properties between the proposed two-layered shock tube and commercially available three-layered shock tubes

	Range of properties of commercial three-layered shock tubes	Range of properties of the proposed two-layered shock tube
Sleep time in oil (hrs)	45 – 50	63 – 66
Average bursts (No. of bursts per linear meter)	Normally 2 to 5 bursts per 5m of tubing	0
Breaking strength (N)	160 N – 200 N	165 – 180
Elongation at break (%)	200 – 300 %	250 - 260
Adhesion strength (N)	8 – 12	3 – 5
Linear thermal shrinkage (%)	5 – 8	10 – 12
Velocity of detonation (m/s)	1800 – 2200	1900 – 2000

It can be seen from Table 4.N that, the proposed material design generates a shock tube with burst strength, breaking strength, elongation at break, and VOD comparable to commercially available high performance three-layered shock tubes. The sleep time is the proposed two-layered shock tube appears to be higher than the commercially available high performance three-layered shock tubes. The peel strength and linear thermal shrinkage of the proposed shock tube are however, much poorer than that of the commercial tubes.

4.14 Comparison between the proposed two-layered shock tube and Stewart's (2002) single-layered shock tubes

Table 4.O shows a comparison of properties and characteristics between the shock tube obtained with the proposed material design and Stewart's (2002) single layered shock tube.

Table 4.O: Comparative properties of single-layered shock tubes design tested by Stewart (2002) and the proposed two-layered shock tube

Characteristics and Properties	Stewart Tube 1	Stewart Tube 2	Stewart Tube 3	Shock obtained with the proposed material design
Outer diameter (mm)	3.1	3.0	3.1	2.9 – 3.1
Inner diameter (mm)	1.4	1.3	1.4	1.2 – 1.4
Core load (mg/m)	18.9	17.9	18.6	14 – 16
Linear shrinkage (after 1 hr @ 80 °C)	2.2	2.6	2.3	8 – 12
Elongation at break (%)	690	520	520	250 - 260

It can be seen from Table 4.O that, the proposed material design generates a shock tube with a linear thermal shrinkage significantly higher than Stewart's (2002) single-layered shock tubes. The elongation at break of Stewart's (2002) single layered shock tubes also appears to be higher than the proposed material design. The differences in linear thermal shrinkage and elongation at break observed between

Stewart's (2002) shock tubes and the proposed material design might result from the difference in processing conditions; In fact, Stewart's (2002) stretching ratio was about 4:1 while the stretching ratio used in this work was 2:1. No comparative data on oil ingression behaviour, burst strength and breaking strength of Stewart's (2002) single-layered shock tube or any other shock tube previously disclosed was available for evaluation.

4.15 Advantages of new material design over current commercial high performance three-layered shock tubes

The two-layered shock tube obtained with the proposed material design is expected to offer various advantages which can include the following:

- It involves two layers and requires two extruders for manufacturing, as opposed to the three-layered structure, which requires three extruders; hence the manufacturing sequence would be simplified and possibly less expensive.

- It only possesses one interface, as opposed to the three-layered shock tubes which possess two interfaces; therefore the numbers of weak points are expected to be minimized.

- The new material design generates shock tubes with a sleep time of about 65 hours in paraffin which is at least 15 hours above the sleep time of commercially available high performance shock tubes. It would, therefore, offer better flexibility for mining, quarrying, and construction operations.

4.16 Weaknesses of new material design over current commercial high performance three-layered shock tubes

- The new material design generates a shock tube with relatively poor adhesion strength between the inner and outer layers. There is therefore a risk of delamination during handling.

- The shock tube obtained with the proposed material design has a relatively high linear thermal shrinkage which might lead to unwanted phenomenon such as strangulation at the detonator's neck or crimp collapse.

4.17 Summary of key findings

The key findings of the investigation can be summarised as follows:

- It was found that, two-layered shock tubes might exhibit bursting characteristics either similar or poorer than the standard three-layered shock tube, depending on the type of materials present in the outer layer.

- The mechanical properties of two-layered shock tubes produced (breaking strength and elongation at break) were found to be comparable to the standard three-layered shock tube.

- The resistance to oil ingression of two-layered shock tubes was found to be similar, better, or worse than the standard three-layered shock tube depending on the type of materials used in the outer layer.

- The linear thermal shrinkage of some two-layered shock tubes was found to be comparable to the three-layered shock tube. Unfortunately, the results generated could not provide sufficient evidence enabling one to establish a relationship between the linear thermal shrinkage and the type of polymeric materials used in the layers.

- The level of adhesion between the inner and outer layers of the two-layered shock tubes was found to be lowered than the standard three-layered shock tube bearing an adhesive layer.

- It was found that, the elimination of the adhesive layer from the structure of a three-layered shock tube combined with the addition of adhesion promoters to polyethylene of the outer layer does not affect the shock tube's VOD.

- A new material design for the manufacture of high performance two-layered shock tubes was proposed. The proposed material design consisted of 60%HDPE/40%HDPE-g-MAH blend in the outer layer, and ethylene based ionomers in the inner layer. When compared to the commercially available high performance shock tubes, the shock tube obtained with the proposed material design was found to have a higher sleep time, but poorer linear thermal shrinkage and structural integrity. The burst strength, elongation at break,

breaking strength, and VOD of both the proposed two-layered shock tube and commercially available high performance three-layered shock tubes were found to be comparable.

4.18 Conclusion

This chapter presented and discussed the results generated from experimental tests. The properties and performance of two-layered shock tubes were compared against the standard three-layered shock tube extruded and the influence of the numbers of polymeric layers on the properties of multi-layered shock tubes was deduced. The effect of varying the outer layer compositions of two-layered shock tubes was also discussed. Based on the results obtained, a new material design for the manufacture of high performance two-layered shock tubes was proposed.

Chapter 5 : Summary and Conclusions

5.1 Summary

The objectives of this investigation were firstly to compare the properties of various recipes of two-layered shock tubes against a standard three-layered shock tube, then deduce the influence of the numbers of polymeric layers on the properties and performance of multi-layered shock tubes. Secondly, to determine the effect of varying the outer layer compositions of two-layered shock tubes on the tubes' properties and performance. Finally, to recommend a material design for the manufacture of high performance two-layered shock tubes.

In order to meet the objectives, a standard three-layered shock tube and various recipes of two-layered shock tubes were extruded using a commercial extrusion line. The three-layered shock tube was made of high density polyethylene in the outer layer, ethylene based ionomer in the inner layer and ethylene acrylic acid copolymer in the intermediate layer. Samples of two-layered shock tubes consisted of ethylene based ionomer in the inner layer and various blends of polyethylene/Adhesion promoter in the outer layer. Two types of polyethylene were used in the outer layer of two-layered shock tubes, high density polyethylene (HDPE) and linear low density polyethylene (LLDPE). The adhesion promoters used in the outer layer of two-layered shock tubes consisted of ethylene based ionomers, high density polyethylene grafted with maleic anhydride (HDPE-g-MAH), and ethylene methacrylic acid copolymers (EMA). The properties of both three-layered and two-layered shock tubes were evaluated using series of tests which included: breaking strength, elongation at break, linear thermal shrinkage, oil ingression, peel-off test, burst strength, and velocity of detonation. The main findings of the investigation can be summarised as follow:

- It was found that, two-layered shock tubes might exhibit a couple of properties similar, superior or poorer than the standard three-layered shock tube, depending on the type of materials present in the outer layer. It was then deduced that, the properties of multi-layered shock tubes are more influenced by the layers' compositions, rather than the numbers of polymeric layers.

- The variation of the outer layer compositions of two-layered shock tubes was found to have a significant impact on some of the shock tube's properties namely:

oil ingression and burst strength. The breaking strength, elongation at break, and velocity of detonation did not seem to be greatly affected by the variation in outer layer materials.

- Based on the results obtained, a new material design for the manufacture of high performance two-layered shock tubes was proposed. The new material design consisted of an ethylene based ionomer in the inner layer, and a blend of 60%HDPE / 40%HDPE-g-MAH in the outer layer. When compared against commercially available high performance three-layered shock tubes, the shock tube obtained with the proposed material design was found to have better resistance to oil ingression, but poorer structural integrity and linear thermal shrinkage.

5.2 Commercial value addition

The work was expected to be value-adding to the explosive and polymer industries with regard to the optimum design of polymeric materials for high performance two-layered shock tubes. This work was also expected to enrich the published literature describing the response of polymeric materials on multi-layered shock tubes.

5.3 Conclusions

The development of high performance two-layered shock tubes with properties either similar or superior to a high performance three-layered shock tube is a real possibility. However, more comprehensive work on materials design toward optimization is required.

5.4 Recommendations for future work

The following recommendations for future work are expected to enhance current understanding and scientific value addition in making high performance shock tubes:

- Further investigations could be value-adding on two-layered shock tube material design; such investigations should involve the modification of inner layer materials that can enhance resistance to oil diffusion and higher level of adhesion with respect to the outer layer materials.

- Investigations on process optimization could be conducted in order to improve some properties of the two-layered shock tubes, such as the linear thermal shrinkage.

- Further investigations on two-layered shock tubes and involving different polymeric materials for the outer layer such as nylon 6, and polypropylene should be considered.

References

Adur, A.M., Schemukler, S., Shida, M., & Machonis, J. 1984. US Patent 4460632.

Awaja, F., Gilbert, M., Georgina, K., Fox, Bronwyn., & Pigram, P.J. 2009. Adhesion of Polymers. *Progress in Polymer Science*, 34 (9): 948-968.

Basin, V.E. 1984. *Progress in Organic Coatings*, Volume 12: 213-250.

Bataille, P., & Schreiber, H.P. 1987. Mechanical Properties and Permeability of Polypropylene and Poly(ethylene terephthalate). *Polymer Engineering Science*: 27-622.

Bateup. 1978. Surface Chemistry and Adhesion. *International Journal of Adhesion and Adhesives*. Elsevier: 233-239.

Bersted, B., & Cohen, S.A. 2008. *Polyolefin Resins*. McGraw-Hill Companies.

Bicerano, J. 1996. *Prediction of Polymer Properties*. New York: Derek M.

Bower, D.I. 2002. *An Introduction to Polymer Physics*. Cambridge: Cambridge University Press.

Brent, G.F., & Harding, M.D. 1993. *Shock Tube Initiator.*: US Patent 5243913.

Brust, G. 2005. http//pslc.ws/macrog/ionomer. [21 June 2010].

Brydson, J.A. 1988. *Plastic Materials*, 5th ed. Oxford: Butterworth- Heinneman: 217-218.

Buchanan, D.R. 1992. *Thermomechanical Responses of Fibres*. Advances In Fibres Science. United Kingdom, the textile institute: 88-111.

Burkdoll, F.B. 1981. Explosive Technology Fairfield, California, Patent No. US4220087.

Chanda, M., & Roy, S.K. 2006. *Plastics Technology Handbook*. 4th ed. CRC Press/ Taylor & Francis Group.

Deanin, R.D. 1972. Polymer Structure. *Properties and Applications*. Cahners Books: 53-316.

Elman, Johs, B.D., Long, T.E., & Koberstein, J.T. 1994. A Neutro Reflectivity Investigation of the Surface Interface Segregation of Polymer Functional end Groups. *Macromolecules:* 5341-5349.

Falsafi, A., Tirrell, M., & Pocius, A.V. 2000. *Compositional Effect on the Adhesion of Acrilic Pressure Sensitive Adhesives.* Langmuir.

Gaydon, A.G., & Hurle, I.R. 1963. *The Shock Tube in High Temperature Chemical Physics.* New York: Reinhold Publishing.

Gladden, E.I., Gary, R., Thureson. Zappalotti, A., Davis. Frank, E.R,. Lucca, J. 1997. *Signal Transmission Fuse*. US Patent 5597973.

Halasz, L., 1993. *Control Methods in Polymer Processing*. Science Direct: 5-10.

Halliday, L.E. 1975. *Introduction to Ionomers*. New York: Wiley.

Han, C.D. 2007. *Rheology and Processing of Polymeic Materials, Volume 2*. Oxford: Oxford University Press.

Hennemann, O.D., Kranz, R., Luschen, Gesang, T., Schett, V., Stohrer, W.D. 1994. The Effect of Flurination on the Surface Characteristics and Adhesive Properties of Polethylene Polypropylene. In: *Adhesion and Adhesive*, Volume 14 (4): 209-271.

Koberstein, J.T., & O'rourke-muisener, P.A.V. 2003. Optimal Chain Architechtures for the Molecular Design of Functional Polymer Surfaces. *American Chemical Society, Macromolecules*: 771-781.

Kristensen, L., Lundborg, H., & Nyqvist, S. 1982. *Low-energy fuse consisting of a plastic tube the inner surface of which is coated with explosive in powder form.* US, Patent 4328753.

Kroschwitz, J.I. 1991. *High Performance Polymers and Composites. Encyclopedia reprint series.* Wiley-Interscience Pubication, John Wiley & Sons.

Kumar, A. & Gupta, R. 2003. *Fundamentals of polymer engineering*, 2nd ed... Marcel Dekker.

Kumar, A., & Gupta, R.K. 1998. *Fundamental of Polymer engineering*, 2nd ed. McGraw-Hill companies: 29-47.

Laksmanan, P.R., & Carrier, P.J. 1989. *Compatible polymer blends useful as melt adhesives (III)*. US Patent 4826909.

Lauren, C., Creton, C., & Leger, I. 2004. Adhesion Promotion Between a Homopolymer Probe and a Glass Substrate Coated with a Block Copolymer Monolayer. *Macromolecules*: 8924-8932.

Longworth, R. 1975. *Ionomic Polymers. Material science series.* Applied science publishers.

Macknight, W.J., & Earnest, J.T.R. 1981. Structure and Propetries of Ionomers. Journal of Polymer Science, *Macromolecular review*, volume 16: 41-122.

Mandelkern, L., & Alamo, R.G. 1999. *Polymer Data Handbook*. Oxford: Oxford University Press.

Meier, L., & Ludwigshafen. 1993. *Plastics Additives Handbook: Stabilizers and Processing Aids, Plasticizers, Fillers, Reinforcements, colorant for thermoplastics.* 4th ed. Hanser Publishers.

Nicholson, J.W. 2006. *The Chemistry of Polymers*, 3rd ed. The royal society of chemistry: 149-152.

Peacock, A.J. 2000. *Handbook of Polyethylene*. Marcel Dekker: 13-30.

Persson, P.A. 1968. US Patent 3590739.

Petrie, E.M. 2007. *Handbook of Adhesives and Sealants*. Graw-Hill: 48-55.

Du Pont. n.d.. *Du Pont Surlyn.*., http://www2.dupont.com/Surlyn/en_US/ [1 July 2010].

Qin, R.Y., & Schreiber, H.P. 1999. *Colloids and Surfaces A: Physicochemical and Engineering Aspects*. Elesevier: 85-93.

Rostami, S., & Miles, I.S. 1992. *Multicomponent Polymer Systems. Polymer Science and Technology Series*. Longman Oublishers: 63-99.

Shida, M., Machonis, J., & Zeitlin, R. J. 1978. *Adhesive Blends.* US Patent 4087587.

Simon, J.R., & Welburn, D.J. 1985. *Reinforced Explosive Shock Tube.* US Patent 4493261.

Sperling, L.H. 2006. *Introduction to Physical Polymer Science*. John Wiley & Sons INC Publication.

Stewart, R.F., Welburn, D.J., Welsh, D.M., & Greenhorn, R.C. 2002. *Low Energy Fuse Method and Manufacture.* US Patent RE37689E.

Stewart, R.F., Welburn, D.J., Welsh, D.M., & Greenhorn, R.C. 1996. *Low Energy Fuse Method and Manufacture*, US Patent 5509355.

Stewart, R.F., Welburn, D.J., & Greenhorn, R.C. 1994. *Low Energy Fuse Method and Manufacture*, US Patent 5317974.

Stewart, R.F. 1992. *Low Energy Fuse. US Patent* 5166470.

Tadmor, Z., & Gogos, C.G. 2006. *Principles of Polymer Processing,* 2nd ed. New Jersey: Wiley Interscience.

Tanabe, H., Ohgaki, A. & Ohsugi, H. 1996. Surface properties of polymer films including multiblock copolymer. *Progress in organic coating*: 167-173.

Taylor, J.R. 1997. *An Introduction to Error Analysis. The Study of Experimental Uncertainties in Physical Measurements*. 2nd ed. University science book.

Thureson, G.R., & Gladden, E.I. 1986. *Laminated fuse and manufacturing process therefor. US* Patent 4607573.

Toro, P., Quijada, R., Murillo, O., & Mehrdad, Y. 2005. *Polymer international*: 4-730.

Tressaud, A., Durand, E., Labrugere, C., Kharitonov, A.P., & Kharitonova, L.N. 2007. Modification of Surface Properties of carbon-bases and Polymeric Materials through Fluorinated Routes; from Fundamental Research to Industrial Applications. *Journal of Fluorine Chemistry*: 378-391.

Vanhoorne, P., & Nicolai, D. 1995. Effect of Blend Ionomers on the Strain Hardening of Polyester-Type Elastomer/Ionomer Blends. *Macromolecules*: 3553-3561.

Vasile, C., & Pascu, M. 2005. *Practical Guide to Polyethylene*. Rapra Technology Limited.

Voyutskii, S.S. 1963. *Autohesion and Adhesion of High Polymers*. New York: John Wiley & Sons Inc.

Wolfensberger, M., Mathieson, I., & Brewis, D.M. 1995. Treatment of Low Energy Surfaces for Adhesive Bonding. *International Journal of Adhesion and Adhesives*, Volume 15 (2): 87-90.

Zhang, J., Subir, D., Rahul, R., Wunder, S., Baran, G.R., Fisher, E. 2006. Chemical surface treatment of ultrahigh molecular weight polyethylene for improved adhesion to methacrylate resins. *Journal of Applied Polymer Science*. Elsevier: 72-1564.

Appendix A: Temperature profile of extruders

Table A 1: Temperature profile of extruder 1

	Pre-set value (°C)	Actual value (°C)
Zone 1	100	99
Zone 2	140	141
Zone 3	170	172
Zone 4	185	181
Zone 5	200	199
Clamp	210	211
Neck	210	210
Head	210	209
Nozzle	210	211

Table A 2: Temperature profile of extruder 3 for the extrusion of sample A1

	Pre-set value (°C)	Actual value (°C)
Zone 1	190	188
Zone 2	240	239
Zone 3	245	245
Zone 4	250	249
Zone 5	250	249
Clamp	250	250
Neck	250	251
Head	250	250
Nozzle	250	249

Table A 3: Temperature profile of extruder 3 for the extrusion of sample A2

	Pre-set value (°C)	Actual value (°C)
Zone 1	155	150
Zone 2	240	238
Zone 3	255	253
Zone 4	260	258
Zone 5	260	259
Clamp	260	261
Neck	265	263
Head	265	264
Nozzle	265	264

Table A 4: Temperature profile of extruder 3 for the extrusion of sample A3

	Pre-set value (°C)	Actual value (°C)
Zone 1	190	189
Zone 2	240	238
Zone 3	245	243
Zone 4	255	254
Zone 5	255	256
Clamp	255	255
Neck	255	255
Head	255	254
Nozzle	260	259

Table A 5: Temperature profile of extruder 3 for the extrusion of sample A4

	Pre-set value (°C)	Actual value (°C)
Zone 1	180	180
Zone 2	190	189
Zone 3	210	208
Zone 4	230	229
Zone 5	240	238
Clamp	240	240
Neck	240	240
Head	240	241
Nozzle	240	240

Table A 6: Temperature profile of extruder 3 for the extrusion of sample B1

	Pre-set value (°C)	Actual value (°C)
Zone 1	180	180
Zone 2	200	202
Zone 3	220	222
Zone 4	230	230
Zone 5	230	232
Clamp	230	231
Neck	230	230
Head	230	231
Nozzle	230	230

Table A 7: Temperature profile of extruder 3 for the extrusion of sample B2

	Pre-set value (°C)	Actual value (°C)
Zone 1	170	170
Zone 2	200	199
Zone 3	210	209
Zone 4	230	232
Zone 5	230	230
Clamp	230	228
Neck	230	230
Head	230	232
Nozzle	230	23

Table A 8: Temperature profile of extruder 3 for the extrusion of sample B3

	Pre-set value (°C)	Actual value (°C)
Zone 1	180	178
Zone 2	200	198
Zone 3	220	222
Zone 4	230	229
Zone 5	235	234
Clamp	235	235
Neck	235	234
Head	235	234
Nozzle	235	234

Table A 9: Temperature profile of extruder 3 for the extrusion of sample B4

	Pre-set value (°C)	Actual value (°C)
Zone 1	160	160
Zone 2	170	169
Zone 3	190	190
Zone 4	210	209
Zone 5	220	221
Clamp	220	219
Neck	220	219
Head	220	219
Nozzle	220	220

Table A 10: Temperature profile of extruder 3 for the extrusion of sample C1

	Pre-set value (°C)	Actual value (°C)
Zone 1	170	168
Zone 2	180	178
Zone 3	210	210
Zone 4	215	214
Zone 5	215	214
Clamp	215	213
Neck	215	214
Head	215	214
Nozzle	215	214

Table A 11: Temperature profile of extruder 3 for the extrusion of sample C2

	Pre-set value (°C)	Actual value (°C)
Zone 1	170	166
Zone 2	180	178
Zone 3	190	188
Zone 4	200	201
Zone 5	210	209
Clamp	210	209
Neck	210	210
Head	210	211
Nozzle	210	210

Table A 12: Temperature profile of extruder 3 for the extrusion of sample C3

	Pre-set value (°C)	Actual value (°C)
Zone 1	170	169
Zone 2	180	179
Zone 3	190	190
Zone 4	220	219
Zone 5	220	219
Clamp	220	220
Neck	220	222
Head	220	221
Nozzle	220	220

Table A 13: Temperature profile of extruder 3 for the extrusion of sample C4

	Pre-set value (°C)	Actual value (°C)
Zone 1	170	167
Zone 2	190	189
Zone 3	210	209
Zone 4	220	219
Zone 5	230	229
Clamp	230	230
Neck	230	230
Head	230	231
Nozzle	230	231

Table A 14: Temperature profile of extruder 3 for the extrusion of sample D1

	Pre-set value (°C)	Actual value (°C)
Zone 1	150	146
Zone 2	180	179
Zone 3	190	189
Zone 4	195	194
Zone 5	210	210
Clamp	210	209
Neck	210	209
Head	210	209
Nozzle	210	210

Table A 15: Temperature profile of extruder 3 for the extrusion of sample D2

	Pre-set value (°C)	Actual value (°C)
Zone 1	150	149
Zone 2	180	179
Zone 3	190	191
Zone 4	200	199
Zone 5	200	201
Clamp	200	200
Neck	200	199
Head	200	200
Nozzle	200	200

Table A 16: Temperature profile of extruder 3 for the extrusion of sample D3

	Pre-set value (°C)	Actual value (°C)
Zone 1	150	148
Zone 2	180	178
Zone 3	200	199
Zone 4	205	204
Zone 5	210	209
Clamp	210	209
Neck	210	209
Head	210	209
Nozzle	210	209

Table A 17: Temperature profile of extruder 2 for the extrusion of the tree-layered shock tube

	Pre-set value (°C)	Actual value (°C)
Zone 1	120	98
Zone 2	140	119
Zone 3	160	158
Zone 4	190	189
Zone 5	205	200
Clamp	205	203
Neck	205	205
Head	205	205
Nozzle	205	205

Table A 18: Temperature profile of extruder 3 for the extrusion of the tree-layered shock tube

	Pre-set value (°C)	Actual value (°C)
Zone 1	140	117
Zone 2	150	136
Zone 3	160	159
Zone 4	190	187
Zone 5	220	218
Clamp	220	219
Neck	220	219
Head	220	220
Nozzle	220	220

Appendix B: Raw data collected during tests

Table B 1: Inner diameters raw data

	Specimens' inner diameters									
Sample	*1*	*2*	*3*	*4*	*5*	*6*	*7*	*8*	*9*	*10*
A1	1.24	1.26	1.28	1.23	1.26	1.25	1.28	1.25	1.26	1.24
A2	1.19	1.2	1.15	1.17	1.22	1.2	1.24	1.26	1.22	1.23
A3	1.2	1.1	1.11	1.1	1.13	1.12	1.18	1.14	1.18	1.14
A4	1.13	1.15	1.12	1.17	1.16	1.14	1.1	1.26	1.15	1.18
B1	1.15	1.2	1.16	1.18	1.12	1.2	1.18	1.24	1.17	1.17
B2	1.22	1.19	1.17	1.21	1.22	1.25	1.21	1.19	1.25	1.25
B3	1.15	1.22	1.12	1.13	1.11	1.15	1.2	1.22	1.14	1.11
B4	1.22	1.28	1.23	1.21	1.23	1.25	1.26	1.28	1.27	1.25
C1	1.12	1.16	1.18	1.12	1.17	1.19	1.15	1.18	1.12	1.23
C2	1.2	1.22	1.19	1.15	1.18	1.23	1.19	1.18	1.155	1.2
C3	1.21	1.18	1.16	1.17	1.22	1.2	1.24	1.21	1.22	1.19
C4	1.13	1.18	1.15	1.11	1.14	1.16	1.09	1.2	1.18	1.2
D1	1.15	1.24	1.18	1.22	1.18	1.11	1.21	1.19	1.22	1.23
D2	1.12	1.18	1.16	1.13	1.19	1.15	1.2	1.14	1.19	1.15
D3	1.23	1.18	1.2	1.16	1.24	1.17	1.19	1.18	1.22	1.25
Three-layered	1.07	1.09	1.05	1.11	1.16	1.08	1.15	1.12	1.09	1.15

Table B 2: Outer diameters raw data

	Specimens' outer diameters									
Sample	*1*	*2*	*3*	*4*	*5*	*6*	*7*	*8*	*9*	*10*
A1	3.05	3.03	3.00	2.95	2.93	3.05	2.99	3.01	2.98	2.96
A2	2.85	2.99	2.89	3.02	2.94	3.01	3.06	3.02	3.01	3.07
A3	2.99	3.01	3.06	3.05	2.99	3.01	3.01	3.01	2.94	2.90
A4	2.98	2.88	2.90	3.04	2.90	2.89	2.98	3.03	2.91	3.07
B1	2.95	3.05	3.03	2.89	3.03	3.04	2.95	2.90	3.02	2.86
B2	2.95	3.03	3.00	2.95	2.93	3.05	2.99	3.01	2.98	2.96
B3	2.90	2.92	2.87	3.01	2.90	3.02	2.86	3.00	2.88	3.04
B4	3.00	2.89	2.87	2.98	2.91	2.88	2.98	2.89	2.85	2.99
C1	3.07	3.02	3.00	2.95	2.93	2.89	2.94	3.02	3.00	3.08
C2	3.06	3.05	2.99	3.00	3.05	2.99	2.89	3.01	2.86	3.05
C3	3.05	2.90	3.02	2.95	2.94	2.99	3.05	2.97	3.07	3.05
C4	2.90	3.02	3.96	2.99	3.01	3.01	2.98	3.05	2.93	3.10
D1	3.05	2.96	2.98	2.89	2.85	2.93	3.06	2.89	3.00	2.94
D2	2.98	2.90	3.00	2.95	2.93	3.06	3.09	3.10	3.04	3.12
D3	3.00	2.95	2.92	2.89	3.06	3.00	2.90	2.86	3.12	3.15
Three-layered	3.01	2.85	3.08	2.99	2.94	3.05	2.99	2.96	2.89	3

Table B 3: Outer layer thickness raw data

	Specimens' thicknesses (mm)									
Sample	*1*	*2*	*3*	*4*	*5*	*6*	*7*	*8*	*9*	*10*
A1	0.40	0.55	0.50	0.41	0.55	0.56	0.47	0.42	0.54	0.38
A2	0.41	0.39	0.45	0.48	0.56	0.59	0.57	0.55	0.57	0.50
A3	0.45	0.49	0.39	0.47	0.46	0.50	0.48	0.44	0.40	0.39
A4	0.50	0.49	0.42	0.54	0.47	0.55	0.48	0.44	0.48	0.41
B1	0.58	0.54	0.59	0.56	0.49	0.52	0.55	0.48	0.52	0.50
B2	0.51	0.51	0.47	0.59	0.45	0.47	0.45	0.41	0.43	0.46
B3	0.53	0.47	0.42	0.47	0.53	0.54	0.43	0.52	0.53	0.55
B4	0.46	0.48	0.46	0.44	0.47	0.43	0.52	0.50	0.43	0.49
C1	0.56	0.58	0.49	0.56	0.49	0.48	0.45	0.50	0.59	0.57
C2	0.47	0.59	0.49	0.58	0.43	0.45	0.54	0.47	0.58	0.54
C3	0.59	0.57	0.54	0.49	0.50	0.53	0.49	0.59	0.57	0.55
C4	0.54	0.47	0.55	0.43	0.41	0.59	0.52	0.54	0.56	0.53
D1	0.57	0.56	0.58	0.58	0.50	0.58	0.56	0.55	0.59	0.55
D2	0.59	0.58	0.56	0.52	0.55	0.46	0.59	0.57	0.54	0.58
D3	0.52	0.48	0.46	0.52	0.49	0.55	0.57	0.54	0.47	0.45
Three-layered	0.47	0.45	0.49	0.48	0.46	0.44	0.45	0.47	0.49	0.48

Table B 4: Inner layer thickness raw data

	Specimens' thicknesses (mm)									
Sample	*1*	*2*	*3*	*4*	*5*	*6*	*7*	*8*	*9*	*10*
A1	0.42	0.46	0.42	0.45	0.40	0.43	0.45	0.42	0.39	0.40
A2	0.43	0.38	0.42	0.38	0.40	0.45	0.50	0.41	0.38	0.40
A3	0.58	0.58	0.55	0.58	0.56	0.53	0.59	0.58	0.59	0.56
A4	0.45	0.47	0.45	0.48	0.53	0.50	0.48	0.45	0.50	0.49
B1	0.53	0.54	0.43	0.57	0.54	0.55	0.46	0.59	0.57	0.54
B2	0.47	0.43	0.52	0.54	0.47	0.45	0.45	0.41	0.43	0.46
B3	0.47	0.53	0.54	0.46	0.53	0.54	0.43	0.52	0.53	0.55
B4	0.44	0.47	0.43	0.52	0.47	0.43	0.52	0.50	0.43	0.49
C1	0.40	0.42	0.48	0.45	0.43	0.40	0.45	0.46	0.42	0.42
C2	0.50	0.43	0.45	0.41	0.43	0.45	0.54	0.47	0.44	0.54
C3	0.49	0.50	0.53	0.49	0.50	0.53	0.49	0.59	0.57	0.55
C4	0.43	0.41	0.59	0.52	0.41	0.59	0.52	0.54	0.56	0.53
D1	0.58	0.50	0.58	0.56	0.50	0.58	0.56	0.55	0.59	0.55
D2	0.52	0.55	0.46	0.50	0.49	0.46	0.52	0.50	0.54	0.52
D3	0.52	0.40	0.44	0.42	0.41	0.55	0.41	0.54	0.47	0.45
Three-layered	0.50	0.42	0.47	0.52	0.45	0.39	0.42	0.46	0.40	0.44

Table B 5: Adhesive layer thickness raw data

	Specimens' thicknesses (mm)									
Sample	*1*	*2*	*3*	*4*	*5*	*6*	*7*	*8*	*9*	*10*
Three-layered	0.1	0.13	0.11	0.09	0.11	0.13	0.09	0.11	0.12	0.09

Table B 6: Core load raw data

	Core load per specimen tested (mg/m)									
Sample	*1*	*2*	*3*	*4*	*5*	*6*	*7*	*8*	*9*	*10*
A1	12	17	15	11	16	14	12	13	12	16
A2	15	12	13	13	17	12	15	14	16	17
A3	17	15	15	14	14	16	14	16	15	15
A4	16	14	12	14	16	15	17	17	16	16
B1	17	17	15	14	16	17	17	14	15	16
B2	15	15	16	17	17	15	16	16	17	17
B3	15	17	16	16	15	13	15	14	14	16
B4	17	15	14	14	16	17	16	12	13	15
C1	16	16	15	15	16	15	17	17	17	11
C2	17	15	11	16	17	14	14	17	16	12
C3	17	16	16	16	13	14	12	12	16	16
C4	11	13	14	14	15	14	12	11	11	11
D1	16	16	16	15	17	17	14	16	15	17
D2	14	17	17	14	15	12	16	17	17	17
D3	12	17	15	14	12	16	17	11	12	11
Three-layered	15	16	12	11	17	15	13	14	12	17

Table B 7: Bursts strength raw data

	Numbers of bursts recorded per specimen tested (burst /m)									
Sample	*1*	*2*	*3*	*4*	*5*	*6*	*7*	*8*	*9*	*10*
D2	8	9	6	7	7	10	10	10	8	7
D3	8	6	8	8	7	6	10	7	9	10
B3	7	7	8	7	8	7	6	8	7	7
B2	6	5	7	6	7	6	5	4	6	6
D1	6	6	8	5	6	6	5	4	7	6
B1	5	5	5	5	6	6	6	5	4	5
B4	5	4	5	6	7	5	4	4	5	6
A2	1	1	0	1	0	0	1	0	1	0
A1	1	0	0	0	1	1	0	0	1	1
C3	1	1	1	0	0	1	0	0	1	0
C1	1	0	1	0	0	1	1	1	1	0
C4	1	1	0	0	1	0	1	1	0	0
A3	0	0	0	0	1	0	0	0	0	0
A4	0	0	0	0	0	0	0	0	0	0
C2	0	1	0	0	0	0	0	0	0	0
Three-layered	2	1	0	1	1	2	1	1	2	2

Table B 8: Breaking strength raw data

	Breaking strength per specimen tested (N)									
Sample	*1*	*2*	*3*	*4*	*5*	*6*	*7*	*8*	*9*	*10*
B3	295	284	317	355	382	325	332	302	289	295
B4	310	293	312	326	286	306	318	296	310	310
B2	308	296	314	291	305	288	309	299	310	308
B1	311	304	308	293	288	286	279	289	296	311
A3	239	215	224	222	202	208	231	224	220	239
C3	222	212	215	233	223	222	225	226	203	222
A4	188	192	182	189	186	188	192	180	190	188
C1	168	175	168	172	161	168	169	171	175	168
D2	190	190	163	179	185	186	173	170	176	190
D3	177	169	175	180	185	166	193	160	178	177
A1	174	189	169	187	175	170	182	175	169	174
C2	172	174	188	170	180	172	173	177	176	172
C4	180	169	167	159	165	182	182	182	175	180
D1	168	160	183	178	166	190	179	159	174	168
A2	164	158	154	167	149	149	171	156	173	164
Three-layered	200	209	162	215	203	180	197	183	214	189

Table B 9: Breaking strength data raw data (continuation)

	Breaking strength per specimen tested (N)									
Sample	*11*	*12*	*13*	*14*	*15*	*26*	*17*	*18*	*19*	*20*
B3	328	298	313	316	303	322	296	314	304	314
B4	301	296	306	312	303	300	295	294	301	293
B2	314	321	305	310	319	296	308	312	308	307
B1	301	297	293	300	284	295	308	285	290	302
A3	231	212	241	242	237	229	234	219	207	220
C3	218	203	224	222	226	217	208	203	219	216
A4	193	181	184	196	199	179	190	196	183	183
C1	163	179	182	163	186	186	183	172	180	178
D2	169	175	184	171	175	190	189	171	178	161
D3	164	170	168	161	149	165	155	153	160	163
A1	178	235	229	228	231	219	201	210	216	230
C2	173	185	177	183	184	172	175	181	170	176
C4	180	188	166	167	179	161	160	166	185	189
D1	176	182	183	163	171	180	159	161	176	162
A2	159	150	160	171	172	163	150	155	157	165
Three-layered	194	203	170	181	188	201	217	161	192	191

Table B 10: Elongation at break raw data

	Elongation at break per specimen tested (%)									
Sample	*1*	*2*	*3*	*4*	*5*	*6*	*7*	*8*	*9*	*10*
D1	372	390	388	420	417	387	382	375	399	375
D3	367	355	360	366	340	351	353	358	368	365
D2	323	347	347	347	353	352	352	353	324	341
A3	248	235	248	243	237	249	274	253	276	268
A1	243	259	227	255	265	266	260	255	254	223
A4	263	216	218	257	234	220	249	214	243	247
A2	220	249	226	227	241	247	241	242	243	251
B4	247	212	211	230	248	231	241	235	217	245
C2	202	228	241	222	214	214	208	245	227	250
C1	204	210	217	219	214	200	223	225	223	211
C3	231	207	225	205	209	218	209	216	203	214
B3	211	231	208	208	207	230	202	222	190	199
B2	217	201	200	225	222	200	213	199	206	217
B1	181	197	212	176	211	179	210	216	195	214
C4	198	180	191	186	208	181	194	210	187	171
Three-layered	232	213	233	243	229	233	238	232	235	246

Table B 11: Elongation at break raw data (continuation)

	Elongation at break per specimen tested (%)									
Sample	*11*	*12*	*13*	*14*	*15*	*16*	*17*	*18*	*19*	*20*
D1	382	377	378	381	392	372	383	376	385	385
D3	360	353	363	348	355	345	343	356	355	355
D2	331	358	330	311	337	338	315	311	335	317
A3	230	251	270	246	267	259	248	252	256	265
A1	267	268	229	229	220	247	250	246	226	262
A4	211	259	221	227	253	253	221	227	227	246
A2	257	234	228	236	223	260	260	236	233	244
B4	210	233	227	212	240	212	231	234	240	230
C2	248	230	203	214	215	247	231	235	237	236
C1	218	204	220	221	216	230	210	216	220	213
C3	214	217	216	211	217	200	209	213	206	218
B3	202	210	229	199	221	227	206	202	196	222
B2	218	203	217	205	218	202	206	212	229	225
B1	211	215	191	190	173	189	211	205	190	192
C4	176	187	178	210	170	186	172	171	192	203
Three-layered	202	237	201	211	242	228	236	234	243	237

Table B 12: Linear thermal shrinkage raw data

	Linear thermal shrinkage per specimen tested (%)									
Sample	*1*	*2*	*3*	*4*	*5*	*6*	*7*	*8*	*9*	*10*
C2	20	24	21	16	23	24	21	15	25	15
B3	19	19	24	18	21	18	15	17	19	16
B2	19	18	15	17	19	19	19	20	20	18
A3	18	16	19	18	19	17	15	20	16	17
A2	18	17	18	17	18	19	19	17	17	19
B1	17	19	15	18	17	17	19	15	19	16
C3	12	13	14	15	12	12	15	13	11	14
A4	11	13	13	12	14	9	12	10	14	13
D1	11	12	9	13	13	9	13	13	9	11
C4	11	13	10	13	9	9	12	10	10	11
D3	10	11	12	9	7	7	10	8	9	12
B4	8	6	8	11	7	9	5	7	9	9
C1	8	8	11	8	8	9	7	7	7	9
D2	6	6	4	5	4	7	6	8	4	4
A1	5	4	5	4	6	3	5	3	5	4
Three-layered	**6**	**7**	**6**	**6**	**8**	**6**	**6**	**8**	**8**	**6**

Table B 13: Sleep times raw data

	Sleep time per specimen tested (hrs)				
Sample	*1*	*2*	*3*	*4*	*5*
A1	65	63	64	66	64
A2	64	65	65	64	65
A3	66	65	65	64	63
A4	63	65	65	66	64
C4	47	47	47	46	46
C1	48	47	47	47	48
C2	46	46	47	47	48
C3	48	46	47	48	48
B3	37	36	38	38	37
B4	36	36	37	36	36
B2	36	36	36	37	38
B1	37	38	36	37	37
D3	25	25	25	26	27
D1	27	27	26	25	26
D2	27	26	25	27	26
Three-layered	48	45	46	46	46

Table B 14: Adhesion strength raw data

	Adhesion strength per specimen tested (N)									
Sample	*1*	*2*	*3*	*4*	*5*	*6*	*7*	*8*	*9*	*10*
D1	4.6	6.1	3.7	4.8	4.5	4.0	4.5	4.7	5.5	3.9
A4	6.3	4.2	4.8	5.9	4.3	4.5	3.7	5.7	3.7	3.1
B4	5.4	5.8	3.2	3.3	6.3	4.0	3.6	4.3	5.9	4.4
B1	4.1	3.3	3.6	3.6	3.0	4.5	3.6	4.7	3.8	3.3
C3	3.7	3.8	4.4	4.0	3.7	3.6	3.7	5.0	4.9	3.6
B2	2.9	3.7	3.9	3.3	3.0	4.9	4.6	4.3	4.9	3.7
C2	3.6	3.2	4.4	3.3	4.3	3.6	4.8	4.3	4.5	3.4
A2	3.2	3.7	3.2	4.5	3.8	4.2	3.1	3.7	3.0	3.4
A3	2.8	2.2	3.0	1.5	1.2	2.4	1.1	2.7	2.6	1.3
D3	1.2	1.5	1.1	2.3	1.7	1.7	2.8	1.4	1.4	1.6
A1	0.7	0.8	1.1	1.0	1.2	0.9	1.2	0.9	0.9	1.2
D2	1.0	1.4	0.8	1.2	1.0	0.8	1.1	1.0	0.8	2.1
C4	0.9	0.8	1.3	0.6	0.8	1.0	0.3	0.9	0.7	0.1
C1	0.3	0.6	0.6	0.7	0.4	0.5	1.7	0.6	0.2	0.6
B3	0.9	0.1	0.3	0.6	0.7	0.3	0.8	1.0	0.9	0.2
Three-layered	11.2	12.1	9.7	8.7	12.1	11.9	7.2	9.3	10.9	11.3

Table B 15: Velocity of detonation raw data

	Velocity of detonation per specimen tested (m/s)									
Sample	*1*	*2*	*3*	*4*	*5*	*6*	*7*	*8*	*9*	*10*
A1	1975	1850	2100	1906	1950	1900	1924	1873	2067	2061
A2	2020	1908	1990	2073	1957	1910	1935	2104	1915	1924
A3	1908	2045	2063	2012	2067	2084	1848	1982	1944	1876
A4	2061	1867	1996	1901	2042	2001	1957	2085	2037	1991
B1	1998	1878	1993	2033	2048	2031	1817	1875	1909	2034
B2	1933	1891	2083	2031	2082	1828	1812	2017	2019	2082
B3	2022	1970	1938	1912	1997	1842	1913	1926	1825	1867
B4	1861	2014	2003	1900	1962	1934	1901	1817	1837	2032
C1	1806	2079	2037	1888	1947	2010	1894	2061	1890	1831
C2	1866	1871	1896	1847	1978	1852	1834	1903	1913	1811
C3	1935	1889	1827	1880	1864	2078	2076	2033	2032	2094
C4	1937	2057	1875	1883	1961	1863	1825	1819	1853	1872
D1	1836	1812	1846	1940	1915	1814	1985	1839	1964	1966
D2	2036	1976	2096	1991	1895	1929	1808	1906	1897	1904
D3	2033	1909	1847	1888	1977	2070	2069	1959	2025	1860
Three-layered	1953	1810	1864	2009	1929	1915	1998	1987	2094	2008